

AD-A035 297

WESTINGHOUSE DEFENSE AND SPACE CENTER BALTIMORE MD  
RADAR PERFORMANCE MONITOR (U)  
MAR 76 A SIAURUSAITIS

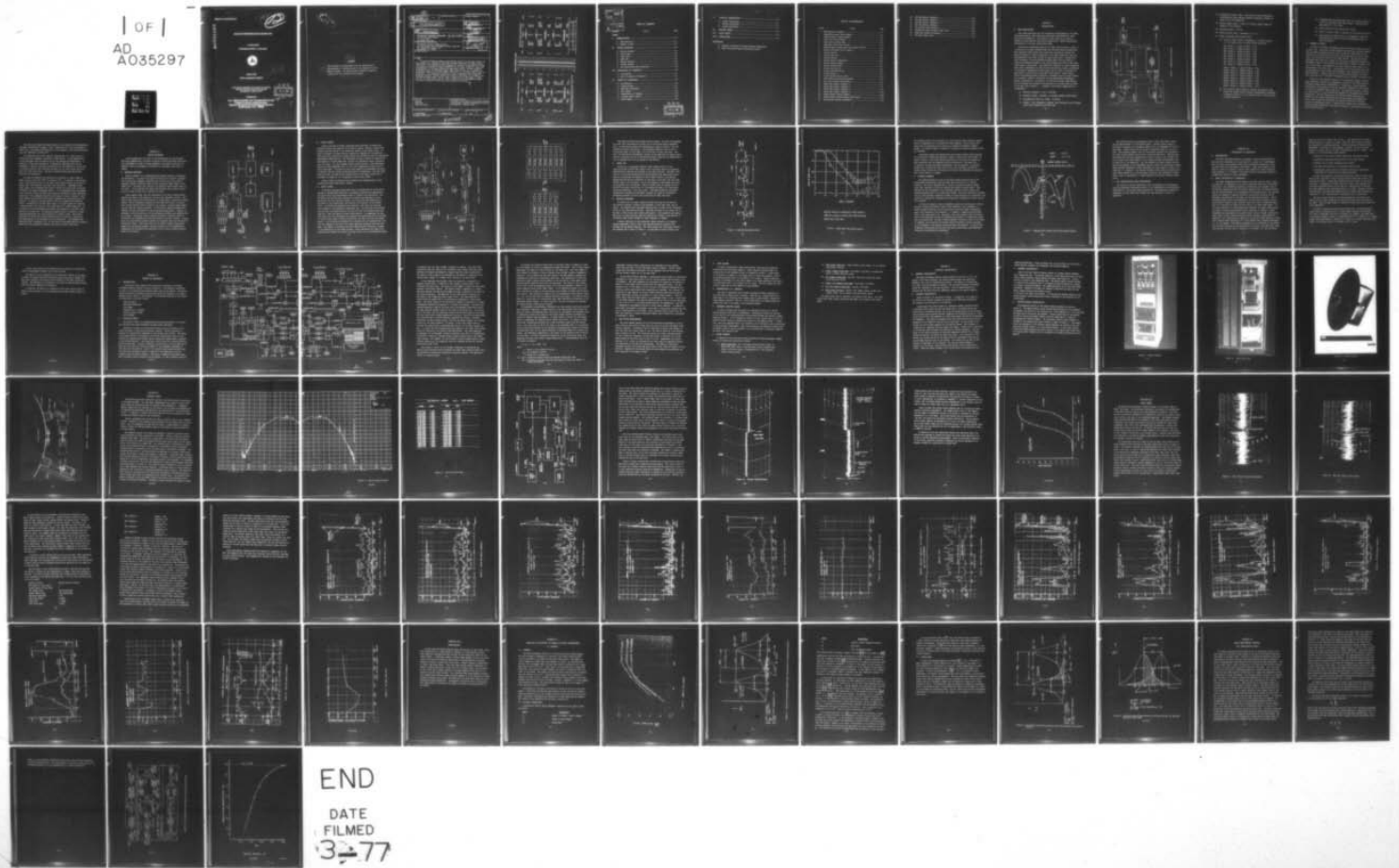
F/6 17/7

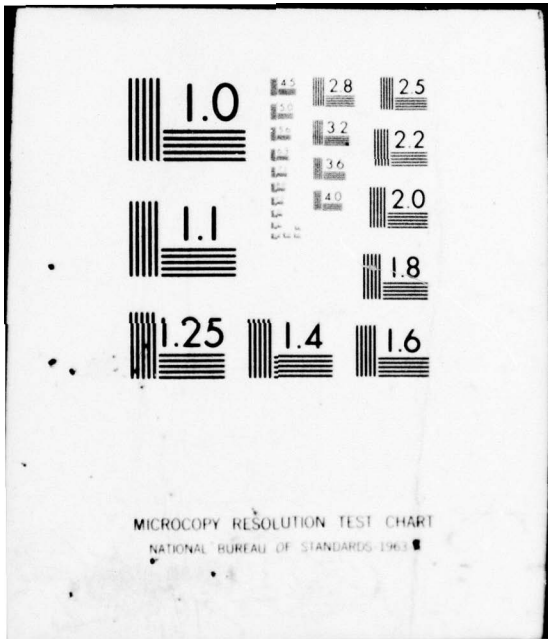
UNCLASSIFIED

FAA-RD-76-121

DOT-FA71WA-2570  
NL

1 OF 1  
AD  
A035297





MICROCOPY RESOLUTION TEST CHART  
NATIONAL BUREAU OF STANDARDS-1963-A

Report No. FAA-RD-76-121

*Handwritten signature or initials*

ADA 035297

**RADAR PERFORMANCE MONITOR**

**A. Slaurusaitis**

**Westinghouse Electric Corporation**



**March 1976**

**FINAL SUMMARY REPORT**

Document is available to the public through the  
National Technical Information Service,  
Springfield, Virginia 22161

**DDC**  
**RECEIVED**  
**FEB 8 1977**

Prepared for

**U.S. DEPARTMENT OF TRANSPORTATION**  
**Federal Aviation Administration**  
**Systems Research and Development Service**  
**Washington, D.C. 20590**

*Handwritten initials*

10

Report No. RAA-70-111

RADAR PERFORMANCE MONITOR

708230ADA

**NOTICE**

This document is disseminated under the sponsorship of the Department of Transportation in the interest of information exchange. The United States Government assumes no liability for its contents or use thereof.

FINAL SUMMARY REPORT

U.S. DEPARTMENT OF TRANSPORTATION  
LIBRARY

Document is available for the public through the National Technical Information Service, Springfield, Virginia 22161

Prepared for

U.S. DEPARTMENT OF TRANSPORTATION  
Federal Aviation Administration  
Systems Research and Development Service  
Washington, D.C. 20590

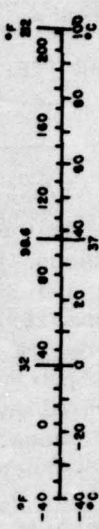
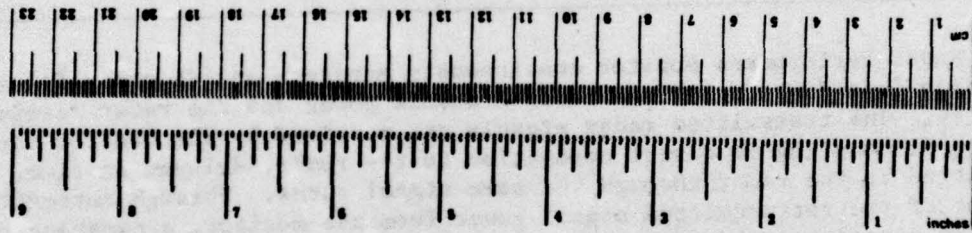
<p>1. Report No.  <span style="border: 1px solid black; padding: 2px;">18</span> FAA-RD-<span style="border: 1px solid black; padding: 2px;">19</span>76-121</p>	<p>2. Government Accession No.</p>	<p>3. Recipient's Catalog No.</p>	
<p>4. Title and Subtitle  <span style="border: 1px solid black; padding: 2px;">6</span> RADAR PERFORMANCE MONITOR.</p>		<p>5. Report Date  <span style="border: 1px solid black; padding: 2px;">11</span> MAR 1976</p>	<p>6. Performing Organization Code</p>
<p>7. Author(s)  <span style="border: 1px solid black; padding: 2px;">10</span> Al/Siaurusaitis</p>		<p>8. Performing Organization Report No.  <span style="border: 1px solid black; padding: 2px;">12</span> 85P.</p>	<p>9. Performing Organization Name and Address</p>
<p>9. Performing Organization Name and Address          Westinghouse Electric Corporation          Defense and Space Center          P. O. Box 1897          Baltimore, MD 21203</p>		<p>10. Work Unit No. (TRAIS)  <span style="border: 1px solid black; padding: 2px;">15</span></p>	<p>11. Contract or Grant No.          DOT-FA71WA-2578</p>
<p>12. Sponsoring Agency Name and Address          DOT-Federal Aviation Administration          Systems Research and Development Service (ARD-243)          800 Independent Avenue, S.W.          Washington, D.C. 20591</p>		<p>13. Type of Report and Period Covered  <span style="border: 1px solid black; padding: 2px;">9</span> FINAL rept.          1971 - 1975</p> <p>14. Sponsoring Agency Code</p>	
<p>15. Supplementary Notes</p>			
<p>16. Abstract</p> <p>The Radar Performance Monitor continuously monitors an ASR radar figure of merit, which is a function of the radar transmit power and the radar receiver sensitivity. The transmitted radar signals are received by the Monitor through free space RF coupling or direct connection to the radar, delayed in time, and retransmitted to the radar through the same signal paths. Through automatic adjustment of the retransmitted signal power from the monitor, a constant retransmitted signal to the radar system noise ratio at the radar video output is maintained. Any significant reduction of radar transmitted power and/or degradation of radar receiver sensitivity causes an adjustment of the Monitor retransmitted signal power level in order to maintain the same signal to noise ratio at the radar video outputs. When a preset Monitor retransmitted power threshold is exceeded, visual and aural alarms are activated.</p>			
<p>17. Key Words          Monitor          ASR Radar          Figure of merit</p>		<p>18. Distribution Statement          Document is available to the public through the National Technical Information Service, Springfield, Virginia 22161.</p>	
<p>19. Security Classif. (of this report)          Unclassified</p>	<p>20. Security Classif. (of this page)          Unclassified</p>	<p>21. No. of Pages          83</p>	<p>22. Price</p>

375450

4/B

# METRIC CONVERSION FACTORS

Approximate Conversions to Metric Measures				Approximate Conversions from Metric Measures			
Symbol	When You Know	Multiply by	To Find	Symbol	When You Know	Multiply by	To Find
<b>LENGTH</b>							
in	inches	2.5	centimeters	mm	millimeters	0.04	inches
ft	feet	30	centimeters	cm	centimeters	0.4	inches
yd	yards	0.9	meters	m	meters	3.3	feet
mi	miles	1.6	kilometers	km	kilometers	1.1	yards
						0.5	miles
<b>AREA</b>							
sq in	square inches	6.5	square centimeters	sq cm	square centimeters	0.16	square inches
sq ft	square feet	0.09	square meters	sq m	square meters	1.2	square feet
sq yd	square yards	0.8	square meters	sq mi	square miles	0.4	square yards
sq mi	square miles	2.6	hectares	ha	hectares (10,000 m <sup>2</sup> )	2.5	square miles
	acres	0.4					acres
<b>MASS (weight)</b>							
oz	ounces	28	grams	g	grams	0.035	ounces
lb	pounds	0.45	kilograms	kg	kilograms	2.2	pounds
	short tons (2000 lb)	0.9	tonnes (1000 kg)	t	tonnes	1.1	short tons
<b>VOLUME</b>							
mp	minim	6	milliliters	ml	milliliters	0.03	fluid ounces
fl oz	fluid ounces	15	milliliters	ml	milliliters	2.1	fluid ounces
cup	cups	30	milliliters	qt	quarts	1.06	quarts
pt	pints	0.47	liters	gal	gallons	0.26	gallons
qt	quarts	0.96	liters	cu ft	cubic feet	36	cubic feet
gal	gallons	3.8	liters	cu yd	cubic yards	1.3	cubic yards
cu ft	cubic feet	0.03	cubic meters				
cu yd	cubic yards	0.76	cubic meters				
<b>TEMPERATURE (exact)</b>							
°F	Fahrenheit temperature	5/9 (after subtracting 32)	Celsius temperature	°C	Celsius temperature	9/5 (then add 32)	Fahrenheit temperature

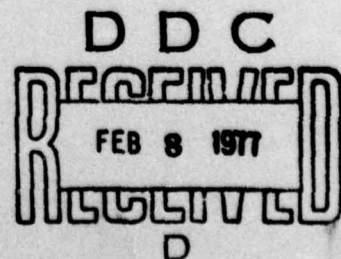


\* 1 in = 2.54 (exact). For other exact conversions and more detailed tables, see NBS Misc. Publ. 256, Units of Weight and Measures, Price \$2.25. SD Catalog No. C13.10.256.

ACCESSION for	
MTIS	White Section <input checked="" type="checkbox"/>
DDC	Buff Section <input type="checkbox"/>
UNANNOUNCED	<input type="checkbox"/>
NOTIFICATION	
BY	
CLASSIFICATION/AVAILABILITY CODES	
AVAIL. and/or SPECIAL	
A	

## TABLE OF CONTENTS

Section	Title	Page
<b>Summary</b>		
<b>I</b>	<b>INTRODUCTION</b> .....	1-1
	A. Task Definition .....	1-1
	B. Summary of Work .....	1-4
<b>II</b>	<b>DESIGN APPROACH</b> .....	2-1
	A. Monitor Accuracy .....	2-1
	B. False Alarms .....	2-3
	C. Delay Lines .....	2-4
	D. Radar STC .....	2-6
	E. Monitor Antennas .....	2-6
	F. Azimuth Sensing .....	2-9
	G. MTI Cancellation Ratio Monitoring .....	2-11
<b>III</b>	<b>PRINCIPLES OF OPERATION</b> .....	3-1
	A. Introduction .....	3-1
	B. Basic Principles of Operation .....	3-1
<b>IV</b>	<b>THEORY OF OPERATION</b> .....	4-1
	A. Introduction .....	4-1
	B. Figure-of-merit .....	4-1
	C. RMS Noise Measurement .....	4-7
	D. Fast Alarms .....	4-8
	E. Transmitter H.V. Sensing .....	4-8
	F. Internal Monitor Alarm .....	4-8
	G. Alarm Summary .....	4-8



V	PHYSICAL DESCRIPTION .....	5-1
	A. General Description .....	5-1
	B. Cabinet Description .....	5-1
	C. Antenna Description .....	5-3
VI	FACTORY TESTS.....	6-1
VII	FIELD TESTS .....	7-1
VIII	CONCLUSIONS .....	8-1

**APPENDIXES**

- A. Analysis of Accuracy of Signal-to-Noise Computation
- B. Radar Performance Monitor Cancellation Ratio

## LIST OF ILLUSTRATIONS

Figure	Title	Page
1	Radar/Monitor Interface.....	1-2
2	Simplified Monitor Block Diagram.....	2-2
3	Improved Monitor Block Diagram.....	2-4
4	Delay Line Block Diagram.....	2-5
5	Recirculating Delay Lines.....	2-7
6	Radar Near Field Power Contour.....	2-8
7	Measured ASR-5 Antenna Near Field Azimuth Pattern .....	2-10
8	Monitor Functional Block Diagram.....	4-3
9	Monitor Cabinet.....	5-2
10	Cabinet Rear View.....	5-4
11	Monitor Antenna.....	5-5
12	Azimuth Sensor Installation.....	5-6
13	Monitor Antenna Pattern.....	6-3
14	Monitor Antenna VSWR.....	6-5
15	Factory Test Set up.....	6-6
16	Average Simulated Noise.....	6-8
17	Figure-of-merit.....	6-9
18	Sliding Window Detector Data.....	6-11
19	ASR-7 Normal Figure-of-Merit/Noise.....	7-2
20	ASR-7 MTI Figure-of-Merit/Noise.....	7-3
21	Normal SWD Outputs, Quadrant 1.....	7-1
22	Normal SWD Outputs, Quadrant 2.....	7-2
23	Normal SWD Outputs, Quadrant 3.....	7-9
24	Normal SWD Outputs, Quadrant 4.....	7-10
25	Normal Channel Figure-of-Merit.....	7-11
26	Average Normal Figure-of-Merit Chart Data.....	7-12
27	Radar Normal Channel Performance.....	7-13

28	MTI SWD Outputs, Quadrant 1.....	7-14
29	MTI SWD Outputs, Quadrant 2.....	7-15
30	MTI SWD Outputs, Quadrant 3.....	7-16
31	MTI SWD Outputs, Quadrant 4.....	7-17
32	MTI Channel Figure-of-Merit.....	7-18
33	Average MTI Figure-of-Merit Chart Data.....	7-19
34	Radar MTI Channel Performance.....	7-20
35	MTI Radar Gated Clock.....	7-21

SECTION I  
INTRODUCTION

**A. TASK DEFINITION**

This report describes the work performed by Westinghouse on the Radar Performance Monitor, FAA Engineering Requirement FAA-ER-240-016, under contract DOT FA71WA-2570. The purpose of this effort was to design a feasibility model Monitor which would automatically indicate sub-standard performance of an airport surveillance radar.

The Monitor continuously monitors the radar figure-of-merit, which is a function of the radar transmit power and the radar receiver sensitivity. The transmitted radar signals are received by the Monitor through free space RF coupling or direct connection to the radar, delayed in time, and retransmitted to the radar through the same signal paths. Through automatic adjustment of the retransmitted signal power from the monitor, a constant retransmitted signal to the radar system noise ratio at the radar video output is maintained. Any significant reduction of radar transmitted power and/or degradation of radar receiver sensitivity causes an adjustment of the Monitor retransmitted signal power level in order to maintain the same signal to noise ratio at the radar video outputs. When a preset Monitor retransmitted power threshold is exceeded, visual and aural alarms are activated. Figure 1 illustrates the ASR System/Radar Performance Monitor configuration. The Monitor is connected to either radar channel and its antennas are located on the perimeter of the radar tower as shown in the plan view of Figure 1. A summary of the Monitor capabilities is listed below:

- (1) Operating frequency - 2700 to 2900 MHz
- (2) Frequency tuning - automatic, 10 seconds maximum tuning period
- (3) Retransmitted target run length - 32 pulses
- (4) Azimuth - four independent azimuths, each adjustable over 90 degree sector with accuracy of one radar PRT.

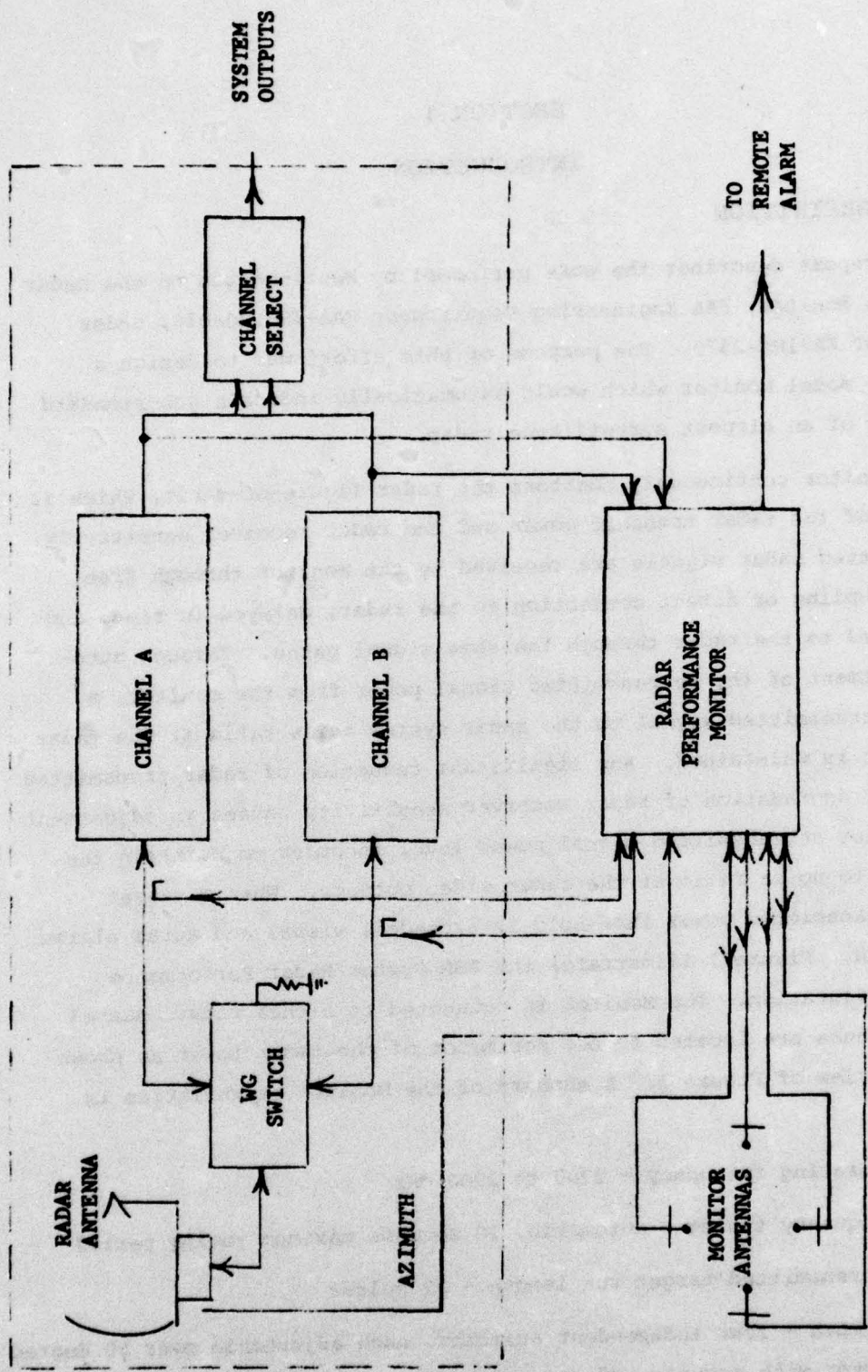


Figure 1. Radar/Monitor Interface

- (5) Retransmitted target range - selectable for 680 microseconds in 20 microsecond steps; MTI-each quadrant separately, Normal-one range for all four quadrants.
- (6) Monitor dynamic range - 60 dB (+10 dB above nominal radar performance to -50 dB below)
- (7) Monitor accuracy -  $\pm 0.5$  dB
- (8) Signal-to-noise ratio - Selectable 1:1 to 3:1.
- (9) Alarms indicating radar system status:

(a) Figure of merit alarms, programmable to indicate alarm in 1 to 200 scans by use of sliding window detectors:

MTI Sector 1, Figure of merit -2 dB  
MTI Sector 1, Figure of merit -3 dB  
MTI Sector 2, Figure of merit -2 dB  
MTI Sector 2, Figure of merit -3 dB  
MTI Sector 3, Figure of merit -2 dB  
MTI Sector 3, Figure of merit -3 dB  
MTI Sector 4, Figure of merit -2 dB  
MTI Sector 4, Figure of merit -3 dB

Normal Sector 1, Figure of merit -3 dB  
Normal Sector 1, Figure of merit -2 dB  
Normal Sector 2, Figure of merit -2 dB  
Normal Sector 2, Figure of merit -3 dB  
Normal Sector 3, Figure of merit -2 dB  
Normal Sector 3, Figure of merit -3 dB  
Normal Sector 4, Figure of merit -2 dB  
Normal Sector 4, Figure of merit -3 dB

(b) Fast figure of merit alarms to indicate catastrophic radar failure for Normal and MTI channels independently; adjustable to declare a fault in 1 to 8 scans and 1/4 to 1 scan to reset to normal condition.

- (c) Independent MTI and Normal RMS noise level alarms to detect +1 dB or +2 dB radar noise level change. Alarm detection adjustable for 1 to 6 scans.
- (d) Radar transmitter high voltage "OFF" alarm.
- (e) Monitor internal alarms to indicate +0.5 dB Monitor accuracy.
- (f) Aural alarms to indicate radar 2 dB degradation (warning), and master aural alarm to indicate unacceptable level of radar performance.

## B. SUMMARY OF WORK

The work on the Radar Performance Monitor feasibility model was started in April 1971. During the initial equipment design stage it became apparent that the Radar Performance Monitor built to meet the requirements of the specification FAA-ER-240-016 would have limited practical use in the field due to the statistical nature of the radar signals. The selected design techniques were sufficient to meet the stability and measuring accuracy requirements; however, the specification restraints on target run length, signal to noise ratio, and probability of alarm detection would result in an unacceptable false alarm rate. A preliminary false alarm analysis was made by Westinghouse and the results were submitted to the government technical representatives. Pending solution of the false alarm problem, the government suspended work on the Radar Performance Monitor contract in January 1972.

During the work suspension period, at the government request, Westinghouse submitted a proposal for mathematical analysis of the radar system to determine optimum Monitor implementation. Alternately, several hardware modifications were proposed to provide additional integration of the alarms to insure an acceptable false alarm rate. The government elected to modify the specification to include additional hardware for selectable test target integration. The main features of the modified specification were the addition of the sliding window detectors for monitoring slow degradation of the radar system and the addition of separate circuitry for fast detection of catastrophic failure. Several other changes were incorporated in the modified specification and some non-essential requirements were deleted from the specification.

The work on the Radar Performance Monitor, as revised by the Engineering Requirement FAA-ER-240-016 changes 1 and 2, dated March 26, 1974, was resumed in April 1974. The design and fabrication of the hardware to the revised specification was completed in October 1974.

The completed Monitor was tested at Westinghouse in a closed loop test hook-up with test equipment simulating a radar system. It was demonstrated to the government that the Monitor met the FAA Engineering Requirements. In addition to exercising the Monitor to demonstrate compliance with the Requirements, a 48-hour continuous reliability test was conducted at the factory. A continuous 48-hour chart recording was made for the scan-to-scan figure-of-merit and video noise level. The data collected proved excellent Monitor stability and reliability.

The monitor equipment was delivered and installed on a ASR-5 radar at NAFEC, Atlantic City, New Jersey in January, 1975. In contrast to the factory tests, the preliminary tests on the ASR-5 radar indicated about +6 dB MTI and Normal radar video baseline long-term noise variations. Independent radar video output noise recordings were taken to verify the radar noise variations recorded by the Radar Performance Monitor. It was determined that the extreme noise variations within the ASR-5 were caused by vibration of radar components, especially in the parametric amplifier and canceller circuit locations. Both radar channels were monitored and similar problems were encountered with both channels. In addition, the MTI channel video noise observed was extremely coarse. Observation of the MTI video output at a single sweep rate indicated a complete absence of noise or a high video spike for a given range cell. At the direction of the government the Monitor was connected to the ASR-7 radar located at the same site. The Monitor acceptance tests, including a 72-hour continuous operation test, were conducted on the ASR-7 radar. The monitor completed the 72-hour test without failure and all functions of the monitor were demonstrated to the satisfaction of the government. The equipment was accepted by FAA in February, 1975. At the time of this report Monitor evaluation tests were being conducted at NAFEC by the FAA at an ASR-7 radar site.

## SECTION II

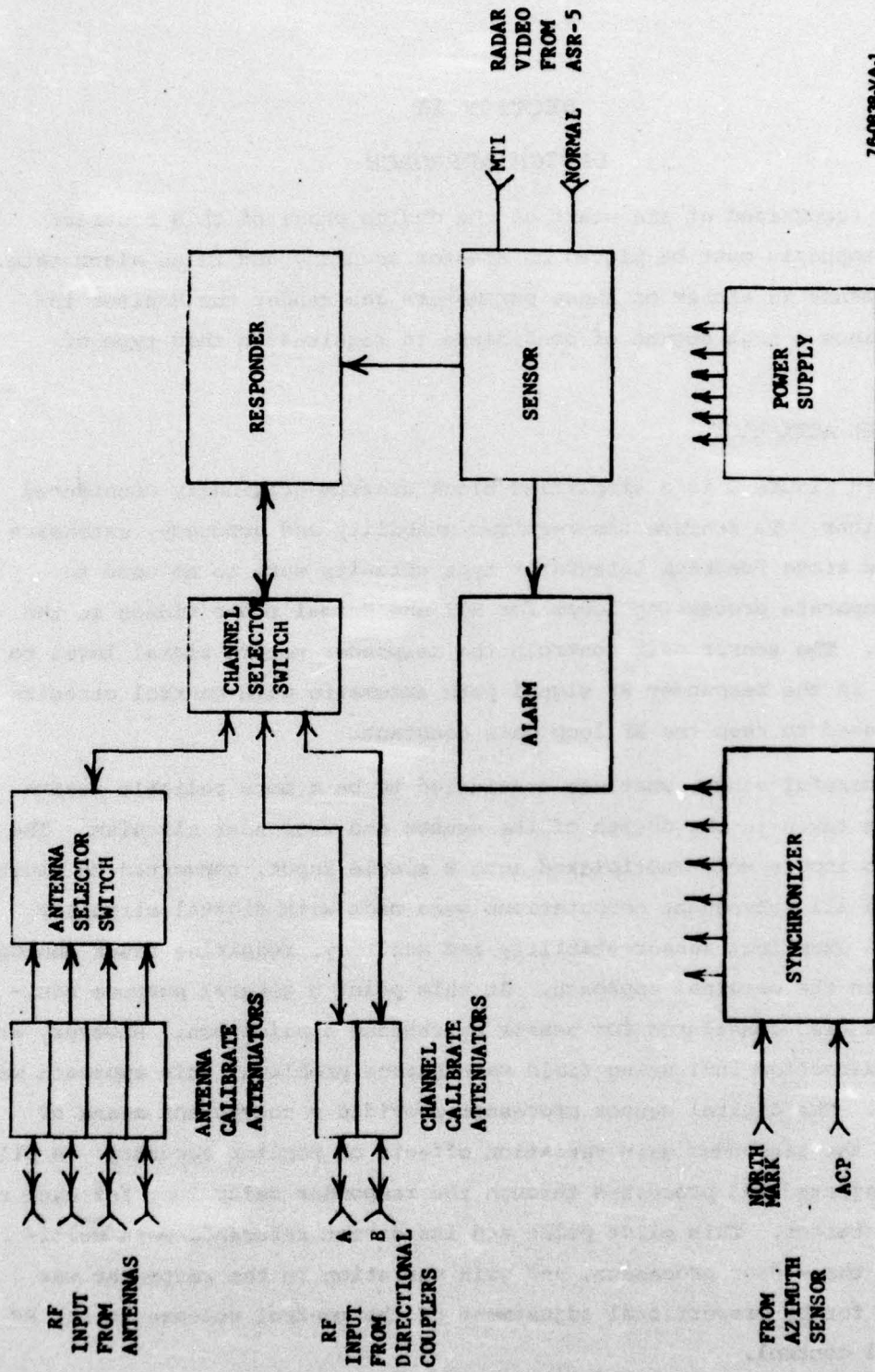
### DESIGN APPROACH

It was recognized at the start of the design phase of this contract that major emphasis must be placed on Monitor accuracy and false alarm rate. Poor performance in either of these parameters can render the Monitor ineffective since a high degree of confidence is required in this type of system.

#### A. MONITOR ACCURACY

Shown in Figure 2 is a simplified block diagram originally considered for the Monitor. To achieve the required stability and accuracy, extensive use of solid state feedback integrator type circuits were to be used to implement separate processing loops for MTI and Normal radar videos in the sensor unit. The sensor unit controls the responder return signal level to the radar. In the responder RF signal path automatic gain control circuits were to be used to keep the RF loop gain constant.

After careful study, what was considered to be a more reliable design approach was taken in the design of the sensor and responder circuits. The sensor video inputs were multiplexed into a single input, converted to digital signals, and all subsequent computations were made with digital circuitry. This insured excellent sensor stability and accuracy, requiring fewer analog circuits than the original approach. At this point a general purpose mini-computer was also considered for sensor processing application. However, at government direction, indicating field maintenance problems, this approach was not pursued. The digital sensor processor provided a convenient means of eliminating the responder gain variation effects on Monitor accuracy. A pilot pulse was injected and processed through the responder delay loop for each re-transmitted target. This pilot pulse and its direct reference were multiplexed into the sensor processor, and gain variation in the responder was compensated for by proportional adjustment of the control voltage to the RF signal level control.



76-0838-VA-1

Figure 2. Simplified Monitor Block Diagram

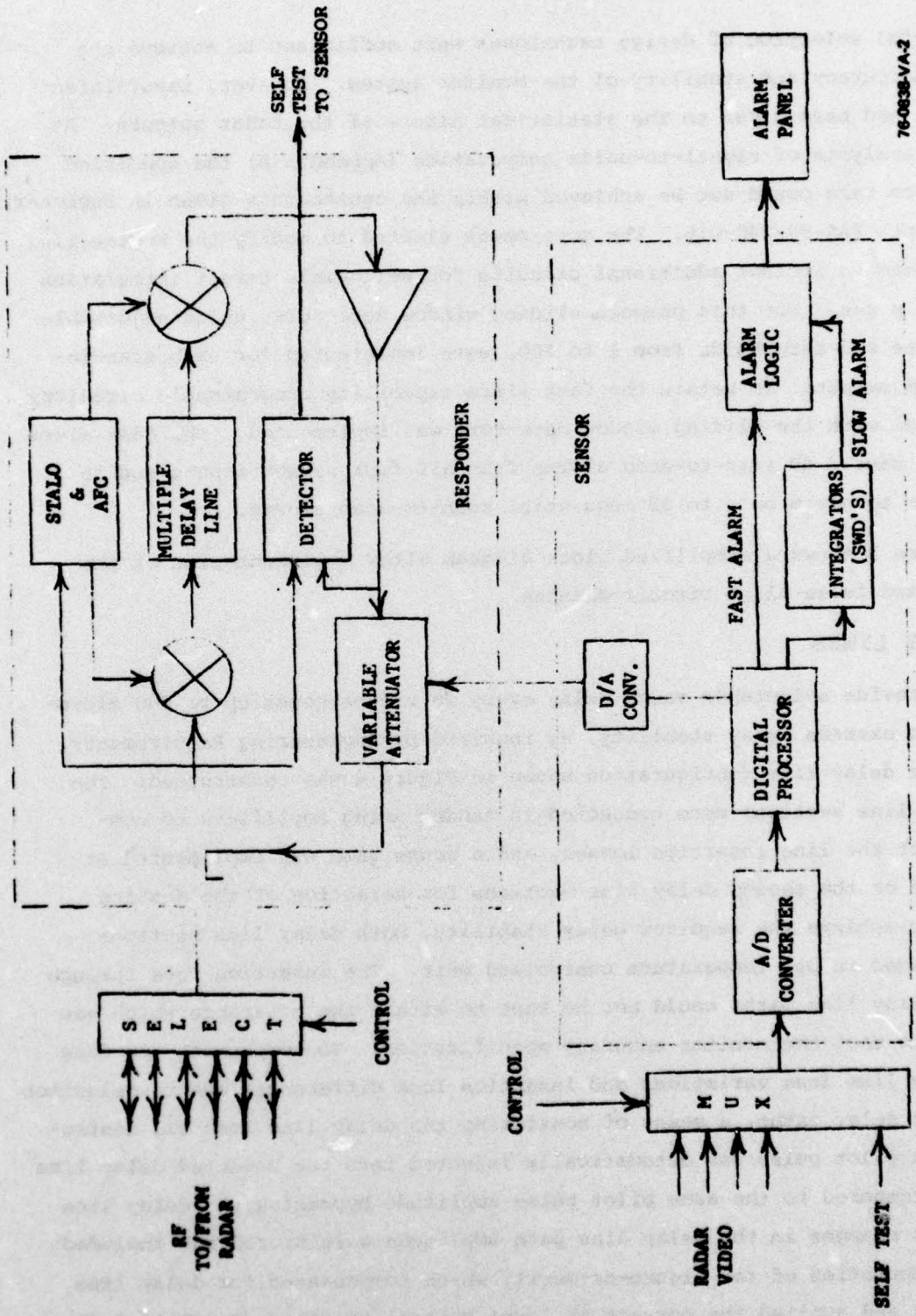
## B. FALSE ALARMS

Careful selection of design techniques were sufficient to achieve the required accuracy and stability of the monitor system. However, insufficient attention had been given to the statistical nature of the radar outputs. As shown in analysis of signal-to-noise computation (Appendix A) the specified false alarm rate could not be achieved within the constraints given in Engineering Requirements FAA-ER-240-016. The government elected to modify the Engineering Requirements to include additional circuits for selectable target integration up to 200 scans. For this purpose, sliding window detectors, using adjustable window size and thresholds from 1 to 200, were implemented for each scan-to-scan alarm output. To retain the fast alarm capability programmable circuitry in parallel with the sliding window detectors was implemented. The fast alarm circuitry uses 3 dB scan-to-scan alarms from all four sensor inputs and is adjustable to alarm on 4 to 32 sequential scan-to-scan alarms.

Figure 3 shows a simplified block diagram after implementation of the accuracy and false alarm circuit changes.

## C. DELAY LINES

To provide selectable range delay every 20 microseconds up to 680 microseconds at extreme delay stability, as required by Engineering Requirements, the quartz delay line configuration shown in Figure 4 was constructed. The two delay line sections were connected in tandem using amplifiers to compensate for the line insertion losses, and a range gate was implemented at the output of the second delay line sections for selection of the desired delay. To achieve the required delay stability, both delay line sections were packaged in one temperature controlled unit. The insertion loss through various delay line paths could not be kept to within the tolerance which was required to meet the monitor accuracy specification. To compensate for long term delay line loss variations and insertion loss differences due to selection of various delay paths, a means of monitoring the delay line loss was instrumented. A pilot pulse was automatically injected into the selected delay line path and compared to the same pilot pulse amplitude bypassing the delay line path. Any changes in the delay line path amplitude were stored and included in the computation of the figure-of-merit, which compensated for delay line variations and applied the correct RF level control to the retransmitted signal.



76-0838-VA-2

Figure 3. Improved Monitor Block Diagram

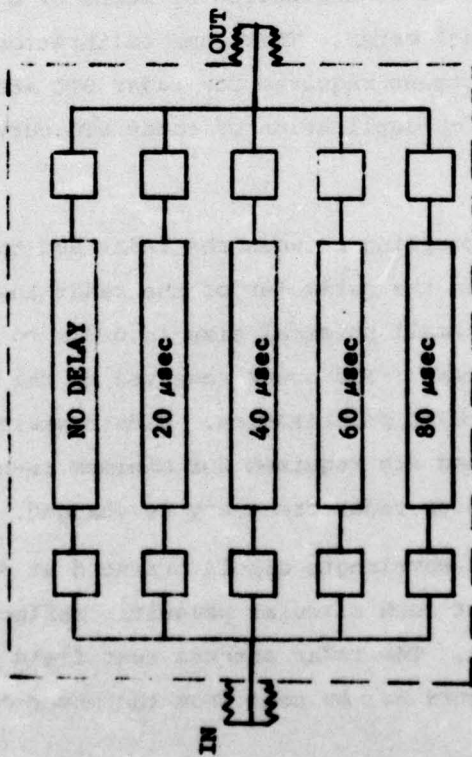
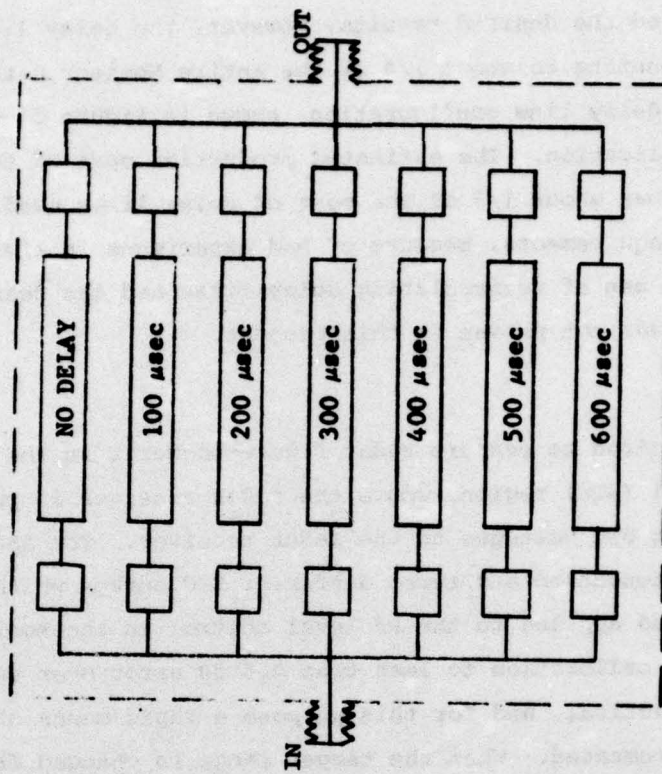


Figure 4. Delay Line Block Diagram

This design achieved the desired results, however, the delay line package is a high cost item amounting to about 1/4 of the entire Monitor materials cost. A recirculating delay line configuration, shown in Figure 5, was considered for Monitor application. The estimated production cost of the recirculating delay line was about 1/3 of the cost of delay lines used. However, the Engineering Requirements, because of bad experience in similar applications, prohibited the use of recirculating delay lines and the feasibility of such an implementation was not proven on this project.

#### D. RADAR STC

The Monitor is required to measure radar figure-of-merit in the sensitivity-time control (STC) region, where the radar receiver is purposely desensitized by applying STC voltages to the radar receiver. The ASR-5 radar uses up to 50 dB STC attenuation and three different STC curves which would have to be duplicated and applied to the RF level control in the Monitor. Maintaining the Monitor calibration to less than 0.5 dB error over such wide dynamic range is not practical, and for this purpose a rapid means of monitor re-calibration was instrumented. When the target range is changed from the Monitor front panel, the Monitor is re-calibrated by means of a front panel switch and observing a front panel meter. This same calibration procedure automatically included the adjustment required for radar STC attenuation, eliminating separate circuitry for duplication of radar STC curves.

#### E. MONITOR ANTENNAS

To provide the free space coupling between the radar and the Monitor, four monitor antennas, located on the perimeter of the radar tower, are required. The antennas must have small physical size in order to have negligible effect on the radar antenna pattern. The power received by the antenna has to be equal in both linear and circular polarization. Wide beamwidth and constant gain over the radar frequency band are required for minimum re-calibration of the Monitor when azimuth targets or radar frequency is changed.

A design consisting of half wavelength dipole oriented at 45 degrees (easily adjustable) with an eight inch circular parasitic reflector was selected for the Monitor antenna. The radar antenna near field power contour was computed and is shown in Figure 6. As seen from the power contour plot

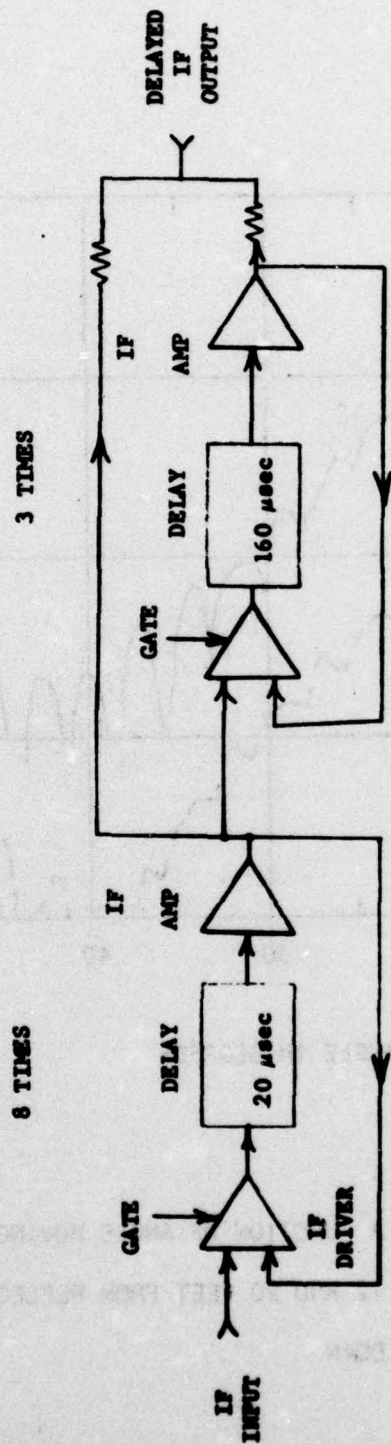
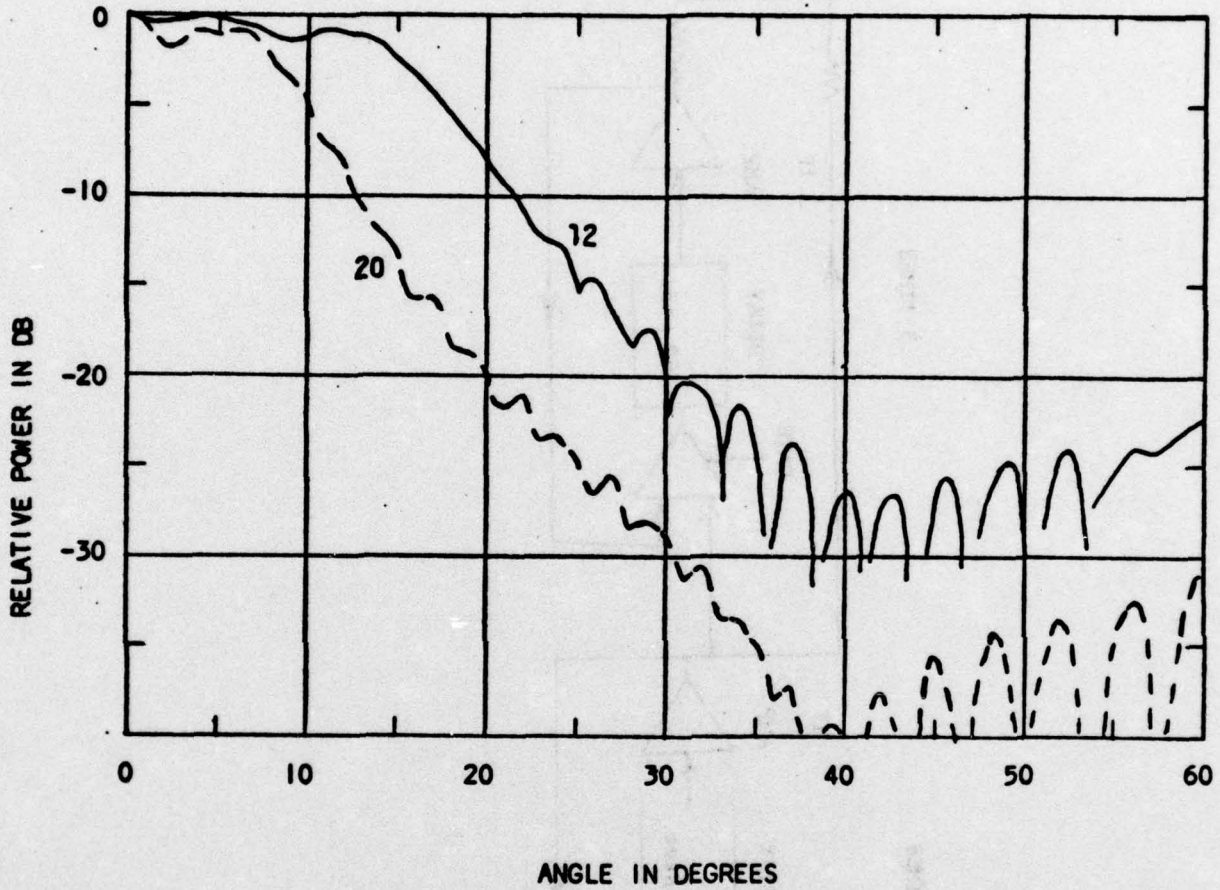


Figure 5. Recirculating Delay Lines



RELATIVE POWER AS A FUNCTION OF ANGLE MOVING A  
 PROBE ON A RADIUS 12 AND 20 FEET FROM REFLECTOR  
 VERTEX AND 2 FEET DOWN

Figure 6. Radar Near Field Power Contour

the optimum location of the antenna is 12 feet from the radar reflector vertex, which is compatible with a standard ASR tower dimension. The plot also indicates that re-calibration of the Monitor is required for moderate azimuth change. For azimuth changes in excess of 15 degrees the Monitor antennas should be relocated.

A prototype antenna was manufactured and the ASR-5 antenna field strength as a function of azimuth was measured at NAFEC, Atlantic City, New Jersey. As shown in Figure 7, the field strength variation as a function of azimuth was more pronounced than was expected from the calculations. The power ratio of linear to circular polarized transmission was not constant. It was concluded that, although the radar near field is not consistent, the Monitor antenna design would serve the purpose, but Monitor re-calibration is necessary when target azimuth is changed.

#### F. AZIMUTH SENSING

The azimuth sensing for each of the radar antenna positions was to be accomplished independently from the radar servo data and to  $\pm 0.1$  degree accuracy. The initial approach was to install an auxiliary azimuth change pulse (ACP) generator to provide accurate and reliable azimuth sensor. This approach was not acceptable to the government because it would require considerable modification to the radar servo system. The use of mechanical switches, such as limit switches, proximity switches and reed switches were considered. For reliability reasons the consideration of mechanical switches for azimuth sensing was discarded.

A variety of magnetic pick-up transducers which are activated by a ferrous material cutting the magnetic field of the transducer, were considered. A typical magnetic pick-up, used for monitoring rotational speed of mechanical gears, was evaluated in the laboratory. In general, a magnetic pick-up would work in this application, but, typically, 0.020 inch distance from the pick-up face to the rotational surface at minimum surface speed of 30 inches per second had to be maintained. The ASR-5 antenna pedestal rotational collar is 28 inches in diameter, and to provide the surface speed for magnetic pick-up a minimum 40 inch diameter at the antenna rotational speed was required. In view of the mechanical difficulties and the risk involved in maintaining close mechanical tolerances this approach was abandoned.

RADIUS - 12.0 FT.

HEIGHT - 7 FT. 2 IN.

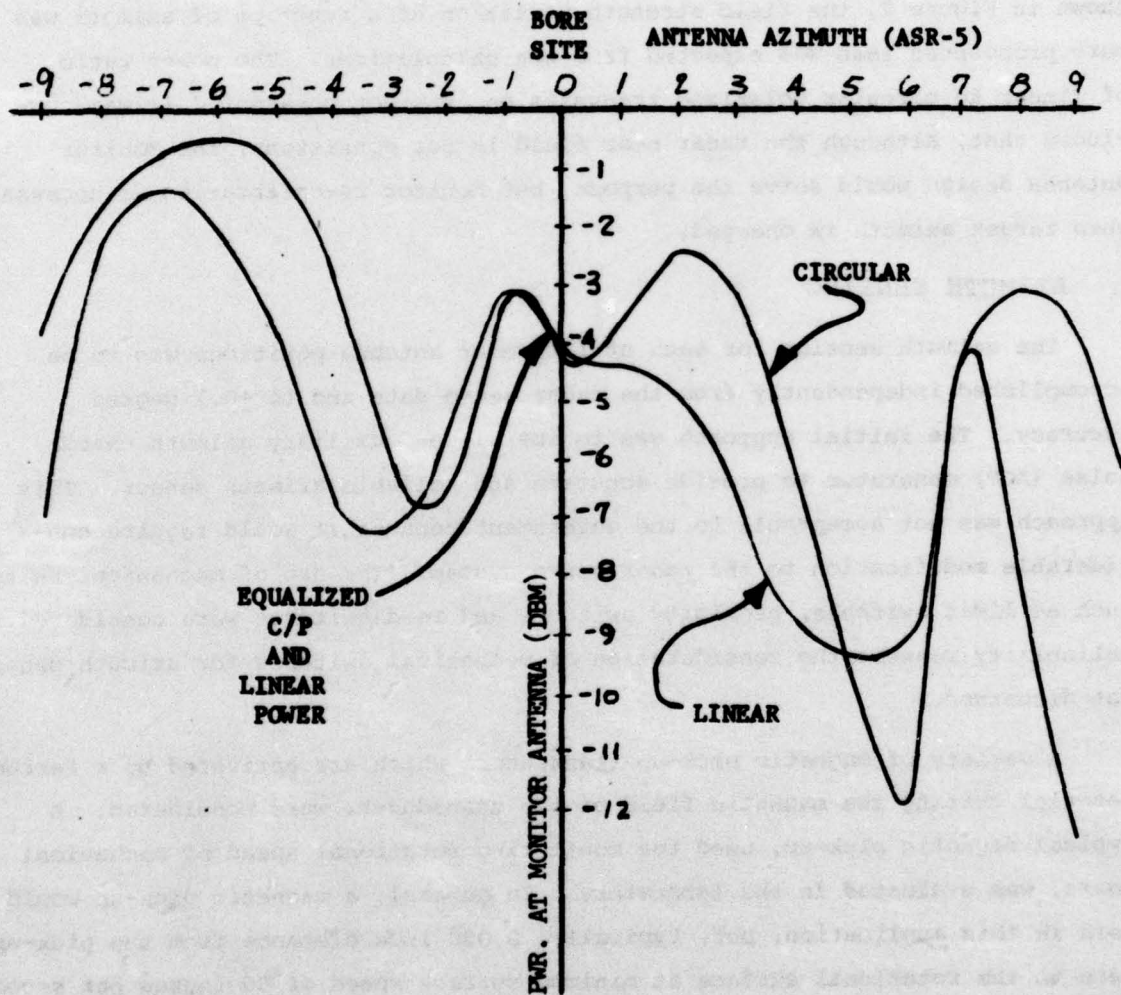


Figure 7. Measured ASR-5 Antenna Near Field Azimuth Pattern

The azimuth sensing was implemented using a solid state switch, where the switching element is a Hall effect sensor. The Hall effect sensor is activated by proximity of a permanent magnet and it is independent of the surface speed. Typical spacing of the switch to permanent magnet is 1/4 of an inch. Four permanent magnets (one for each monitor antenna) were attached to the radar antenna pedestal collar with a stainless steel belt. Theoretically, the magnets and thus the azimuth pulses could be located at any azimuth, however to adjust the target azimuth to  $\pm 0.1$  degree accuracy the procedure could be laborious if not impossible. For this purpose the azimuth pulses from the sensor were applied to four independent digital circuits in the Monitor cabinet, which provided independent vernier adjustment for each azimuth in steps on one radar PRT ( 0.1 degrees). The absolute azimuth (north) pulse was generated by using double magnet for one of the magnet locations, thus generating a double pulse, which is recognized as a unique azimuth by the Monitor azimuth synchronizer.

#### G. MTI CANCELLATION RATIO MONITORING

The option of the MTI cancellation ratio was deleted by the government from the Engineering Requirements and it is not implemented in the feasibility model Monitor. The initial design approach of a MTI cancellation monitor as applicable to ASR-5 radar with a delay line type canceller, is given in appendix B.

SECTION III  
PRINCIPLES OF OPERATION

A. INTRODUCTION

The Radar Performance Monitor is designed to prove the feasibility of monitoring the performance of an ASR system to a given set of requirements. When the radar system degrades below preset performance thresholds, visual and audio alarms are indicated by the Monitor. These alarm outputs can be used as a basis for decision to switch radar channels to retain continuous radar operation, or to provide a continuous record of the Monitor outputs to indicate past history of radar performance.

B. BASIC PRINCIPLES OF OPERATION

The Radar Performance Monitor measures the radar figure of merit, which, by definition, is dependent on the radar transmitted power level and receiver sensitivity. The transmitted signals are received by the responder unit of the Monitor through free space RF coupling employing four (4) dipole antennas (one for each 90 degrees) on the periphery of the antenna tower. The received signals are delayed in range by selected 20 microsecond intervals and sequentially retransmitted to the radar via the same dipole antennas. The retransmitted power levels are automatically controlled by the Monitor sensor, which detects changes in radar receiver sensitivity and/or transmitted power level by evaluating the signal-to-noise ratio at the radar video output. If the radar sensitivity or transmitted power degrades, the sensor output causes the amount of power retransmitted from the responder to increase. Preset thresholds are implemented on the sensor output control voltage, and when the radar figure of merit degrades beyond a preset threshold, alarm pulses are generated. The alarm pulses are applied to the sliding window detectors, which have a window length adjustment of 1 to 200 samples and a threshold adjustment of 1 to 200 samples. Each sample corresponds to one revolution of the antenna, thus the alarm criteria can be selected from a one scan, very high false alarm rate and fast reaction time (1 revolution = 4 seconds), to a very low false

alarm rate but slow reaction time (13 min.). The outputs of the sliding window detectors are applied to visual (lamp) and audio alarms to indicate the degradation of radar performance. The above process of figure-of-merit measurement is repeated for each quadrant (4 times), for MTI and Normal channels (2 times), and at 2 dB and 3 dB degradation levels (2 times). This results in 16 figure-of-merit alarm outputs.

In addition to the figure-of-merit monitoring, the Monitor system:

- monitors the absolute RMS noise level of the radar receiver
- detects loss of radar transmitter high voltage
- provides fast alarm due to catastrophic radar failure
- continuously checks itself for accuracy and gives an appropriate alarm when not operating within required accuracy

The RMS noise alarms are indicated by the Monitor when the video noise levels at the radar MTI or Normal channel change by more than 1 dB or 2 dB from nominal levels. Either noise threshold can be prewired in the Monitor circuitry. To determine the radar video noise level, noise samples from all antenna quadrants during any one scan are evaluated and, in addition, the noise sampling time is selectable from 1 to 6 scans. Separate controls are provided so that RMS noise alarms for MTI or Normal radar channels are indicated in 1 to 6 antenna scans as selectable from the front panel.

The loss of high voltage to the radar transmitter is sensed by the Monitor using a direct connection to the high voltage control circuitry of the radar. When the high voltage is disabled the audio and visual alarms are given immediately.

To sense a catastrophic radar system failure the 3 dB figure-of-merit alarms from all quadrants prior to sliding window detectors are combined. A fast alarm (catastrophic failure) is indicated if X number 3 dB alarms occur in continuous sequence, where X is selectable from 4 to 32 alarms (1 to 8 scans). Normal system performance is declared if Y number of no alarm conditions occur, where Y is selectable from 1 to 4 alarms (1/4 to 1 scan).

Finally, test circuits are provided within the Monitor to continuously check its measurement accuracy to  $\pm 0.5$  dB or better.

The Monitor is also connected to the directional coupler of the radar. By means of a manual switch the monitoring signal path may be changed from free space coupling via antenna to hard coupling at the radar directional coupler. The operation of the Monitor is the same as described above except that the antenna components are bypassed.

In addition, the Monitor is connected to both radar channels and, by manual switch selection, it can be operated with either channel without re-tuning.

## SECTION IV

### THEORY OF OPERATION

#### A. INTRODUCTION

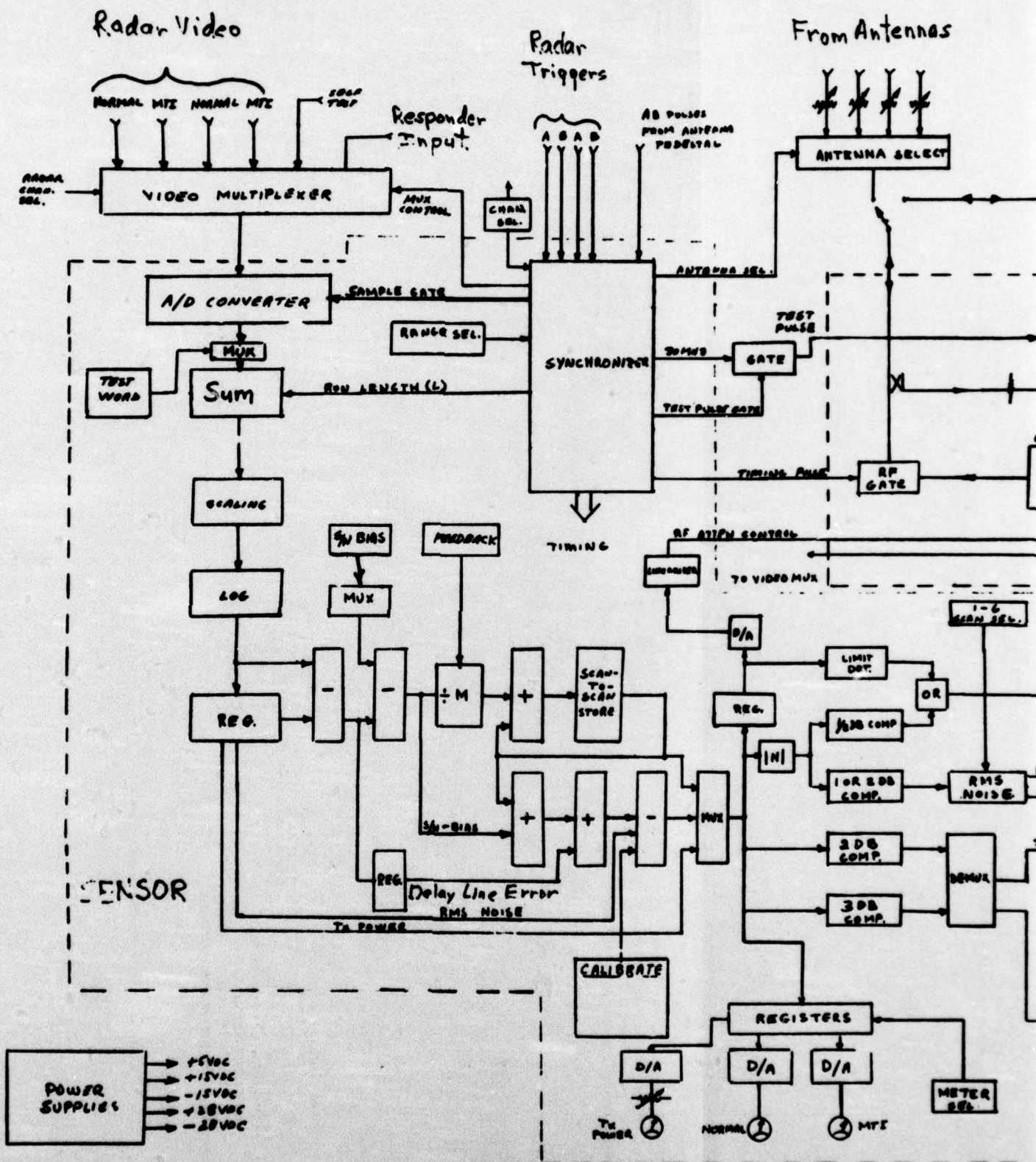
A functional block diagram of the electronics contained in the Radar Performance Monitor cabinet is given in Figure 8. The diagram is simplified in order to illustrate system function rather than circuit design. The Monitor dipole antennas and azimuth pick-up circuits which are located on the antenna pedestal are not shown in this diagram. The following functions of the Monitor are described in the order listed:

- Figure-of-merit,
- RMS noise measurement,
- Fast alarm,
- Transmitter H.V. sensing,
- Monitor Internal Alarm,
- Alarm Summary

#### B. FIGURE-OF-MERIT

The figure of merit is continuously monitored by the Monitor, and alarms are indicated when radar degradation exceeds preset thresholds.

Referring to Figure 8, the transmitted radar pulse is received via four dipole antennas or from radar directional couplers. Signals received via antennas are sequentially commutated by the antenna select switch. The timing for antenna selection is provided by the Monitor synchronizer which in turn receives the azimuth start pulses from an independent azimuth sensor installed on the antenna pedestal. The directional coupler selection is manual from the Monitor front panel. Variable attenuators are provided at all six radar RF inputs such that equal RF signals are applied to the Responder regardless of which RF source is selected. Part of the transmit pulse energy received from the radar via directional coupler is applied to the Responder by use of a coupler within the Monitor cabinet. This pulse is sampled and provides automatic frequency control reference for the Monitor, so that no Monitor retuning





is required when the radar transmit frequency is changed. The other input connections from the radar are MTI and Normal video outputs from both radar channels, and Master and Modulator triggers from both radar synchronizers. All cables to both channels are provided and the Monitor is switched to the desired radar channel by a common switch located on the front panel.

In the Responder, the RF pulse, after the selection, is applied to a summing network which, in addition to the transmit RF pulse input, has a secondary self-test input. The output of this summer is split into two paths through a directional coupler. The coupled output is applied to a S-band amplitude detector through another summer and then is applied to the input of the video multiplexer. The amplitude of the video pulse is directly proportional to the transmitter power output level. The video amplitude is evaluated by the sensor and it is continuously displayed on a front panel meter. The direct output of the directional coupler is converted to a 30 MHz intermediate frequency and applied to the delay line network. The delay line network generates a comb of 35 pulses with 20 microsecond inter-pulse period for each received transmit pulse at the input of the delay line. At the output of the delay line the range gate selects the desired pulses as controlled from the front panel through synchronizer circuitry. Then the selected pulses are converted back to the RF frequency, amplified and through a variable attenuator, RF gate, antenna select, and roof-top dipole antenna, are retransmitted into the radar receiver. Of course, if the radar coupler path is selected the target pulse is retransmitted directly to the radar receiver input. In either case the retransmitted pulse appears at the radar video outputs which are connected to the Monitor video multiplexer. The video amplitude is dependent on the Responder variable attenuator value which is automatically controlled to maintain a constant preset signal-to-noise ratio at the radar video outputs. For example, for any decrease in radar transmit power or radar receiver sensitivity the attenuator value will decrease raising the retransmitted pulse power level.

The automatic control of the variable attenuator is achieved by the Monitor sensor processor which evaluates the radar video signal-to-noise ratio and generates a proportional attenuator correction voltage. The sensor processor is a digital device.

To evaluate the signal-to-noise ratio of the radar video, 32 samples of video and 1024 samples of noise are independently summed and stored. The 32 video samples approximate the number of target returns for one radar scan. The large number of noise samples is averaged to assure constant noise average as shown in Appendix A, Figure A1. The two quantities are then scaled to the same number of samples and independently converted to logarithmic quantities. The subtraction of these log quantities yield a signal-to-noise measure in dB from which a fixed number representing desired signal-to-noise ratio is subtracted. The result of this subtraction is zero if the retransmitted signal level from the responder is equal to the preset signal-to-noise at the radar output. If the subtractor output is not zero then a correction is made to the scan-to-scan store output to adjust the RF attenuator control. The correction is made at the rate determined by the M factor (equal to 1, 1/2, 1/4 or 1/8) which is selected from the front panel. At M factor setting equal to 1, since this is a closed servo loop, some overshoots are expected in the attenuator control signal. At lower M factors, the error correction is smoother, but slower reaction time must be accepted.

To instrument the performance thresholds the video signal-to-noise and selected bias (S/N-Bias) difference is added directly to the scan-to-scan store output and from this result (disregarding delay line error for the moment) the calibrate value is subtracted yielding zero output to the sensor output processor threshold circuitry for nominal radar performance. A unique feature is built into the Monitor design to compensate for amplitude drift (delay line error). An internal 30 MHz test pulse is generated by gating the 30 MHz oscillator output from the synchronizer. This test pulse is fed to the input to the Responder where it is converted to RF and processed through the two responder processing paths (direct and through selected delay line) and the sensor processor as described above for a normal test target. The subsequent computation in the sensor is the insertion loss of the delay line path. As the RF attenuation changes due to the active servo loop, compensation for delay line change is made automatically. The performance error can be written as follows:

$$e = A_R + \Delta + \text{D.L. LOSS} - \text{CAL},$$

where,

$e$  = Error to the threshold circuits,

$A_R$  = RF attenuator control,

$\Delta$  = Actual S/N - desired S/N,

D.L. Loss = Difference between direct and delayed signal paths, and

CAL = Calibration inserted from the front panel to yield zero output for normal performance.

Independent figure-of-merit computations are performed for each quadrant (four times per scan) for MTI and Normal receiver channels. The MTI target ranges are individually selectable for each quadrant from the front panel. The four Normal targets are at the same range.

If the figure-of-merit degrades, a proportional error output is continuously displayed on a front panel meter in dB for one MTI quadrant and one Normal channel quadrant. The other quadrants are selectable for display on the meters by means of a front panel switch located below the appropriate meter. The performance error is also applied to the 2 dB and 3 dB threshold comparators producing an alarm output pulses when thresholds are exceeded. The 2 dB and 3 dB alarm data is then applied to sliding window detectors (SWD) which produce an output alarm when  $m$  alarms are present in a given window length  $n$ . Both the alarm count  $m$  and the window length  $n$  are adjustable from 1 to 200. Since there are two radar channels, four monitor quadrants and two levels of error detection, a total of 16 ( $2 \times 4 \times 2$ ) sliding window detectors are implemented. Each SWD is independently programmable and has an alarm output indicator. In addition a three digit LED display is provided on each SWD to continuously indicate the number of alarms present in the window. The 16 figure-of-merit alarms from the SWD's are combined to produce prescribed summary alarm indications as described in paragraph G. below.

#### C. RMS NOISE MEASUREMENT

The noise samples obtained for the figure-of-merit measurements are also used to monitor the value of video base line noise of the MTI and Normal radar receiver channels. A calibrate value is subtracted from the noise samples in each case such that nominal input to the 2 dB (may be wired for 1 dB) absolute noise threshold is zero. The threshold outputs are stored, and when present for four consecutive quadrants, an RMS noise alarm is indicated if the scan select switch on the front panel is set to 1 scan. Independent scan select switches (1 to 6 scans) are provided on the front panel for improved accuracy and consistency of the RMS noise measurement. The number of consecutive thresholds required to declare RMS noise alarm is four times the number of scans selected. Separate MTI and Normal RMS noise alarm lamps are provided and are also connected to the summary alarms.

#### D. FAST ALARMS

To sense a catastrophic radar system failure, fast reacting alarms are provided for MTI and Normal channels. These alarms are derived from 3 dB alarms from all four quadrants prior to integration by SWD's. A fast alarm is indicated if X number of 3 dB alarms occur in continuous sequence, where X is switch-selectable from 4 to 32 alarms (1 to 8 scans). Normal system performance is declared if at any time Y number of no alarm conditions occur where Y is selectable from 1 to 4 alarms (1/4 to 1 scan). The fast alarms are indicated by lamps and are also applied to alarm summary.

#### E. TRANSMITTER H.V. SENSING

The loss of transmitter high voltage is sensed by direct connection to the radar high voltage control circuitry. When the H.V. voltage goes off an alarm lamp is lit indicating this condition and an alarm signal is applied to alarm summary circuitry. When H.V. "off" alarm occurs the sliding window detectors are reset to no alarms in the selected windows.

#### F. INTERNAL MONITOR ALARM

In order to assure that the Monitor is performing within  $\pm 0.5$  dB measuring accuracy a self-test is implemented. Calibrated DC levels are applied to the input of the video multiplexer and processed through the system in normal computing fashion. If the computation results in error greater than  $\pm 0.5$  dB, an internal monitor alarm is indicated and applied to the summary alarms. In addition, since the responder delay line insertion loss is allowed to vary as described in figure-of-merit measurement, limit level detectors are employed to assure that the dynamic range of the RF attenuator is not exceeded due to excessive change of the delay line insertion loss.

#### G. ALARM SUMMARY

In addition to the individual alarms described in above paragraphs, summary alarms are derived and indicated as follows:

- (a) Master Alarm Lamp - Any 3 dB Normal figure-of-merit alarm, or Normal RMS noise alarm, or MTI RMS noise alarm, or Normal fast alarm, or MTI fast alarm, or Transmitter H.V. "off" alarm or Internal Monitor alarm.

- (b) Audio Alarm, High Tone - Same as Master Alarm except 1 to 10 seconds (adjustable) duration.
- (c) Normal (common) Alarm Lamp - Any Normal 3 dB alarm, or Normal fast alarm, or Normal RMS Noise alarm.
- (d) MTI (common) Alarm Lamp - Any MTI 3 dB alarm, or MTI Fast Alarm or MTI RMS Noise alarm.
- (e) Normal 2 dB (common) Alarm Lamp - Any Normal 2 dB alarm.
- (f) MTI 2 dB (common) Alarm Lamp - Any MTI 2 dB alarm.
- (g) Audio Alarm, Low Tone - Normal 2 dB (common) alarm, or MTI 2 dB (common) alarm, and not Master (high tone audio) alarm.

The Master Alarm lamp is located on the cabinet front panel. All other listed alarm lamps, except individual SWD lamps, are located on the sensor output.

## SECTION V

### PHYSICAL DESCRIPTION

#### A. GENERAL DESCRIPTION

The Radar Performance Monitor system consists of one 78.5" x 22" x 22" cabinet, four dipole antennas, one antenna azimuth sensor and associated hardware, and a set of interconnecting cables. The cabinet is located near the radar receiver/transmitter cabinets, and the dipole antennas and azimuth sensor are installed on the tower platform. A set of cables connect the antennas and the radar receiver/transmitter signals to the Monitor cabinet.

#### B. CABINET DESCRIPTION

Shown in Figure 9 is the Monitor cabinet. A hinged 28" x 19" panel at the front of the cabinet contains the controls and indicators required for the operation and calibration of the Monitor.

Located below the control panel is a slide-out chassis containing plug-in printed circuit cards (16) and one planar array. The planar array contains plug-in integrated circuits (up to 100 per planar array) and the printed circuit boards have soldered discrete components and integrated circuits. Below the printed circuit card assembly is an RFI-tight drawer containing the Responder RF components. The drawer is mounted on pull-out slides and the access to the components is by removal of the top lid of the drawer. At the bottom of the cabinet are the DC power supplies for the Monitor system. Each assembly is a separate unit removable from the cabinet for repair. Figure 10 is a rear view of the Monitor Cabinet showing the locations of various components. The top panel of the cabinet contains the switching components required for RF input switching functions and serves as cable entry panel. All connections to the Monitor are through the top of the cabinet and all maintenance functions can be performed from the front of the cabinet. The access from the rear of the cabinet is desirable but not required. The top most wired assembly in Figure 10 is the sensor, which contains four planar arrays of digital circuitry. Below the sensor assembly is the quartz delay line package with its

associated amplifiers. Below the delay line, top to bottom, are the sliding window detector assembly, the responder, and the power supplies.

### C. ANTENNA DESCRIPTION

Each of the four Monitor antennas consist of a dipole antenna assembly and a supporting mast. The Monitor antenna is a half-wave dipole with an eight inch circular reflector located behind the dipole (See Figure 11). The reflector is bolted to the supporting mast. The dipole support extends through the center of the reflector and it is rotated for equal reception of linearly or circularly polarized signals. The supporting masts are 10 feet high wooden structures. Normally, the masts are located 12 feet from the center of the ASR-5 antenna rotation and secured in place on the top of the tower roof surface. To eliminate the weather effects on the dipole antenna a small weather-proof dome is attached to the reflector at the installation.

### D. AZIMUTH SENSOR DESCRIPTION

The mechanical details of the azimuth sensing hardware are shown in Figure 12. The magnet holders, which provide the positioning of the permanent bar magnets, are secured to the rotating part of the pedestal by a 1-1/2 inch wide stainless steel band around the pedestal. Angular positioning of the magnets is made by sliding the magnet holders along the clamp band to a position corresponding to desired azimuth. The stationary azimuth sensor assembly is attached to the antenna motor mount channel as shown in Figure 12. The magnets around the periphery of the rotating antenna pedestal are aligned to pass the stationary azimuth sensor at 1/4 inch radial distance. As the radar antenna rotates each magnet passing the sensor results in an azimuth pulse output from the azimuth sensor assembly which is connected to the Radar Performance Monitor cabinet.

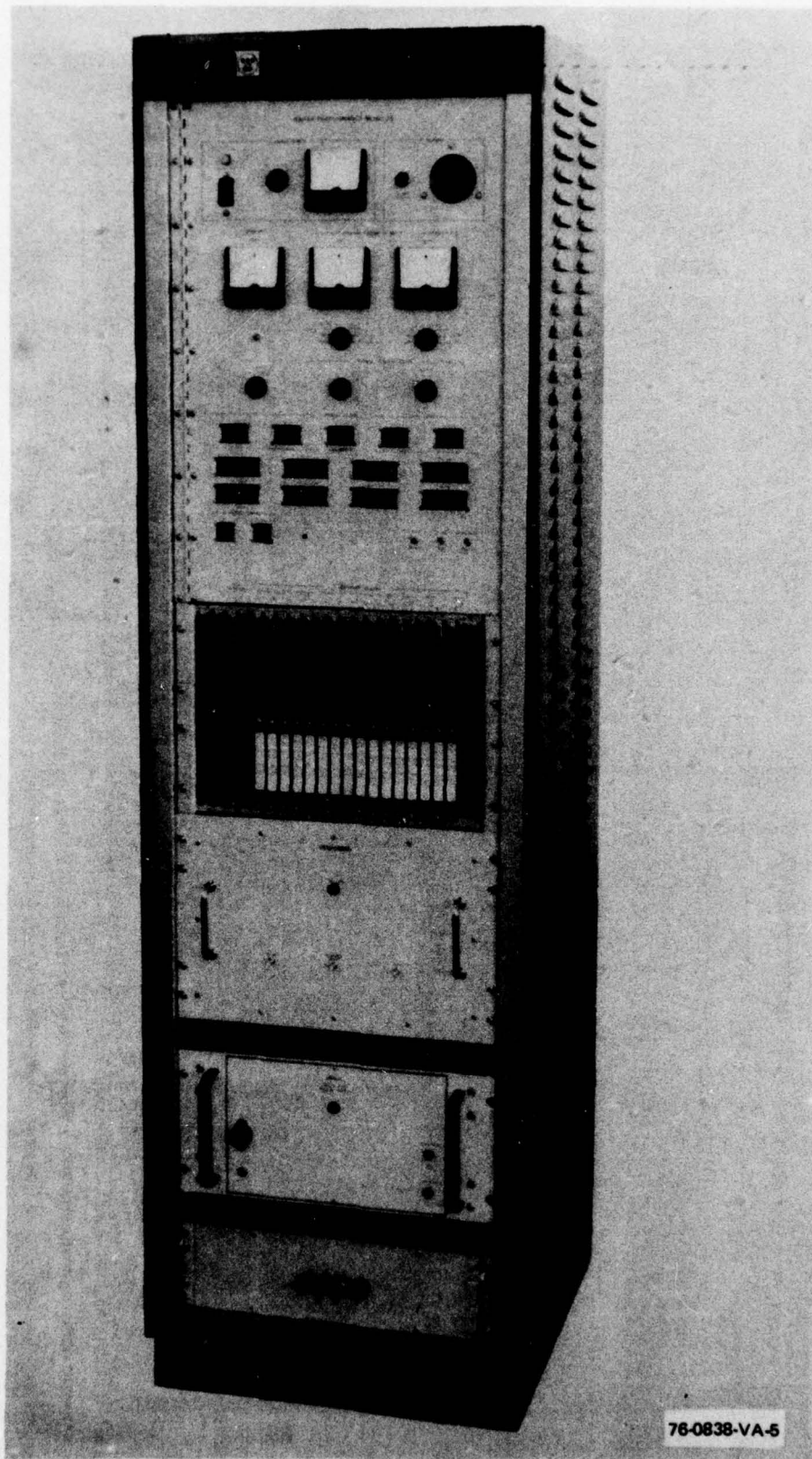
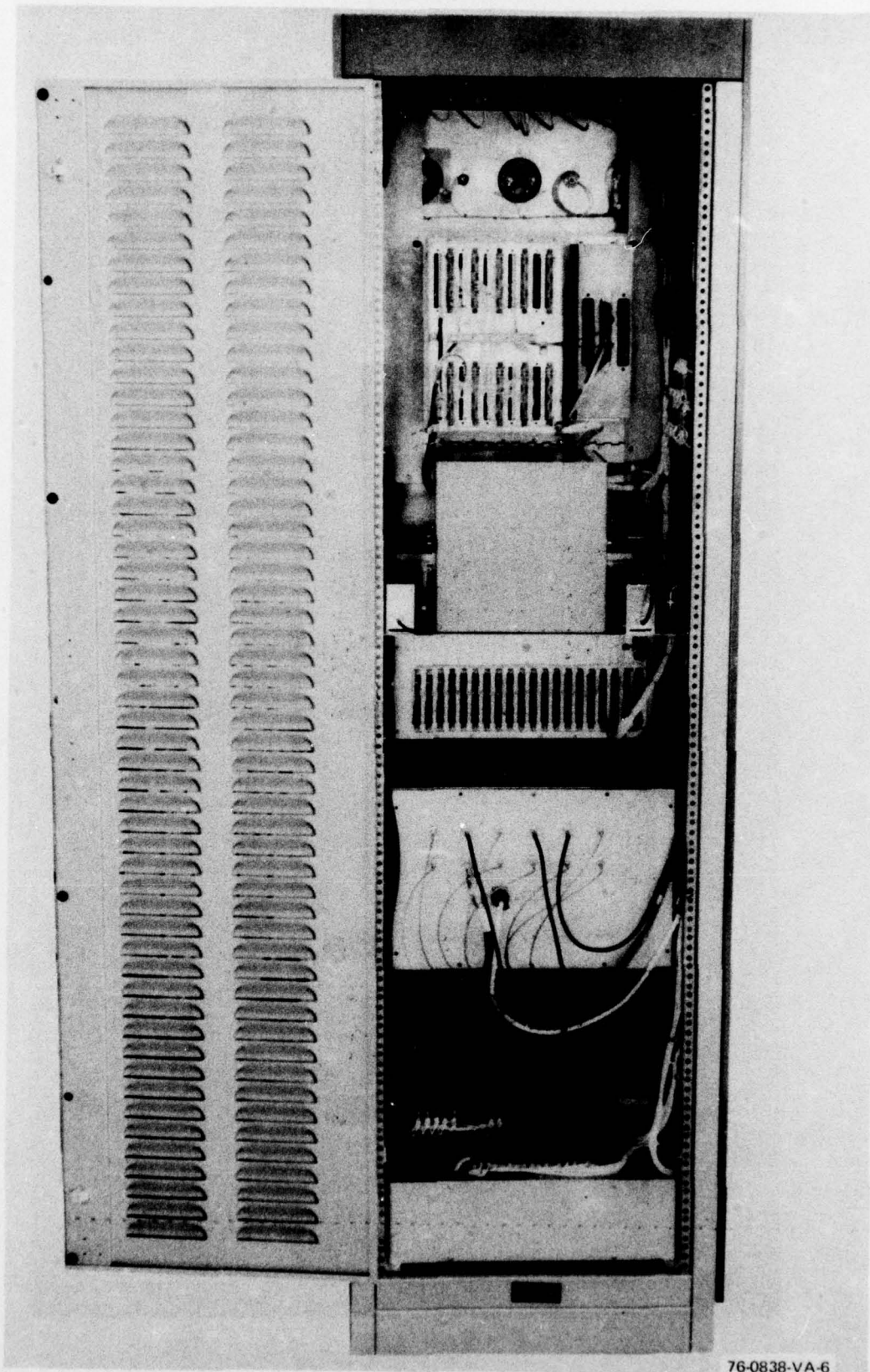


Figure 9. Monitor Cabinet

*Bank 1*



76-0838-VA-6

Figure 10. Cabinet Rear View

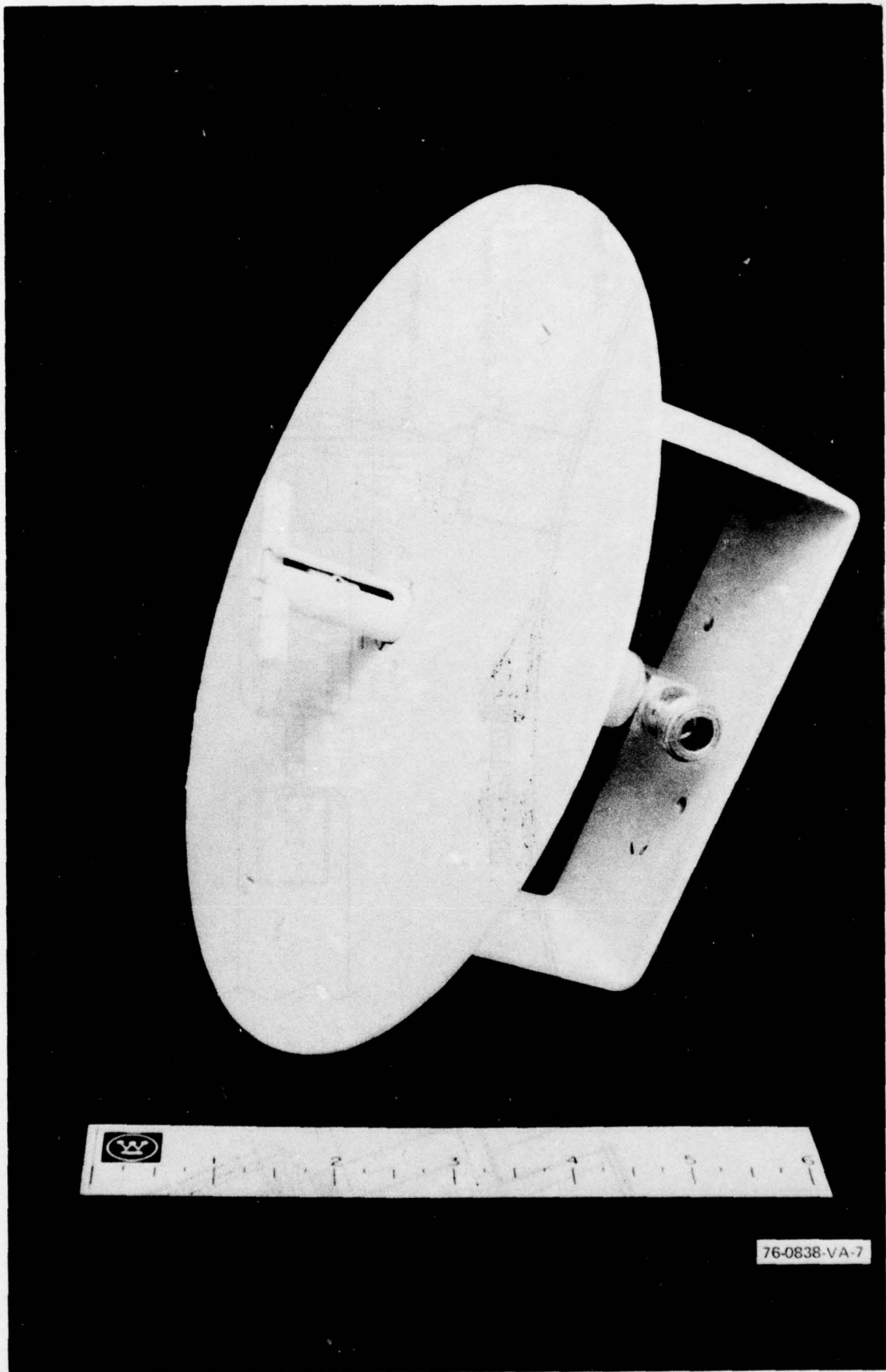


Figure 11. Monitor Antenna

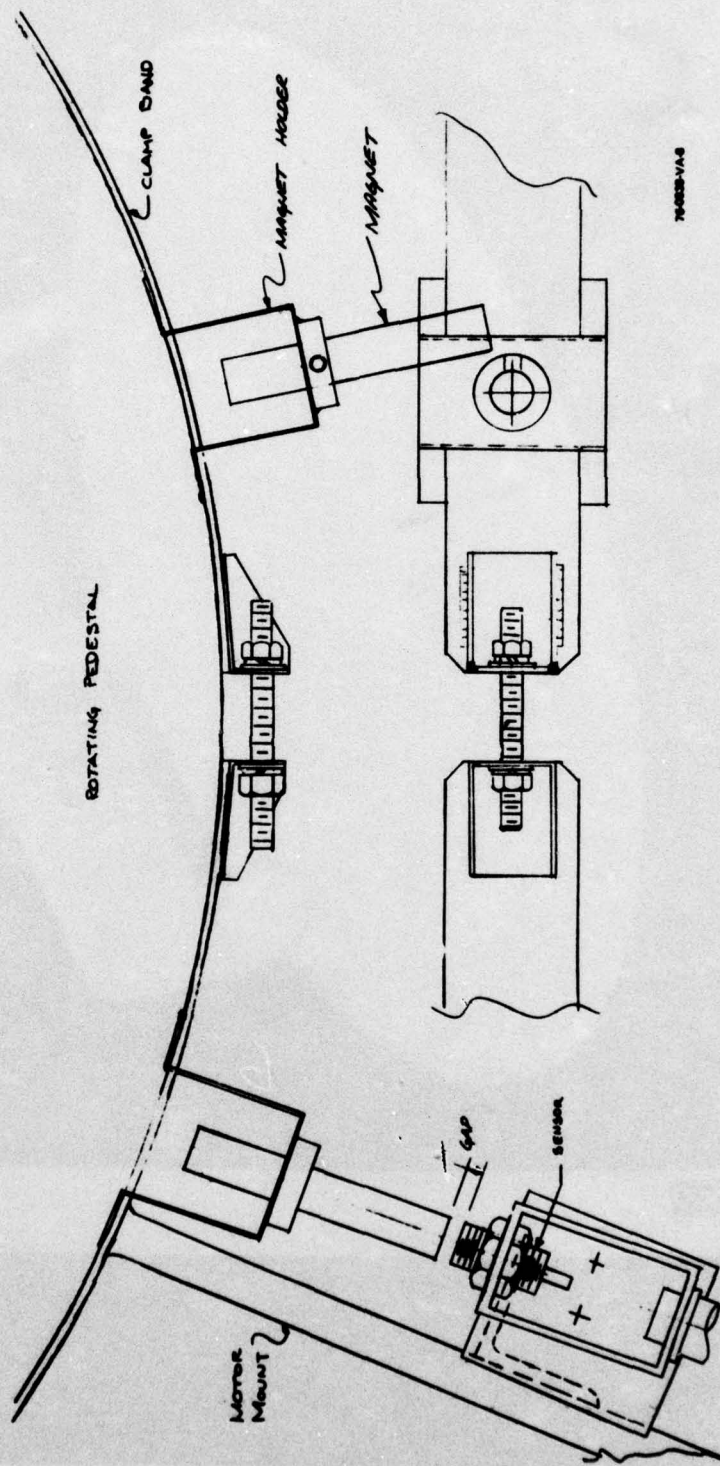


Figure 12. Azimuth Sensor Installation

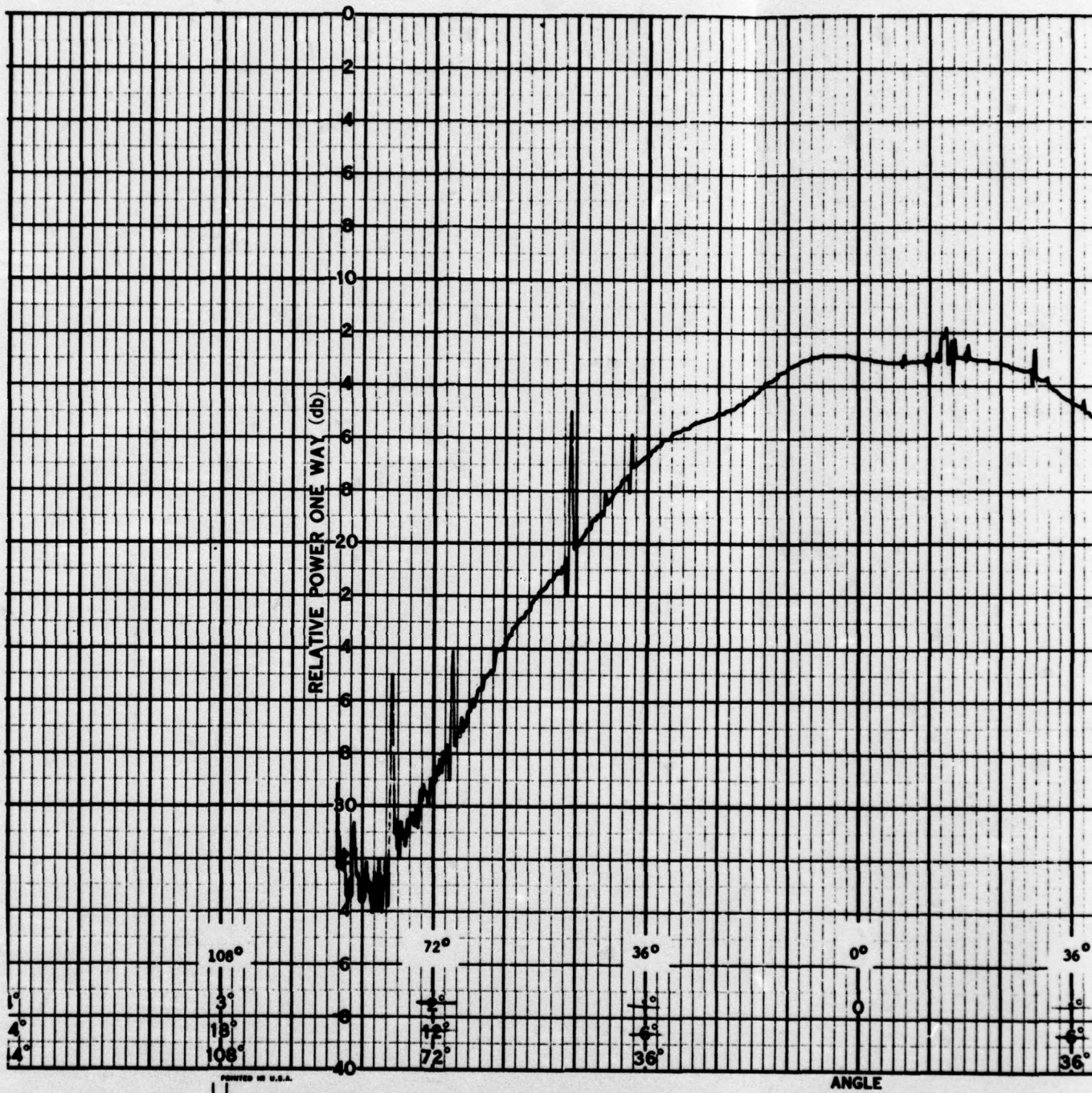
## SECTION VI

### FACTORY TESTS

The Monitor system was extensively tested in the factory before installation on the radar at NAFEC. All individual subassemblies were tested to assure that their electrical performance met the required design parameters. A composite monitor system test was conducted at the factory, and the Monitor performance per the Engineering Requirements FAA-ER-240-016 was demonstrated to the satisfaction of FAA. In addition, a 48-hour continuous operation test was conducted to assure the monitor hardware stability and reliability.

Typical subassembly test results are shown in Figure 13 and 14 for a Monitor antenna. Figure 13 is the antenna pattern measured for  $\pm 84$  degrees from its bore-sight. The 3 dB beamwidths as seen from the graph, is approximately 76 degrees. Figure 14 shows the VSWR measurements made on the automatic network analyzer for the same antenna.

The composite Monitor test setup was designed to exercise the Monitor functions simulating an actual connection to the radar. Figure 15 shows the Monitor composite test setup. This hook-up is equivalent to the radar field connection when the Monitor RF inputs are selected from the radar multicoupler and the transmitter is switched to the dummy load. The transmit pulse is generated by a stable S-band signal generator which is followed by a calibrated precision attenuator allowing accurate calibration of the RF input pulse to the Monitor responder. The delayed Monitor pulse is returned through the same path and through a directional coupler (equivalent to radar multicoupler) is applied to a simulated radar receiver. The receiver sensitivity control is provided to simulate receiver sensitivity degradation up to 60 dB to demonstrate the dynamic range of the responder. The frequency converter consists of a low noise TWT followed by a double balanced mixer converting the S-band signal to 30 MHz IF. The 30 MHz IF pulse is amplified in an IF receiver with 3 MHz bandwidth and linearly detected. A wide-band excess IF noise source is provided to the IF receiver to exercise the Monitor noise circuitry. The figure-of-merit tests are conducted with the excess noise attenuator at maximum and the receiver output noise level is determined by the receiver gain. The detected video pulse is applied to both the Normal and MTI video inputs of the Monitor sensor through a calibrated attenuator. The Monitor sensor evaluates the signal to noise



108°

72°

36°

0°

36°

1°  
4°  
14°

3°  
15°  
108°

12°  
72°

1°  
6°  
36°

1°  
6°  
36°

PRINTED IN U.S.A.

ANGLE

02

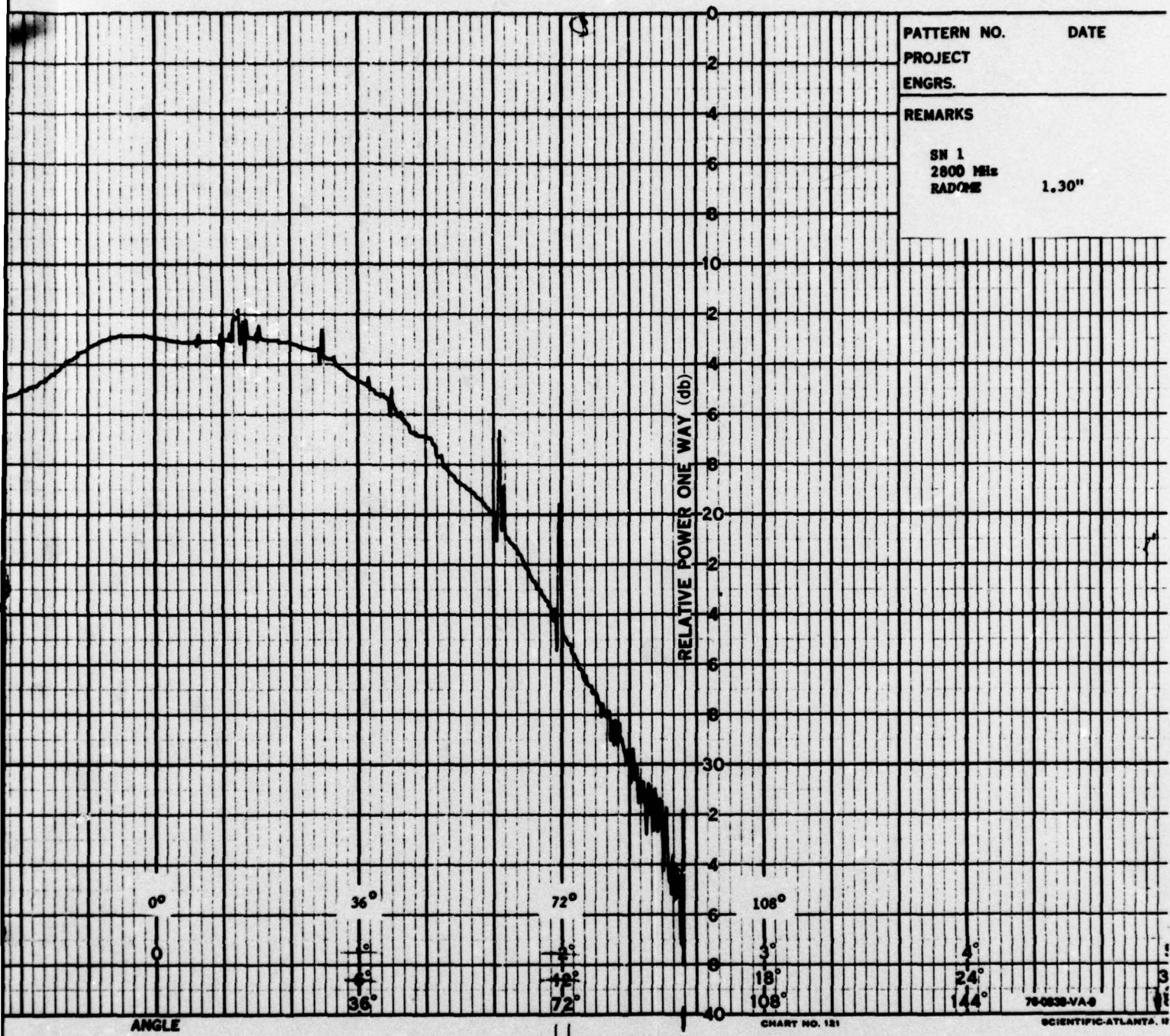


Figure 13. Monitor Antenna Pattern

6-3/6-4

2

CALIBRATION		ANTENNA	SN 1	WITH RADOME
FREQ	VSWR	FREQ	VSWR	
2700.000	1.005	2700.000	1.100	
2710.000	1.003	2710.000	1.094	
2720.000	1.004	2720.000	1.064	
2730.000	1.005	2730.000	1.062	
2740.000	1.006	2740.000	1.056	
2750.000	1.007	2750.000	1.049	
2760.000	1.006	2760.000	1.044	
2770.000	1.006	2770.000	1.046	
2780.000	1.003	2780.000	1.058	
2790.000	1.001	2790.000	1.050	
2800.000	1.003	2800.000	1.061	
2810.000	1.005	2810.000	1.089	
2820.000	1.005	2820.000	1.093	
2830.000	1.006	2830.000	1.127	
2840.000	1.002	2840.000	1.090	
2850.000	1.003	2850.000	1.104	
2860.000	1.001	2860.000	1.142	
2870.000	1.002	2870.000	1.150	
2880.000	1.003	2880.000	1.156	
2890.000	1.005	2890.000	1.147	
2899.999	1.002	2899.999	1.165	

Figure 14. Monitor Antenna VSWR

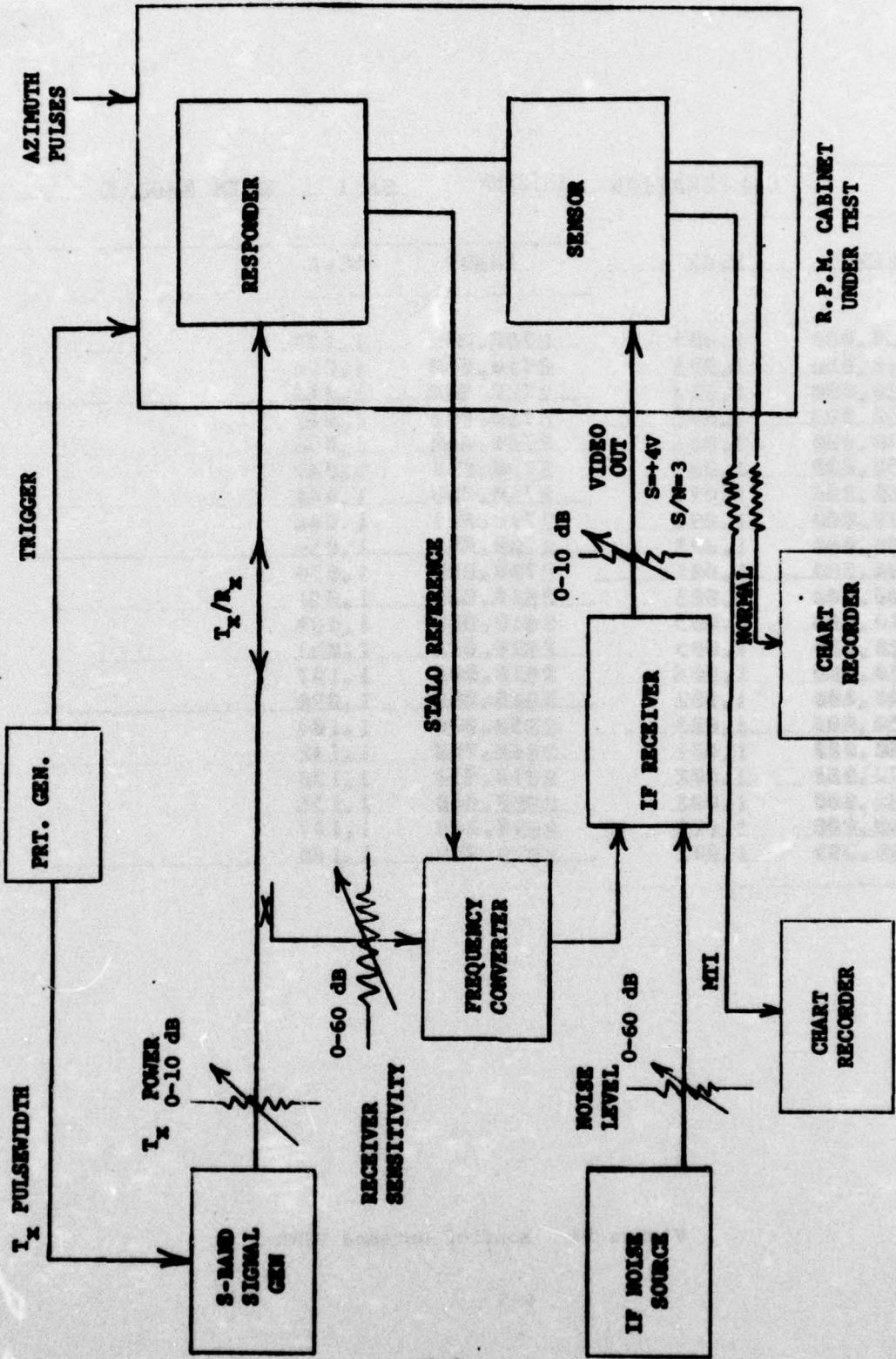


Figure 15. Factory Test Setup

ratio of the video pulse and internally applies the control voltage to the delayed pulses of the Monitor completing the loop as in actual installation on the radar. The chart recorders are connected to the sensor to record the control voltage which is used to control the delayed RF pulse amplitude on a scan-to-scan basis. Since a common video input to the sensor is used, both chart recorders can be used to assure identical performance of MTI and Normal Monitoring, or one recorder is used for the figure-of-merit resulting from the Tx power level and receiver sensitivity, and the second recorder is used to record noise, delay line insertion loss, or self-test (calibrate) as selected by front panel switch. The range synchronization is provided by a pulse generator at radar PRF. The azimuth pulses are produced by using the actual Monitor azimuth sensing hardware. One permanent magnet is attached to a variable speed motor shaft at a right angle, and the azimuth sensor is located at the proper distance from the pole of the magnet. The motor speed is adjusted to simulate the azimuth pulses at four times the radar antenna rotation rate, since four azimuths per antenna rotation are processed in the actual radar monitoring process.

The chart recorder data of Figure 16 shows the averaged scan-to-scan noise level of the simulated radar video output. The lower portion of the chart shows the noise level at nominal (calibrated) condition and the upper portion of the chart shows the noise level at an intentionally increased video gain of 1 dB, hence the noise level recorded is 1 dB higher. This noise average is used for figure-of-merit computation as well as activating the noise alarm when the threshold is exceeded. The number of samples averaged is 1024 per scan, and as seen from the recording the average is less than 0.5 dB peak-to-peak, which is sufficient for accurate figure-of-merit computation even at one scan rate.

Figure 17 shows a scan-to-scan record of the figure-of-merit using the same noise average and 32 signal-plus-noise samples. The lower portion of the chart is at nominal receiver sensitivity and the upper portion is at a 1.5 dB intentional receiver sensitivity degradation. Observation of the recording indicates proper calibration of the Monitor and excellent stability, which was demonstrated by continuous recording for 48 hours. However, the

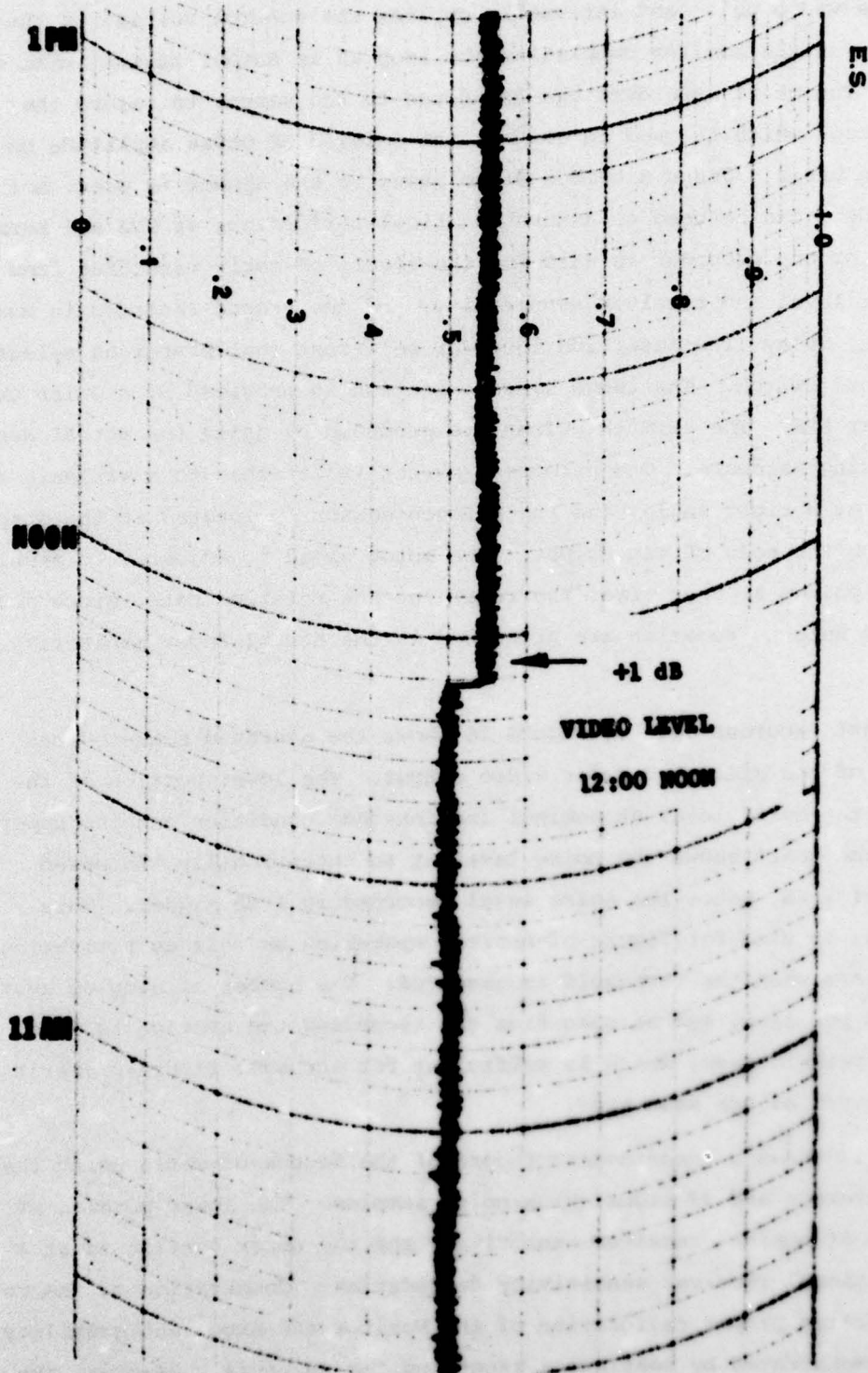


Figure 16. Average Simulated Noise

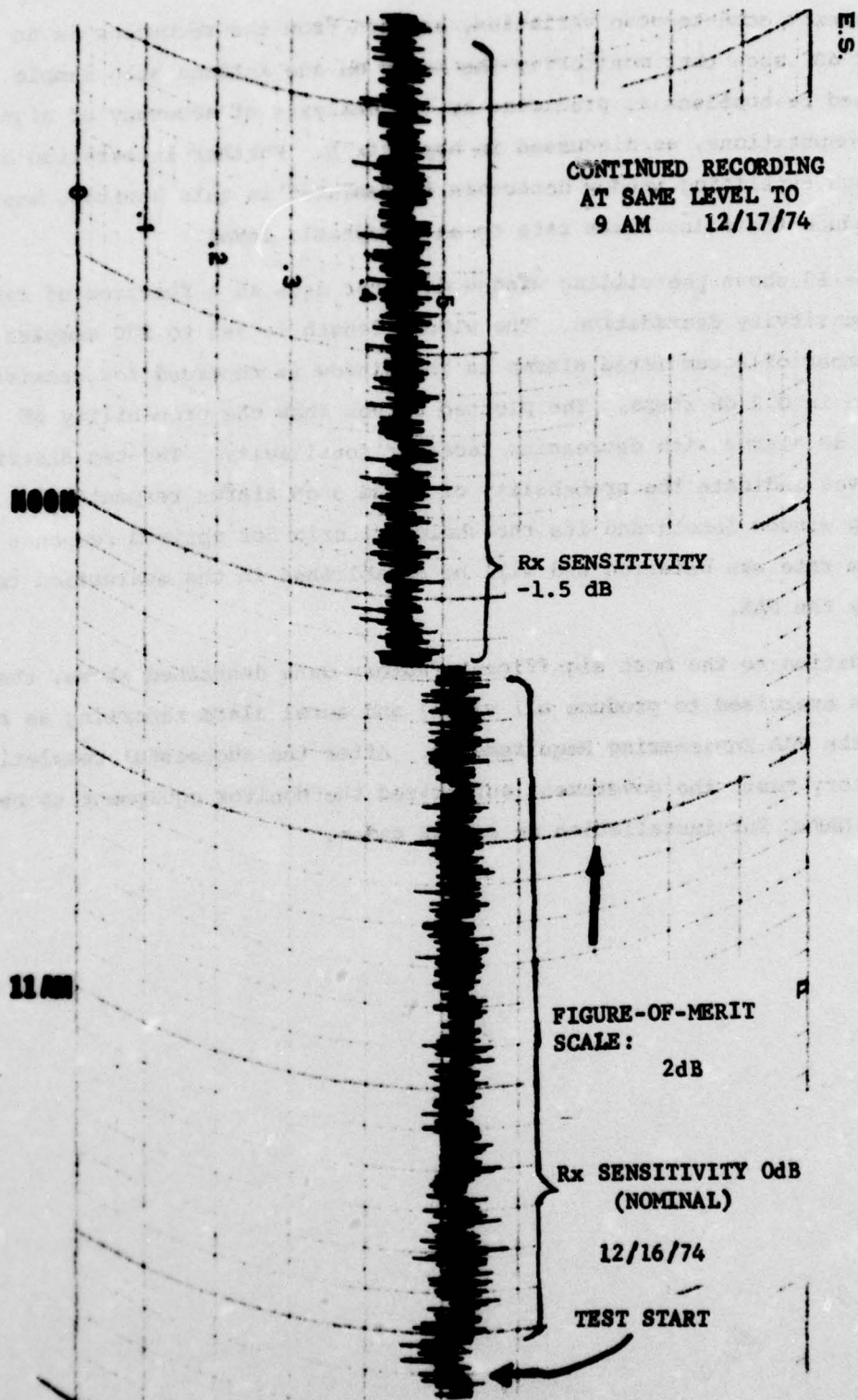


Figure 17. Figure-of-merit

figure-of-merit scan-to-scan variation, as seen from the recording is an order of 2 dB, such that monitoring the radar on one antenna scan sample would indeed be hopeless as predicted by the analysis of accuracy of signal-to-noise computations, as discussed in Appendix A. Further integration of the alarms, such as sliding window detectors implemented in this Monitor, must be used to reduce the false alarm rate to an acceptable level.

Figure 18 shows the sliding window detector data as a function of radar receiver sensitivity degradation. The window length is set to 200 samples, and the number of accumulated alarms in the window is recorded for receiver degradation in 0.2 dB steps. The plotted curves show the probability of 2 dB and 3 dB alarms with decreasing receiver sensitivity. The two distribution curves indicate the probability of 2 and 3 dB alarms respectively. The sliding window length and its threshold criteria for optimum response time/false alarm rate was deferred and will be established in the evaluation tests at NAFEC by the FAA.

In addition to the most significant factory data described above, the Monitor was exercised to produce all visual and aural alarm reporting as required by the FAA Engineering Requirements. After the successful completion of the factory tests the government authorized the Monitor equipment to be shipped to NAFEC for installation on an ASR radar.

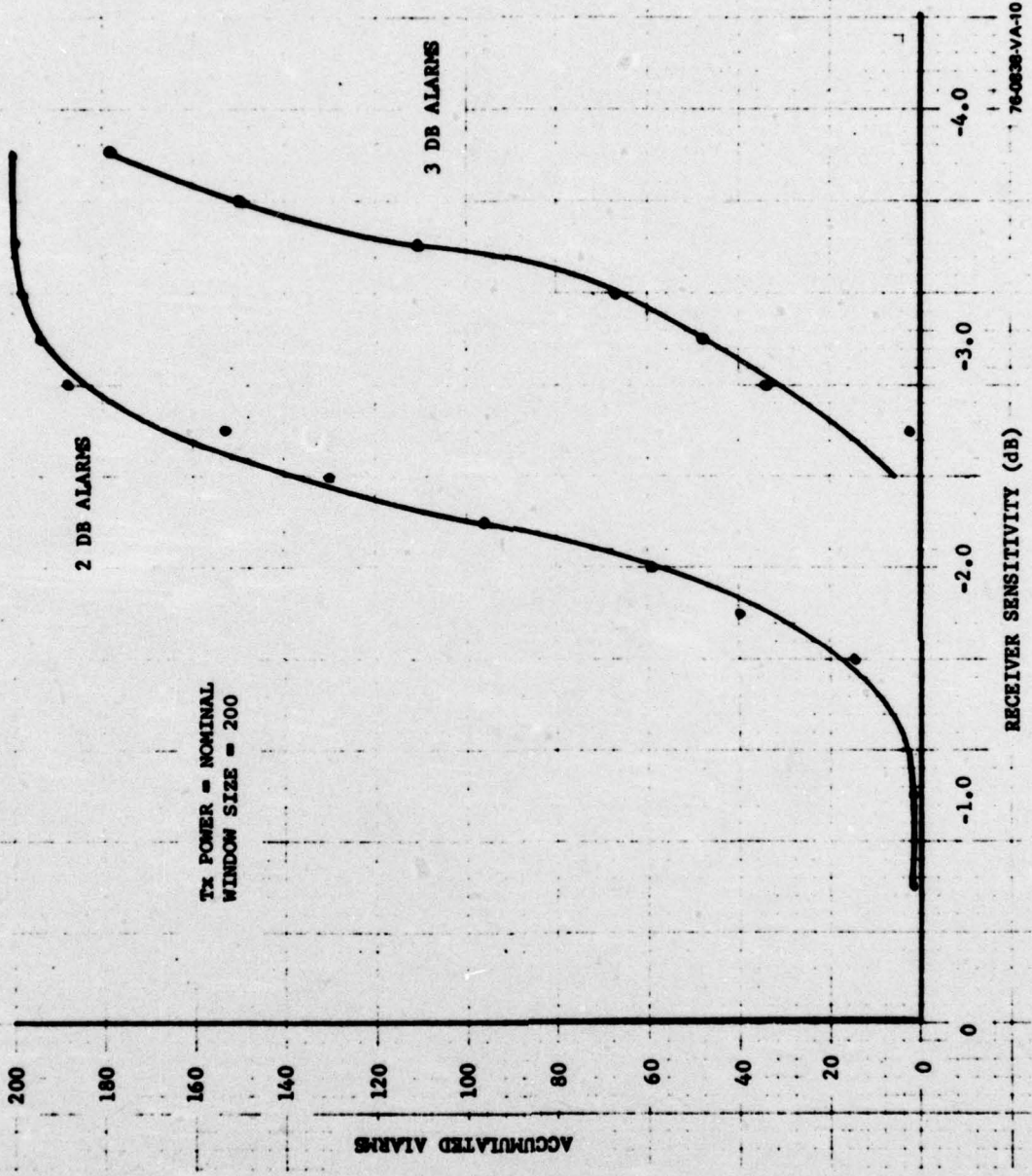


Figure 18. Sliding Window Detector Data

6-11/6-12

## SECTION VII

### FIELD TESTS

The Monitor was connected as shown in Figure 1 to the ASR-5 radar at NAFEC, New Jersey. The preliminary checkout of the Monitor was accomplished on the ASR-5 radar by varying the radar performance parameters. The radar receiver sensitivity degradation was simulated by inserting calibrated attenuation levels at the input to the parametric amplifier. The average transmit power was monitored with an RF voltmeter at the radar multicoupler and the transmitter high voltage was adjusted to vary the transmitter output power. Independent radar video noise measurement was instrumented to verify noise measurements made by the Monitor. To collect the alarm data two chart recorders (one for MTI and one for Normal channel) were connected to the scan-to-scan outputs of the Monitor as in factory tests. Latching alarm indicators were connected to the Monitor summary alarm outputs to store the alarms when the equipment operated unattended.

The preliminary tests with either of the two ASR-5 radar channels indicated extremely high variations of the radar video output noise (in order of  $\pm 6$  dB). The greatest variation was observed during the high level of activity hours at the site. It was determined, by observation of radar noise recorded on the Monitor and independent metering of the radar video noise, that the noise variations were caused by the vibration of radar components, especially the parametric amplifier and MTI canceller. In addition, the MTI video noise texture was extremely coarse. Observation of MTI video noise on a single radar sweep time-base indicated a complete absence of noise or a high level spike for a given range cell. The ASR-5 radar was used to check out the Monitor channel switching, Monitor antenna calibration and other tests, but since the figure-of-merit measurement is based on a good radar noise sample, no meaningful figure-of-merit data could be obtained due to unpredictable radar video noise output.

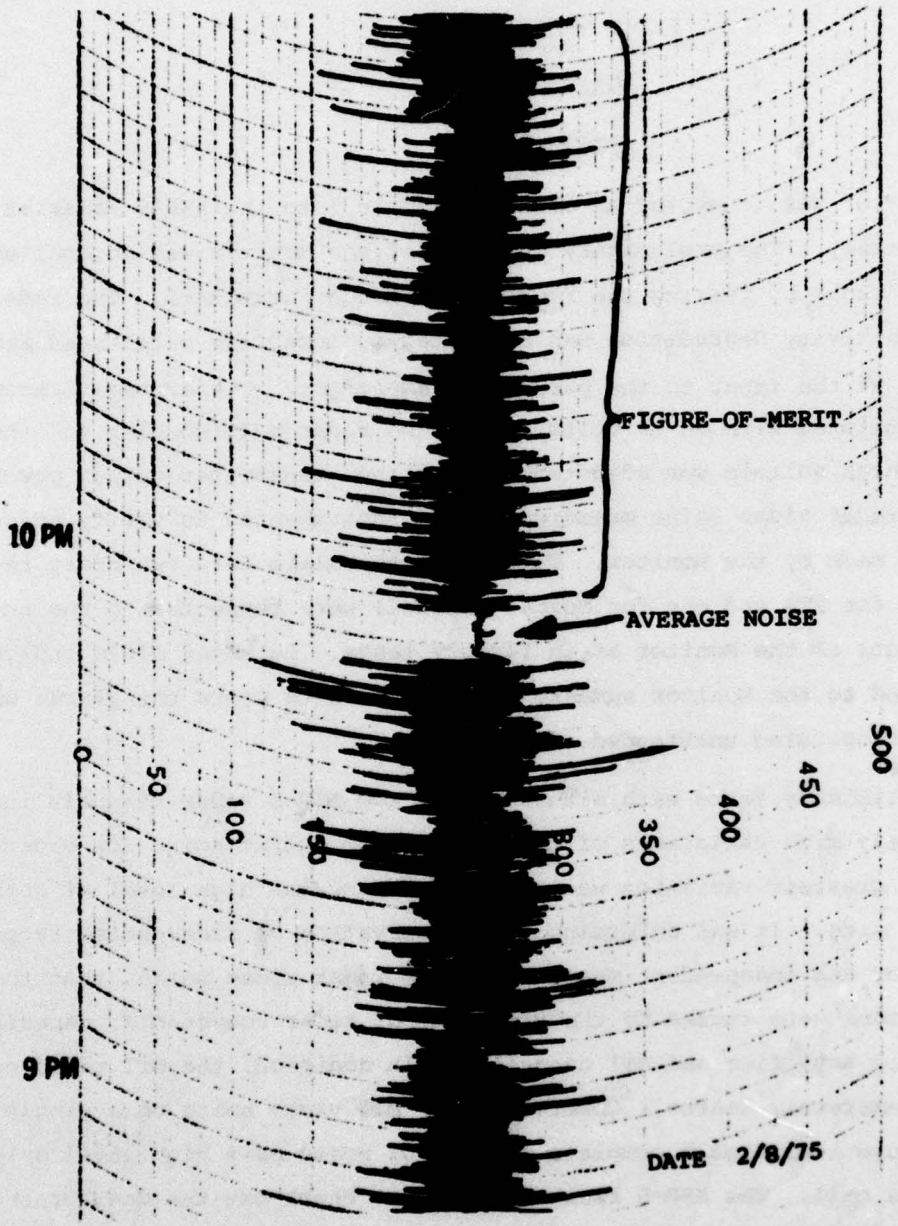


Figure 19. ASR-7 Normal Figure-of-Merit/Noise

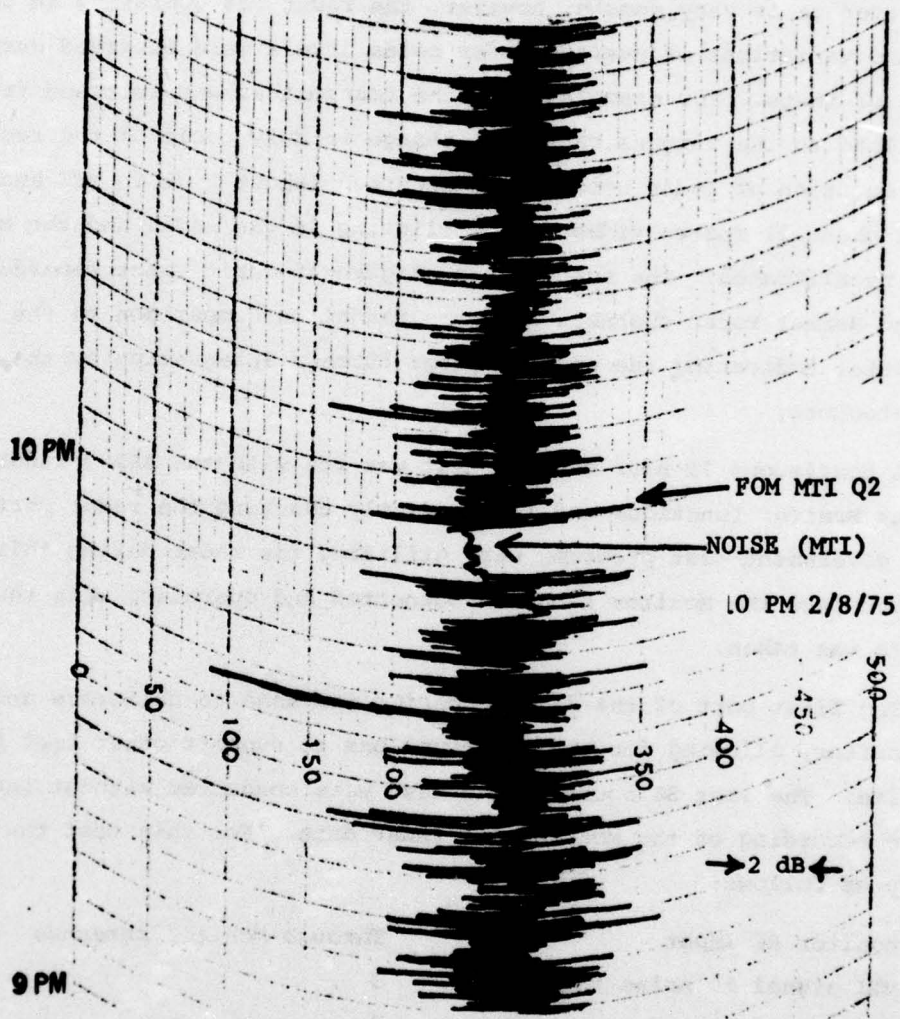


Figure 20. ASR-7 MTI Figure-of-merit/Noise

At the direction of the government the Monitor was connected to the ASR-7 radar located at the same site. Figure 19 shows a scan-to-scan chart record of ASR-7 Normal channel figure-of-merit and average noise. Figure 20 shows the same parameters recorded for the MTI channel. The scale in all cases is 2 dB per large division. As seen from these two chart records, the noise average is very smooth, however, the radar was operating in the non-CFAR mode and variations of average radar noise levels were observed during the course of tests. For example, when the transmitter was switched from the dummy load to the antenna causing a change in duty cycle of the received signal, reduction of radar noise level occurred (about 2 dB in MTI and 6 dB in Normal channel) due to video bottom clipping in the radar and the Monitor had to be recalibrated. The scan-to-scan figure-of-merit chart records for both MTI and Normal radar channels are more random in comparison to the factory test data, indicating the necessity for further integration by the sliding window detectors.

A continuous 72-hour Monitor test was run with the ASR-7 radar exercising various Monitor functions and independently checking the radar performance. Other government test programs were utilizing the radar during this test period, in which case the Monitor remained connected and operating with the radar but no data was taken.

The first part of the 72-hour period was used to calibrate and exercise the Monitor, allowing for the interruptions to support other test programs at the site. The last 36 hours of the test were conducted without interruptions in the recording of the Monitor and radar data. For this test the Monitor was set up as follows:

Monitor RF Input	Through Monitor antennas
MTI signal to noise ratio	3
Normal signal to noise ratio	3
MTI target range	300 microseconds
Normal target range	620 microseconds
RMS noise thresholds	2 dB
RMS noise alarms	6 scans
Fast alarm	16 scans
Fast alarm reset	1 scan

SWD, quadrant 1	Window = 200
	Threshold = 100
SWD, quadrant 2	Window = 100
	Threshold = 50
SWD, quadrant 3	Window = 50
	Threshold = 25
SWD, quadrant 4	Window = 25
	Threshold = 13

Figures 21 through 27 show the data collected for the Normal channel during the test period. Figures 21 to 24 are the outputs from the sliding window detectors showing the number of scan-to-scan alarms present in SWD windows for quadrants 1 through 4 recorded at half-hour intervals. The data was collected at nominal radar performance with an intentional radar sensitivity reduction at the end of the test. The thresholds for each SWD are indicated on each plot. In general, the data for all four quadrants is consistent and becoming more random when the window size gets smaller, as expected. For the window length of 25 the 2 dB alarms and 3 dB alarms are seen overlapping. The estimated average of 2 dB alarms for the test run at nominal radar performance is 10-14% with maximum alarms in the window not exceeding 22%. The average for 3 dB alarms is about 3% with maximum not exceeding 4%. Figure 25 is the sliding window (200) detector outputs recorded at one minute intervals. Figure 26 is scan-to-scan figure-of-merit data for quadrant 2, recorded on a chart recorder during the test period. The plot is an estimated average figure-of-merit from the chart record. The independent radar checks were also recorded at half-hour intervals and are shown in Figure 27. The transmit power and receiver noise figure checks are consistent and sufficiently accurate to indicate radar performance, however, the MDS and video noise measurements, by conventional means available at the radar site, are not sufficiently accurate to be used as a reference for the Monitor. In general, a survey of the Normal channel plotted data indicate stable and accurate Monitor performance, and no figure-of-merit alarms are occurring during the test at nominal radar performance.

Simultaneously with the Normal channel data, the same set of data was taken for the MTI channel, and the results are plotted in Figures 28 through 34. The examination of results show large, slowly changing variations of accumulated

alarms in all MTI sliding windows. Quadrant 3 is seen alarming at 0630 hours. This drift effect was investigated and found to be caused by the MTI radar amplitude quantizing error. The MTI radar gated clock rate was periodically checked and is shown in Figure 35 in percent of its average rate. The clock change shown in the plot results in about 0.5 microsecond apparent range variation for a Monitor test target at 300 microseconds. This was also confirmed by period observation of MTI video delay with respect to the Monitor sample gate. The Monitor sampling of the radar videos was designed for a constant radar processing delay as in ASR-5 radar, which has a delay line type MTI. For the ASR-7 the Monitor sample gate was adjusted to sample the MTI video range cell with the highest target amplitude, but this was varying as a function of the MTI gated clock and resulting in erroneous figure-of-merit variation.

Since considerable redesign effort was required to compensate for the ASR-7 MTI sampling loss, the tests were continued, and the Monitor concluded the tests without failure. The equipment was accepted by the government for further evaluation.

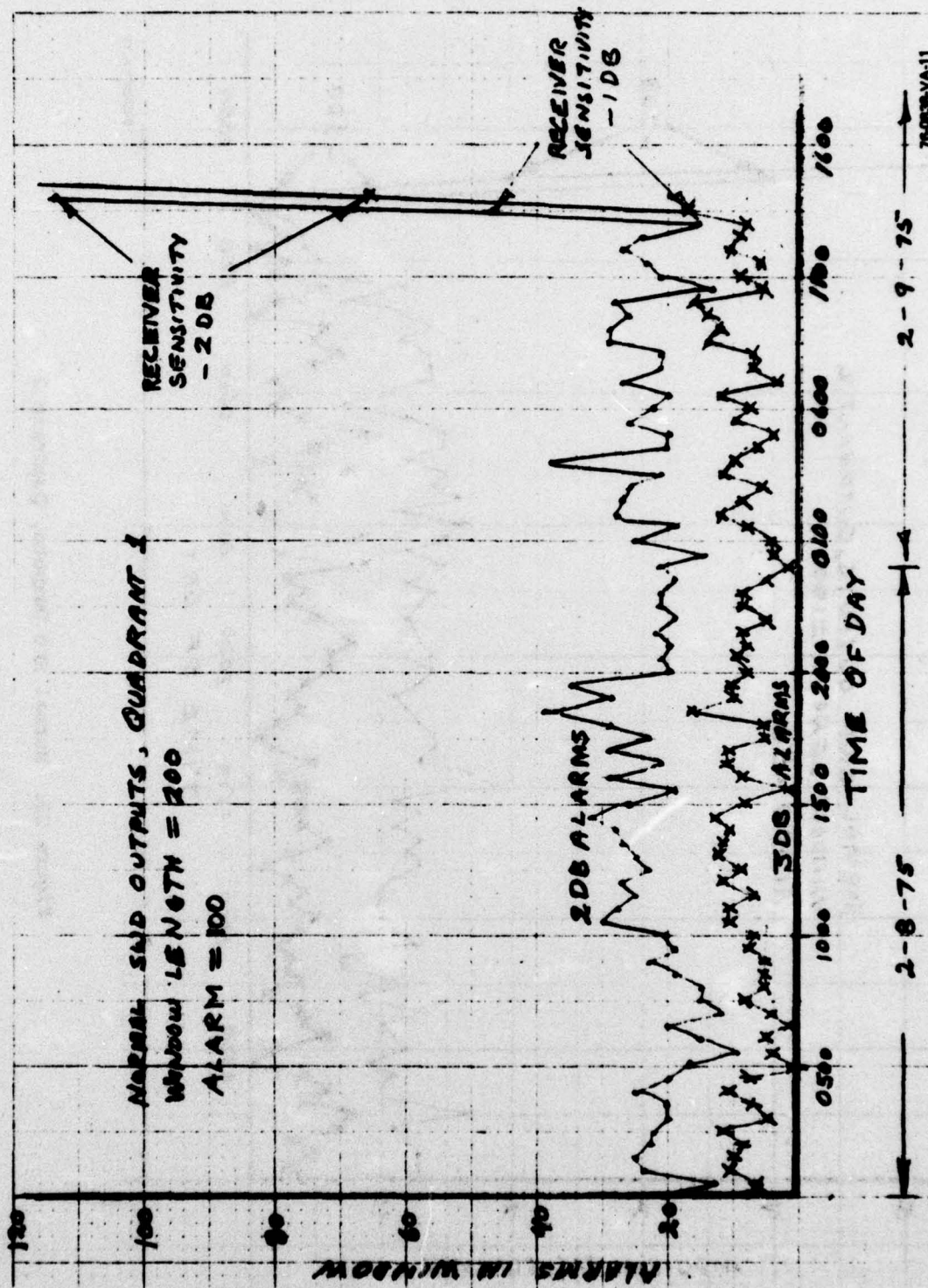


Figure 21. Normal SWD Outputs, Quadrant 1

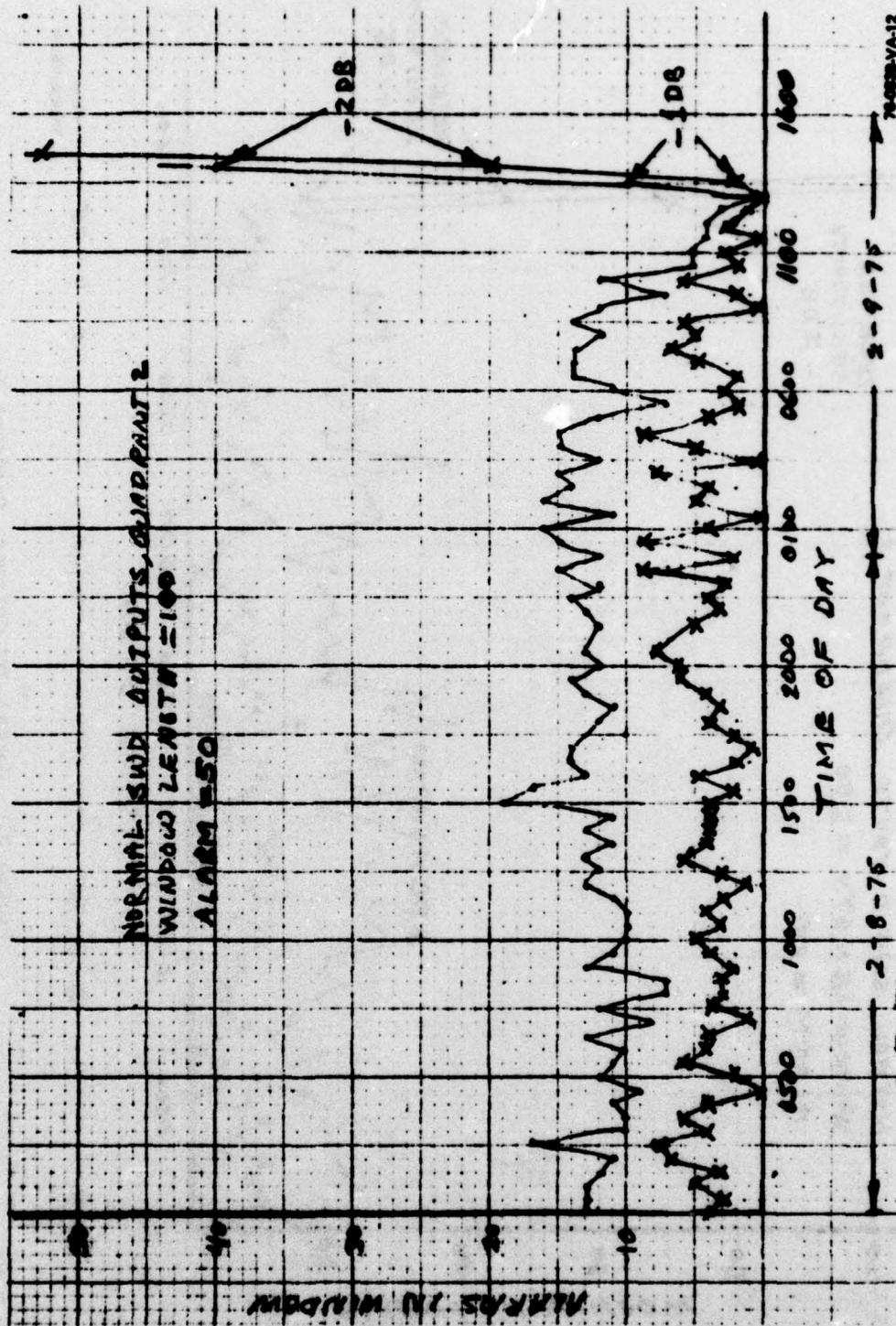


Figure 22. Normal SMD Outputs, Quadrant 2

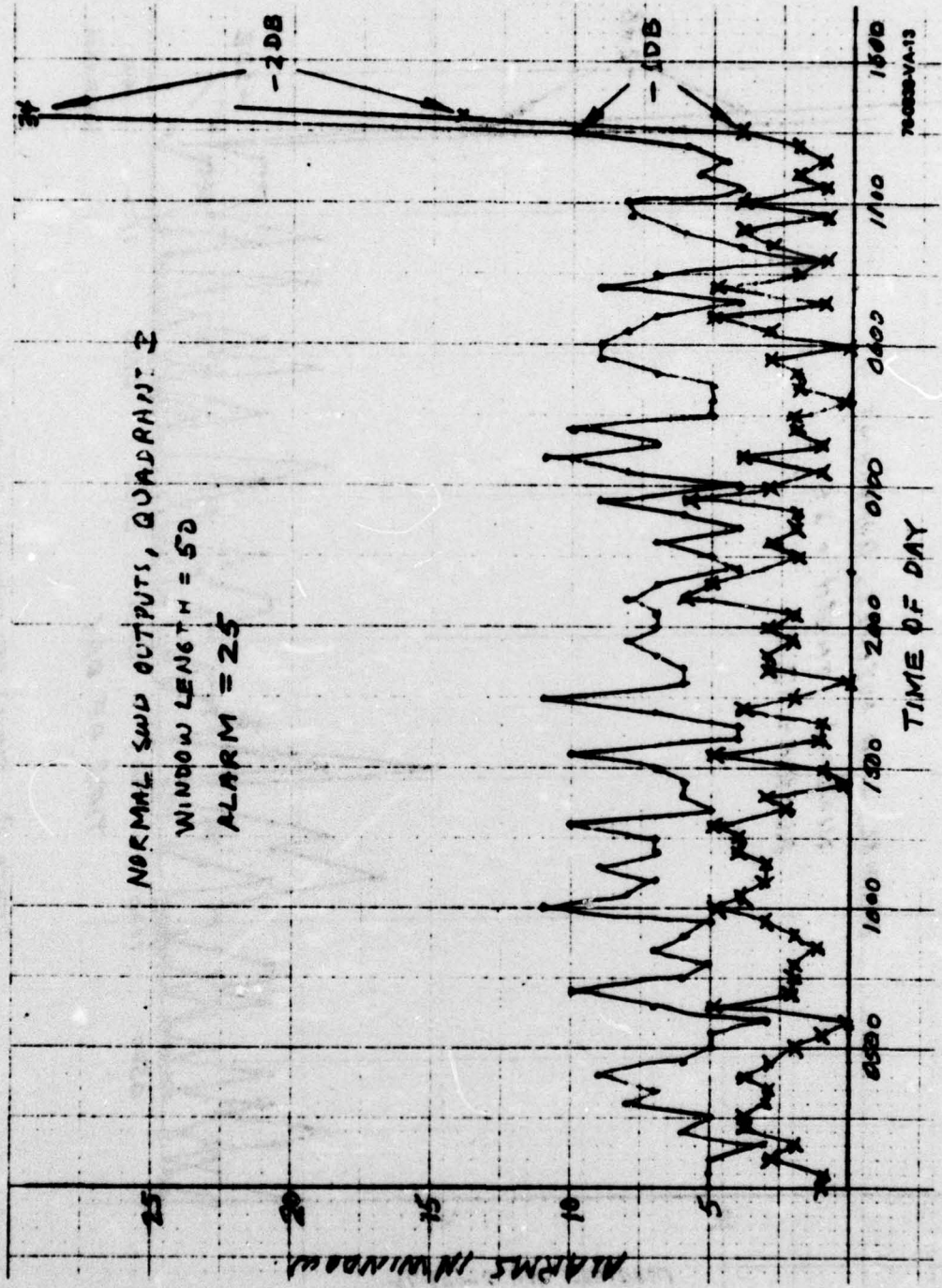


Figure 23. Normal SWD Outputs, Quadrant 3

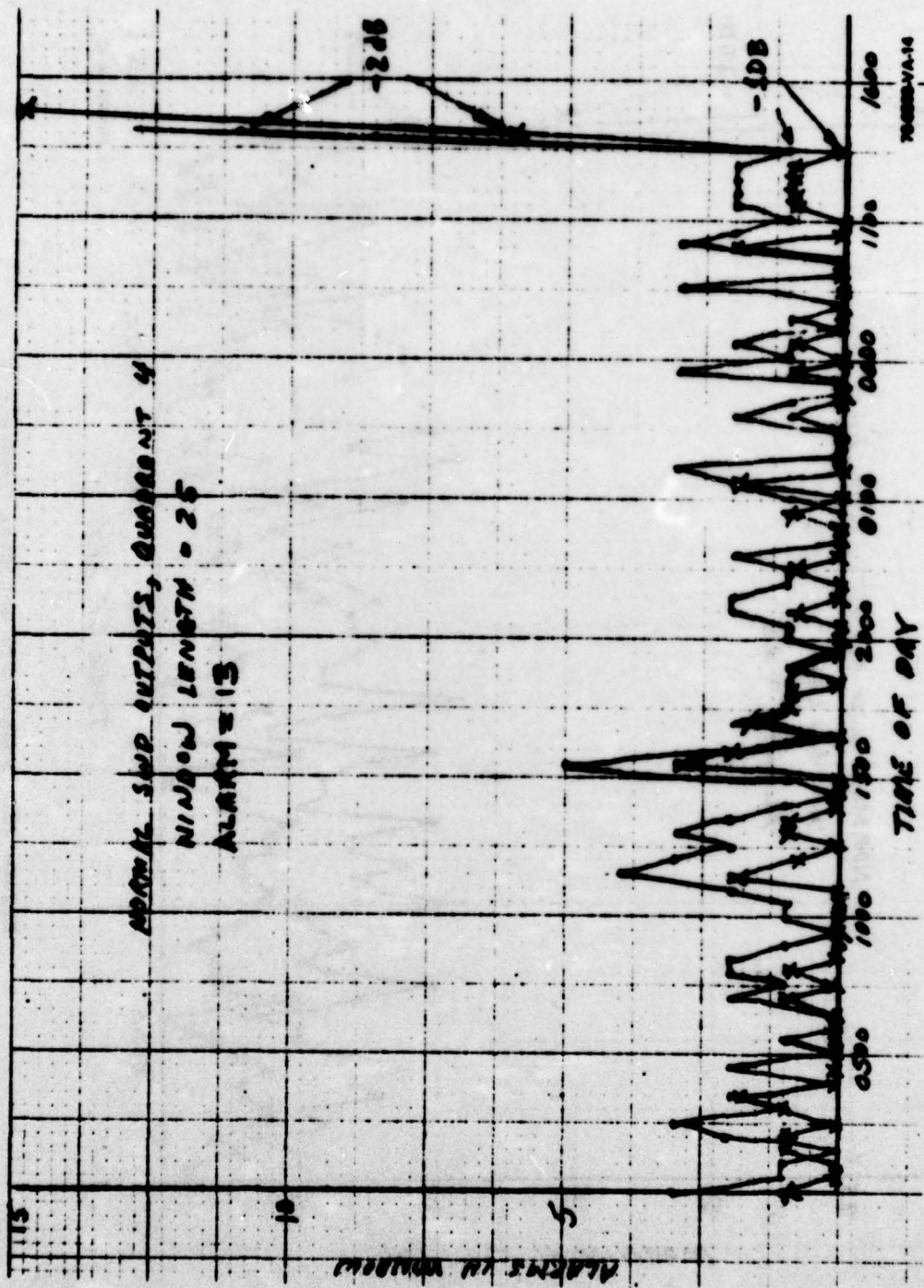


Figure 24. Normal SMD Outputs, Quadrant 4

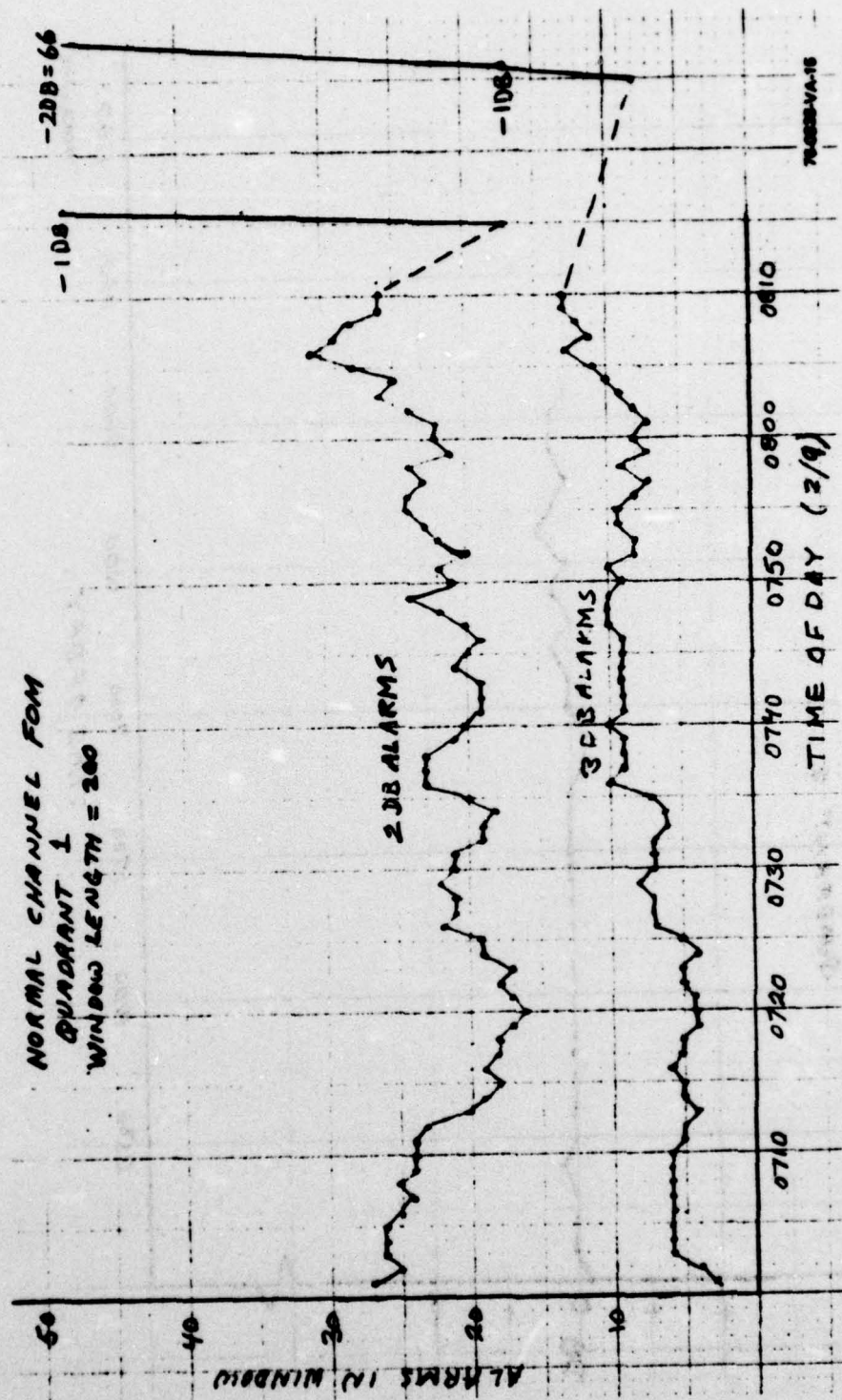


Figure 25. Normal Channel Figure-of-Merit

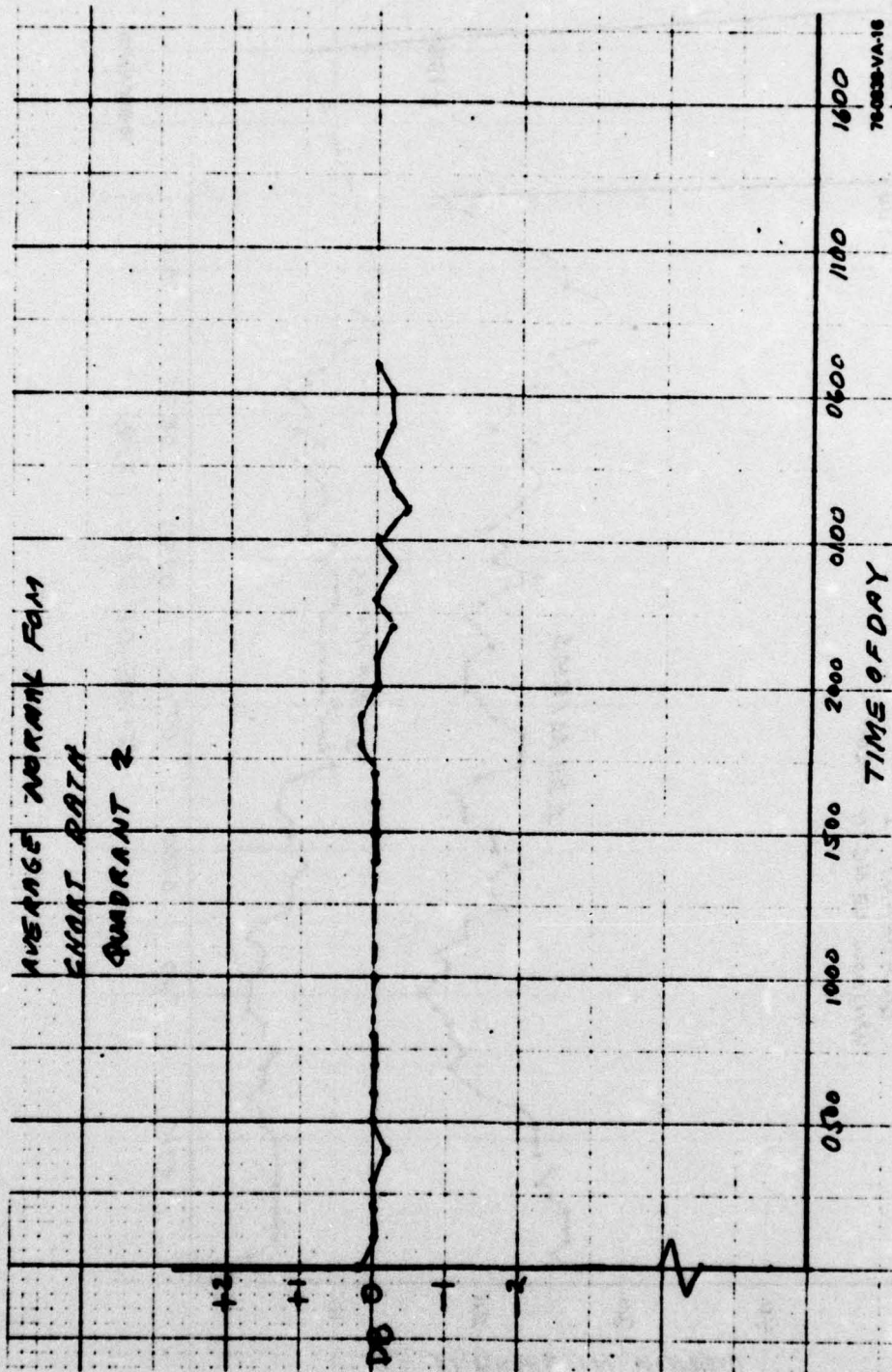


Figure 26. Average Normal Figure-of-Merit Chart Data

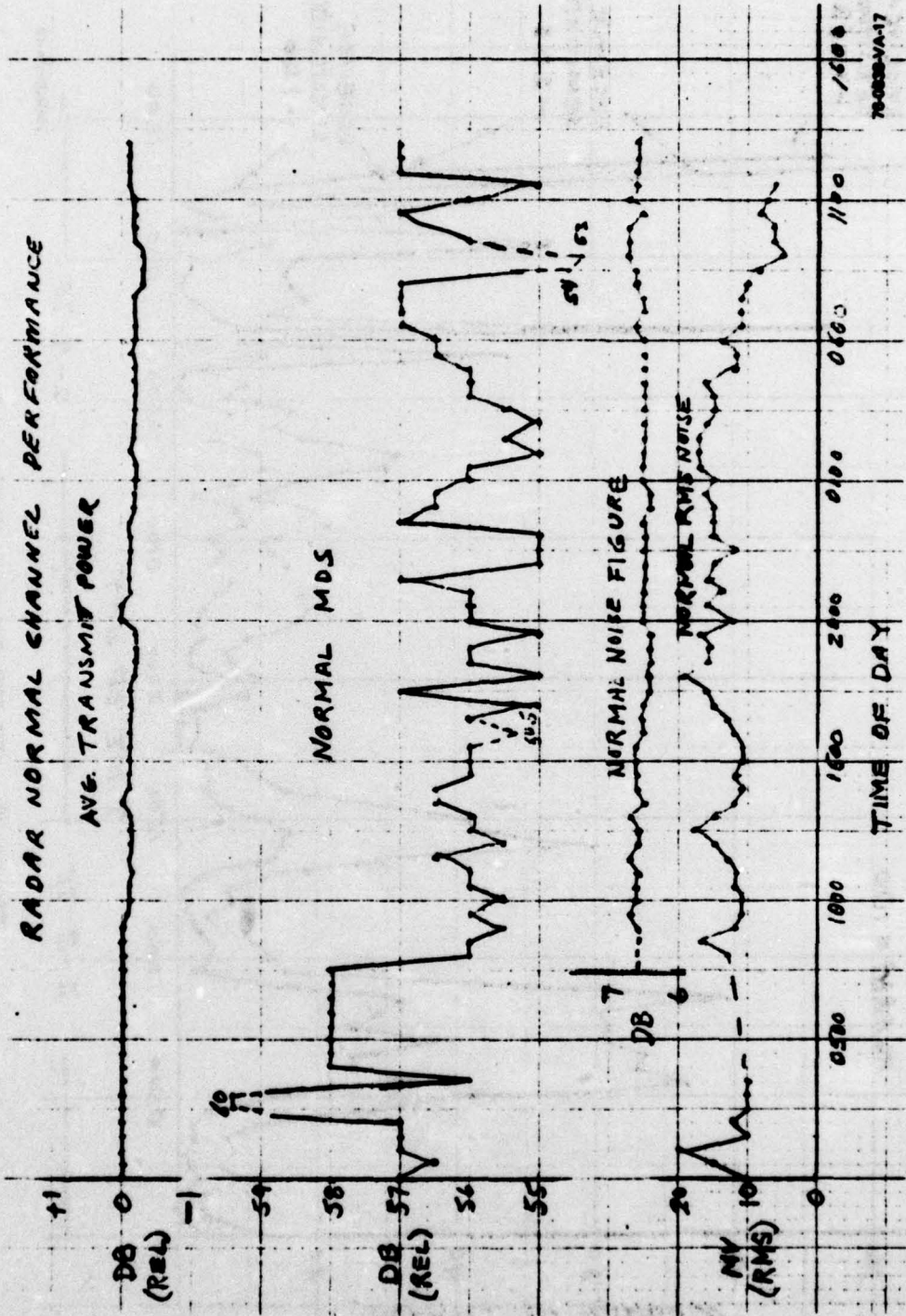


Figure 27. Radar Normal Channel Performance

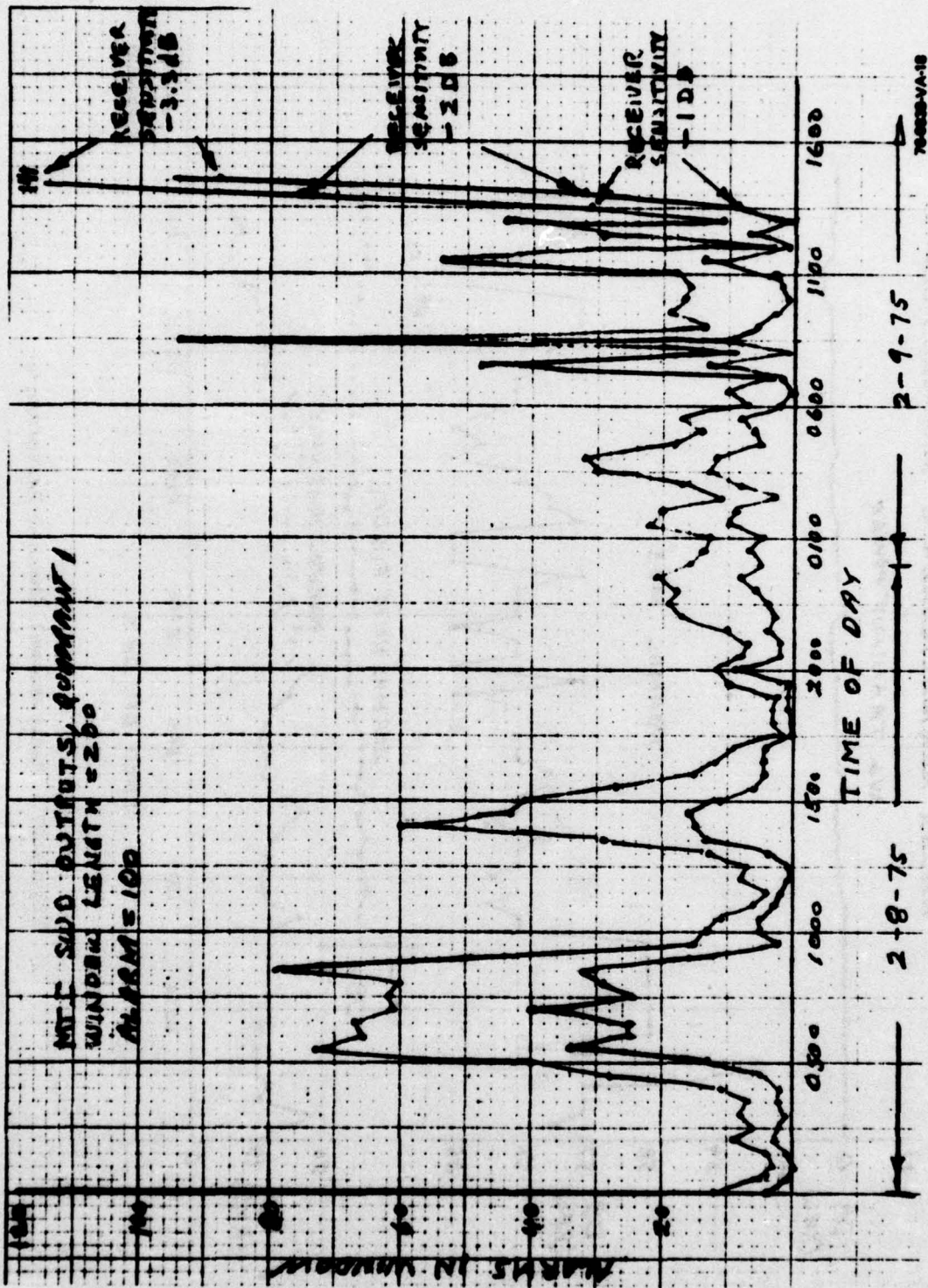


Figure 28. MTI SMD Outputs, Quadrant 1

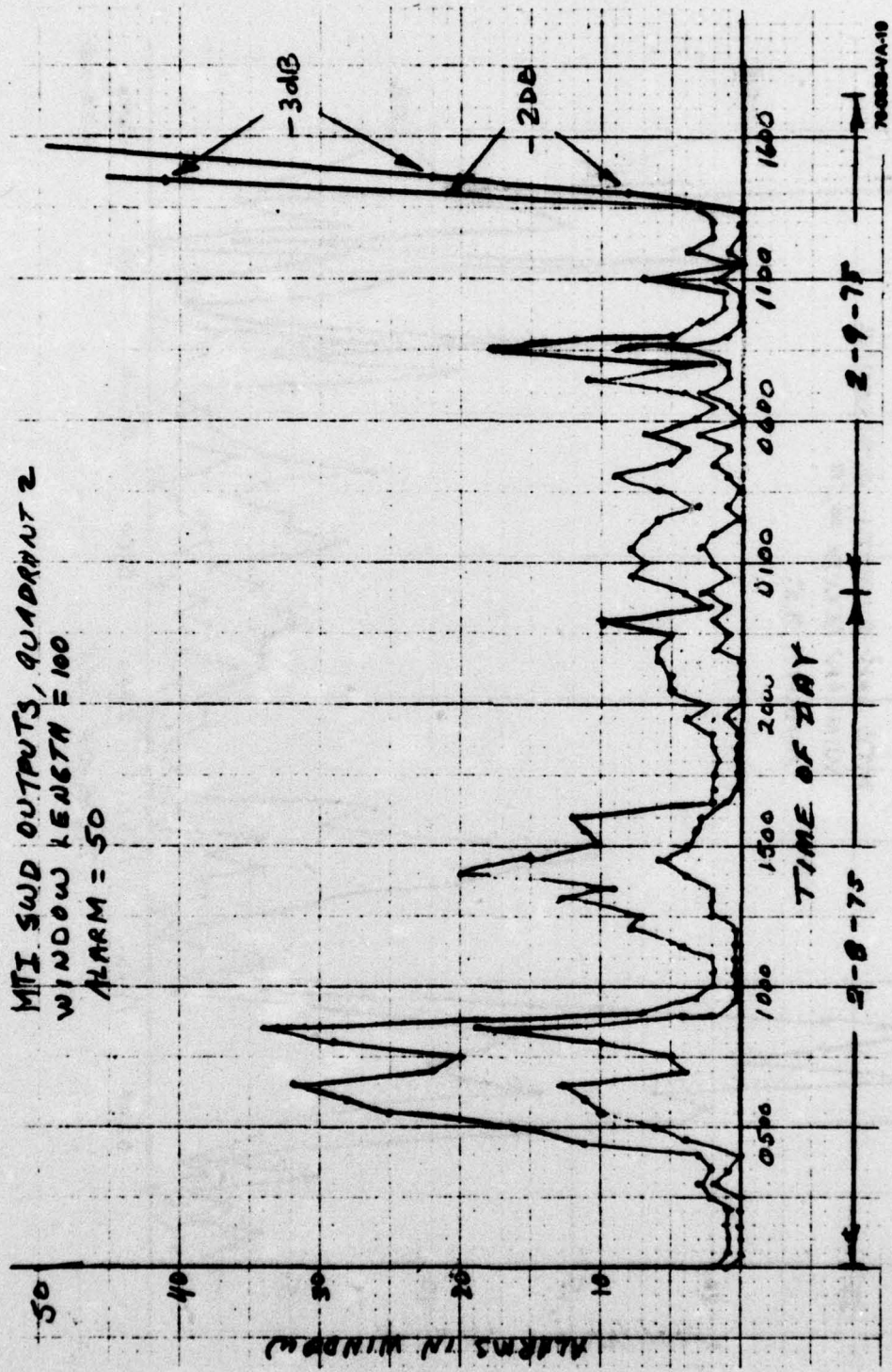


Figure 29. MTI SWD Outputs, Quadrant 2

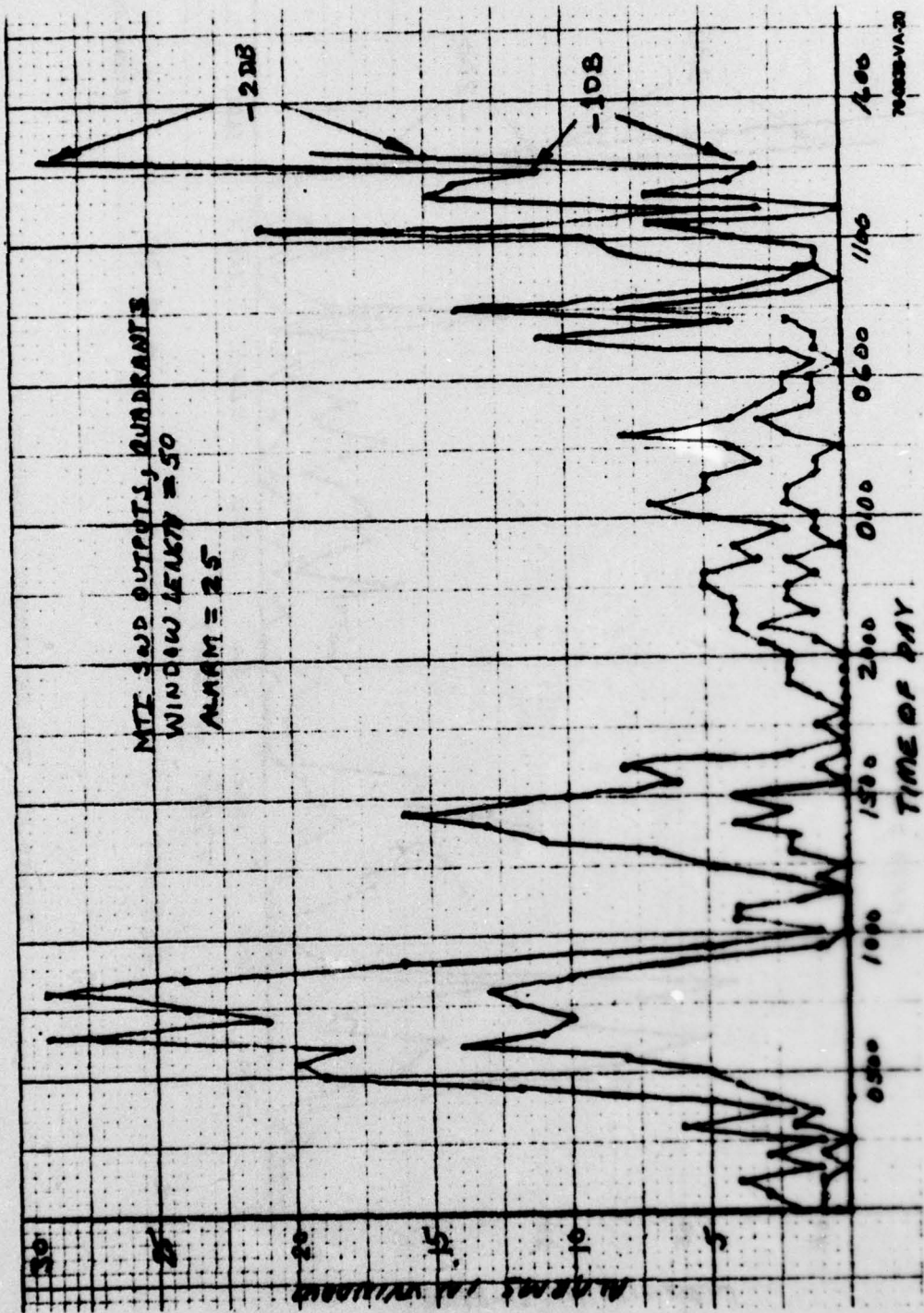


Figure 30. MTE SMD Outputs, Quadrant 3

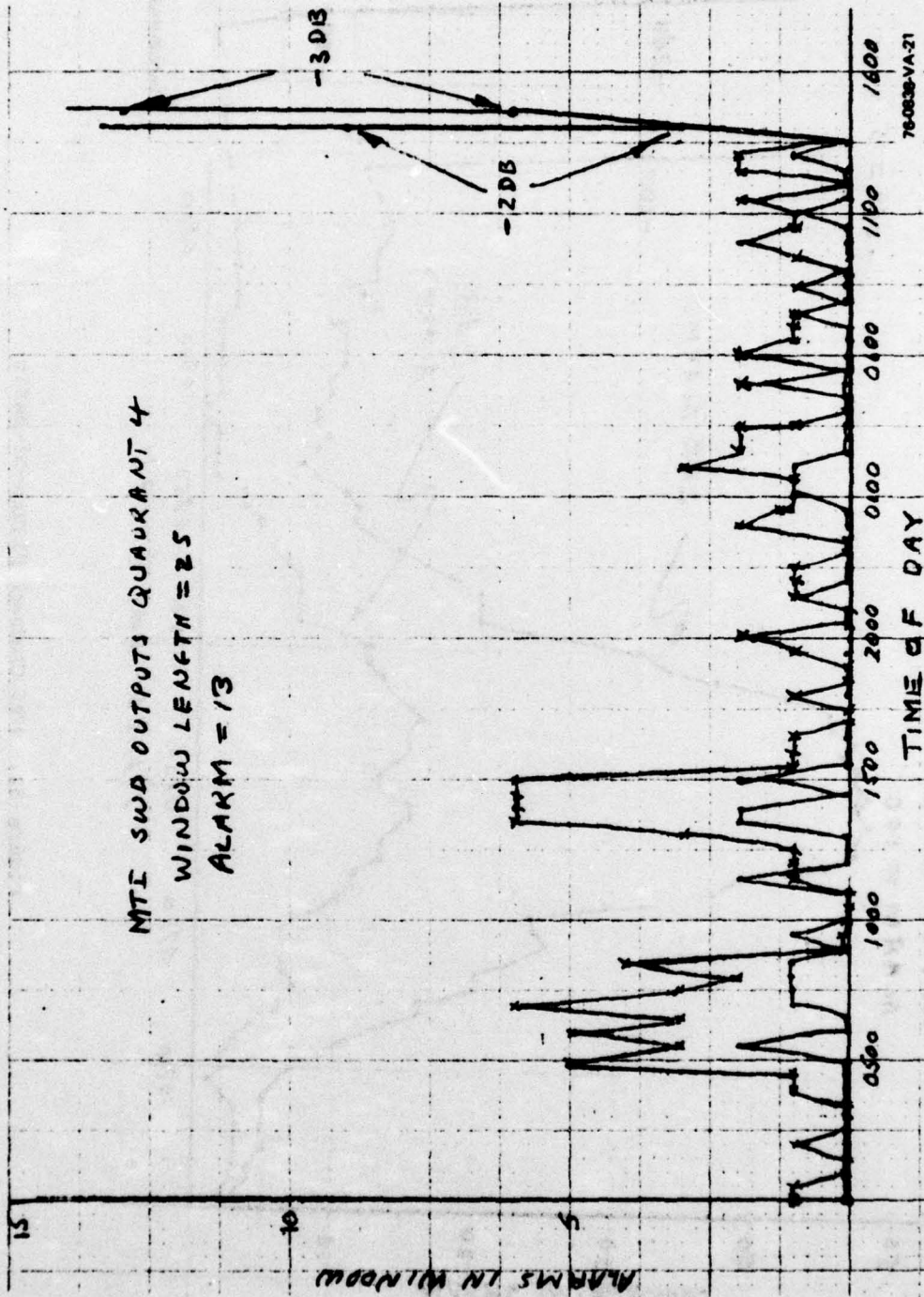


Figure 31. MTE SWD Outputs, Quadrant 4

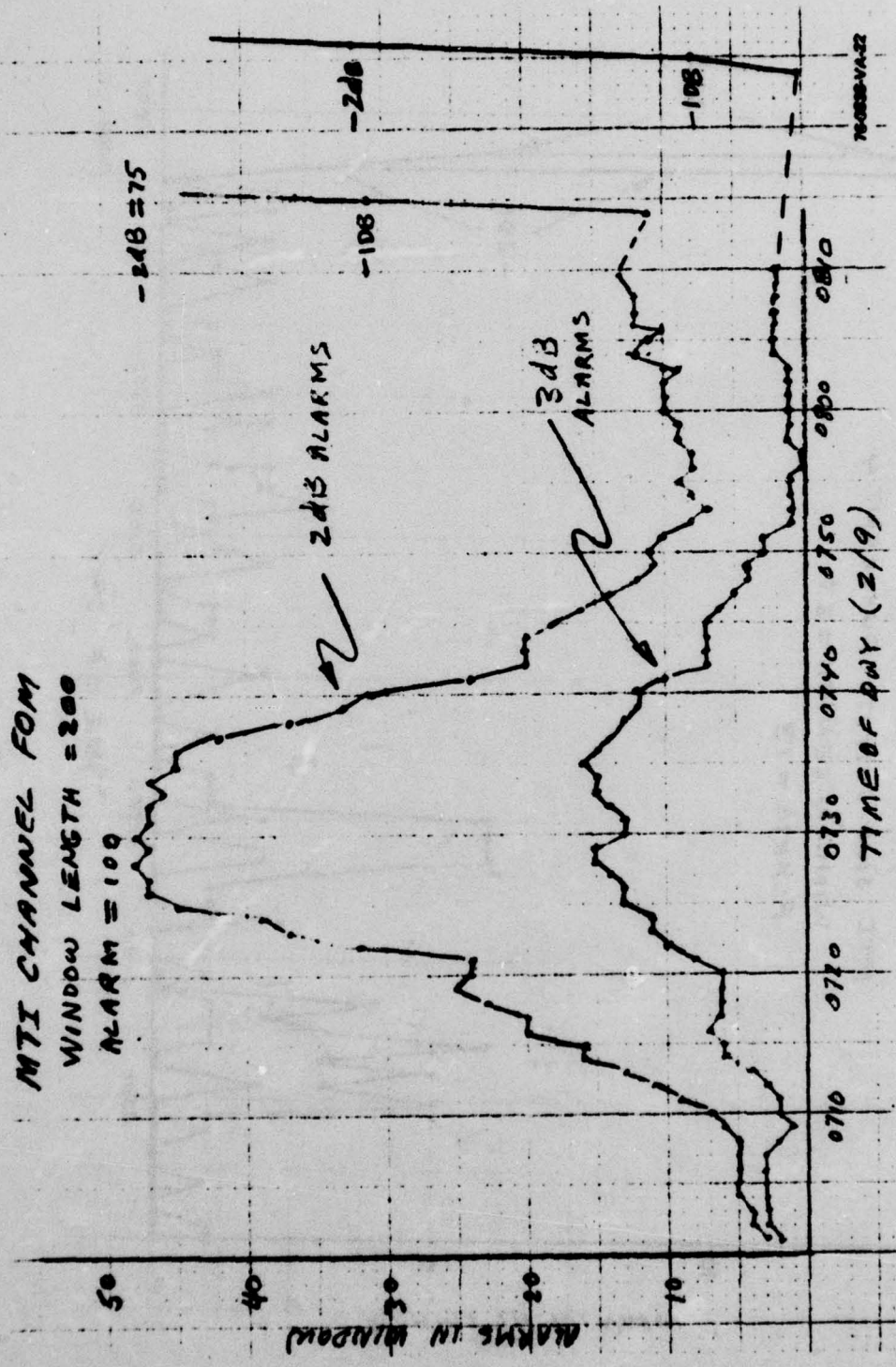


Figure 32. MTI Channel Figure-of-Merit

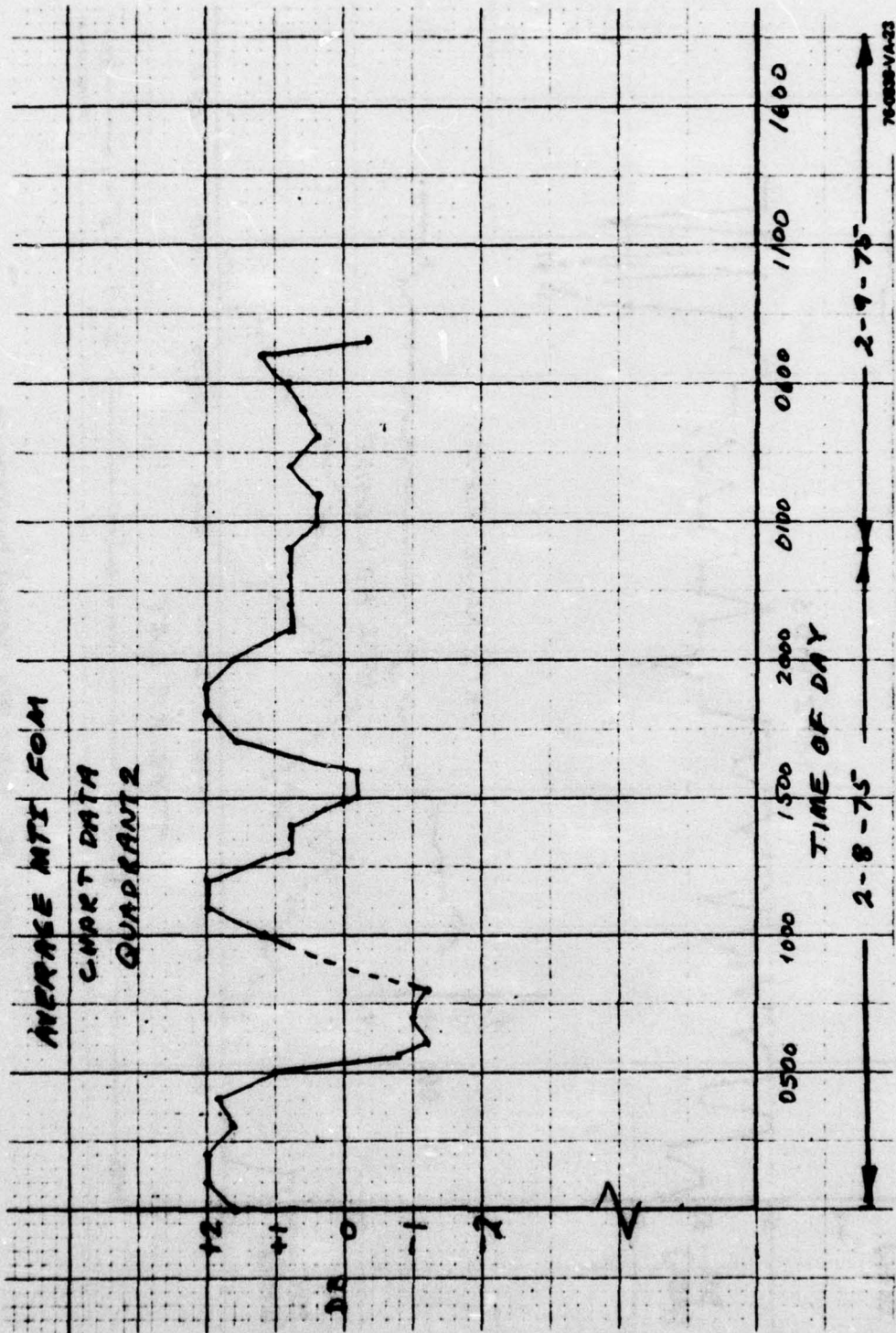


Figure 33. Average MTI Figure-Of-Merit Chart Data

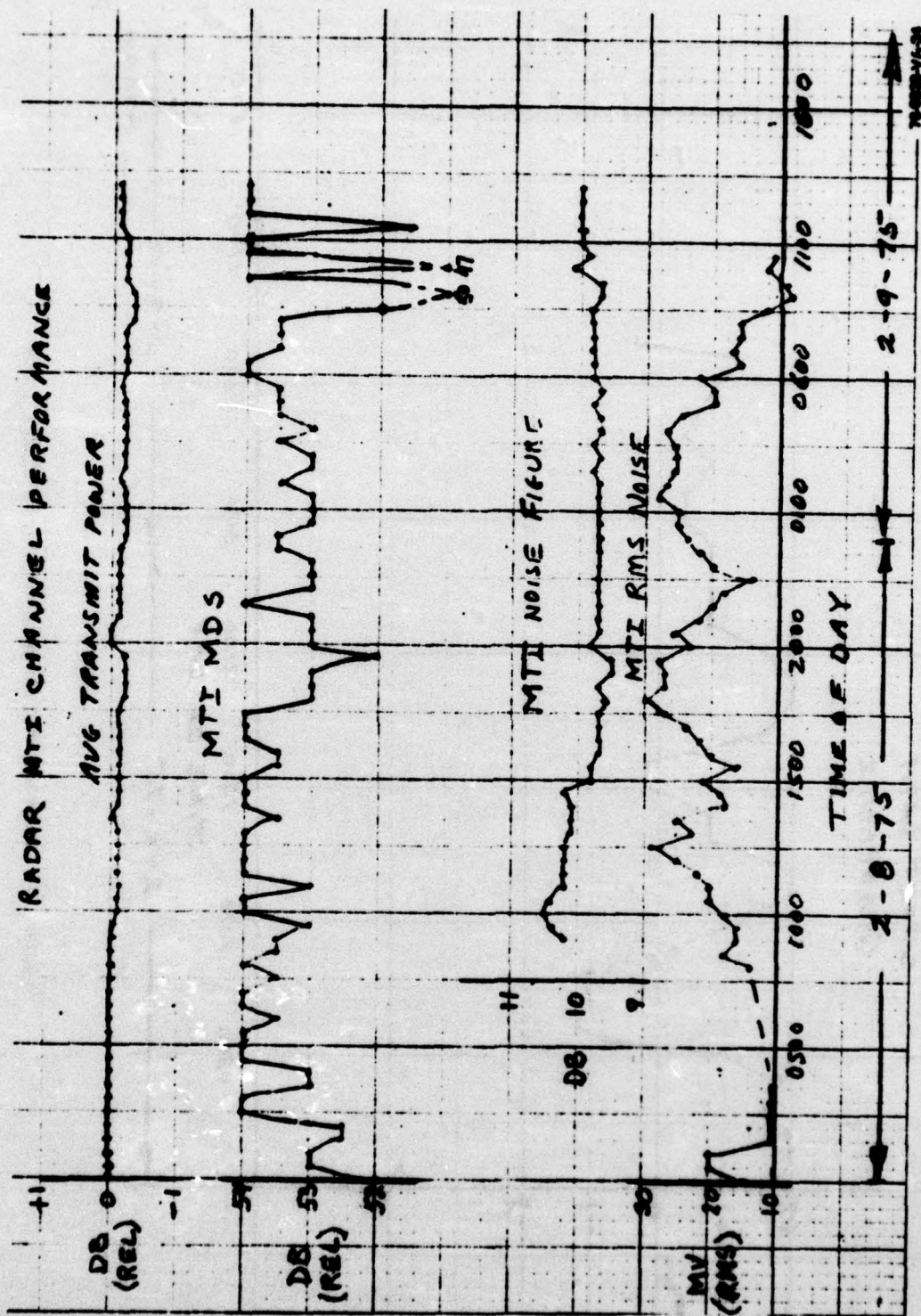


Figure 34. Radar MTI Channel Performance

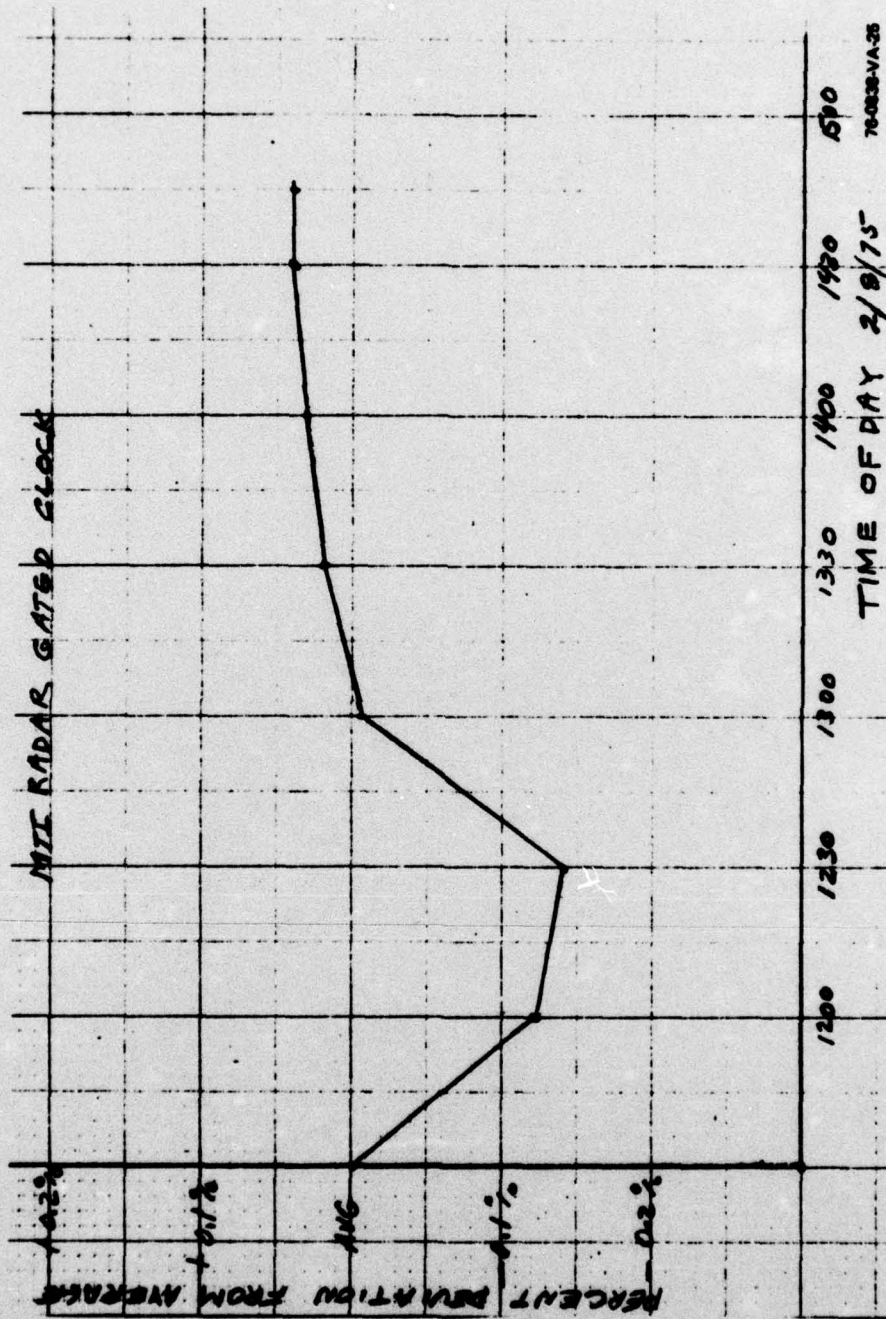


Figure 35. MTI Radar Gated Clock

7-21/7-22

## SECTION VIII

### CONCLUSIONS

As seen from the numerous Monitor tests and the data of this report, automatic monitoring of a radar system is feasible, but the pitfalls are many. Most important considerations must be given to the statistical nature of the radar outputs. A sufficient number of radar output samples (still to be determined in the Monitor evaluation tests) must be averaged before an accurate measure of signal to noise ratio can be made. Another important consideration is radar video noise output. Since the radar figure-of-merit computation is based on signal-plus-noise to noise ratio at the radar output, any alteration of this ratio due to signal limiting or bottom clipping of the noise is reported as figure-of-merit change. In a non-CFAR radar system moderate receiver gain changes allow accurate figure-of-merit measure if no top limiting or bottom clipping variations are present, but monitoring the video noise level at  $\pm 1$  dB thresholds becomes impractical. Furthermore, the Monitor must be tailored for each radar system to include all its modes of operation and peculiarities of the system.

## APPENDIX A

### ANALYSIS OF ACCURACY OF SIGNAL-TO-NOISE COMPUTATION

G. VAUGHAN

#### 1.0 GENERAL

The Radar Performance Monitor is a closed loop control system whereby the error voltage is computed as a function of the video signal-to-noise ratio as measured at the output of the video line drivers. The number of signal samples and signal plus noise samples is finite. The specification dictates that the video signal-to-noise ratio shall be regulated over a voltage range of from 3/1 to 1/1. Since there is no practical way of separating signal and noise during the signal sample, the ratio of signal plus noise-to-noise is considered. The signal plus noise-to-noise ratio shall be controlled over the range of 4/1 to 2/1. The specification states that a decrease of (S+N/N) of either 2 dB or 3 dB shall be monitored and the accuracy of the measurement shall be  $\pm 0.5$  dB for all cases. Further, a maximum of 32 (S+N) samples are allowed per sector. The specification places no limit on the number of noise samples per azimuth sector.

The problem is, of course, statistical in nature by virtue of the noise inputs. Intuitively, we know that the solution is also statistical; however, intuition does not tell us if a usable solution results from the specified inputs. Therefore, the problem was simulated on a high speed digital computer. The results of the simulation are outlined in Section 2.0.

#### 2.0 DIGITAL SIMULATION

A program was devised (BASIC LANGUAGE) consisting of six inputs listed as follows:

<u>INPUT</u>	<u>DESCRIPTION</u>
$Z_1$	Number of (Signal + Noise) Samples
$Z_2$	Number of Noise Samples
$M_1$	Signal Mean

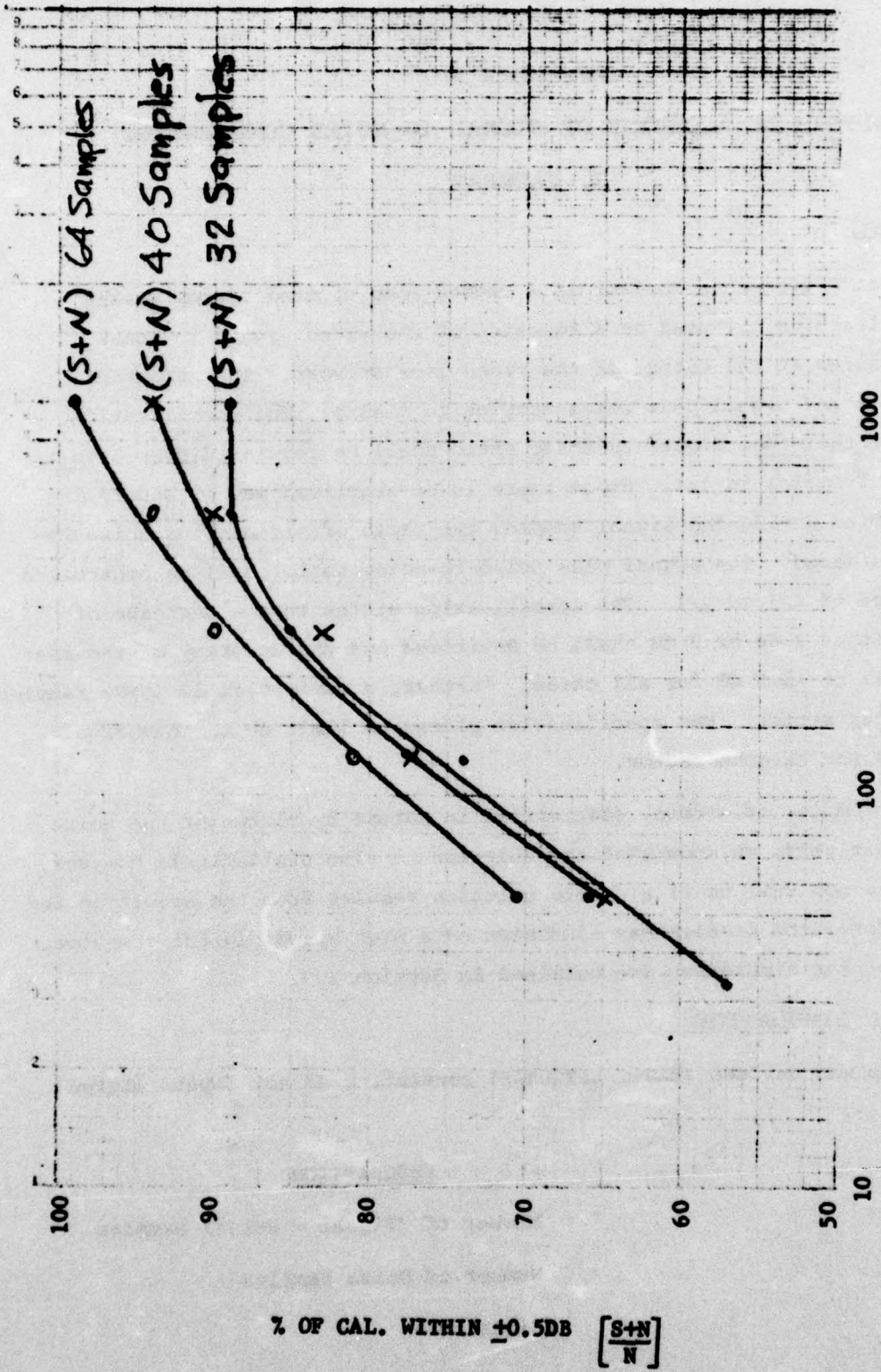
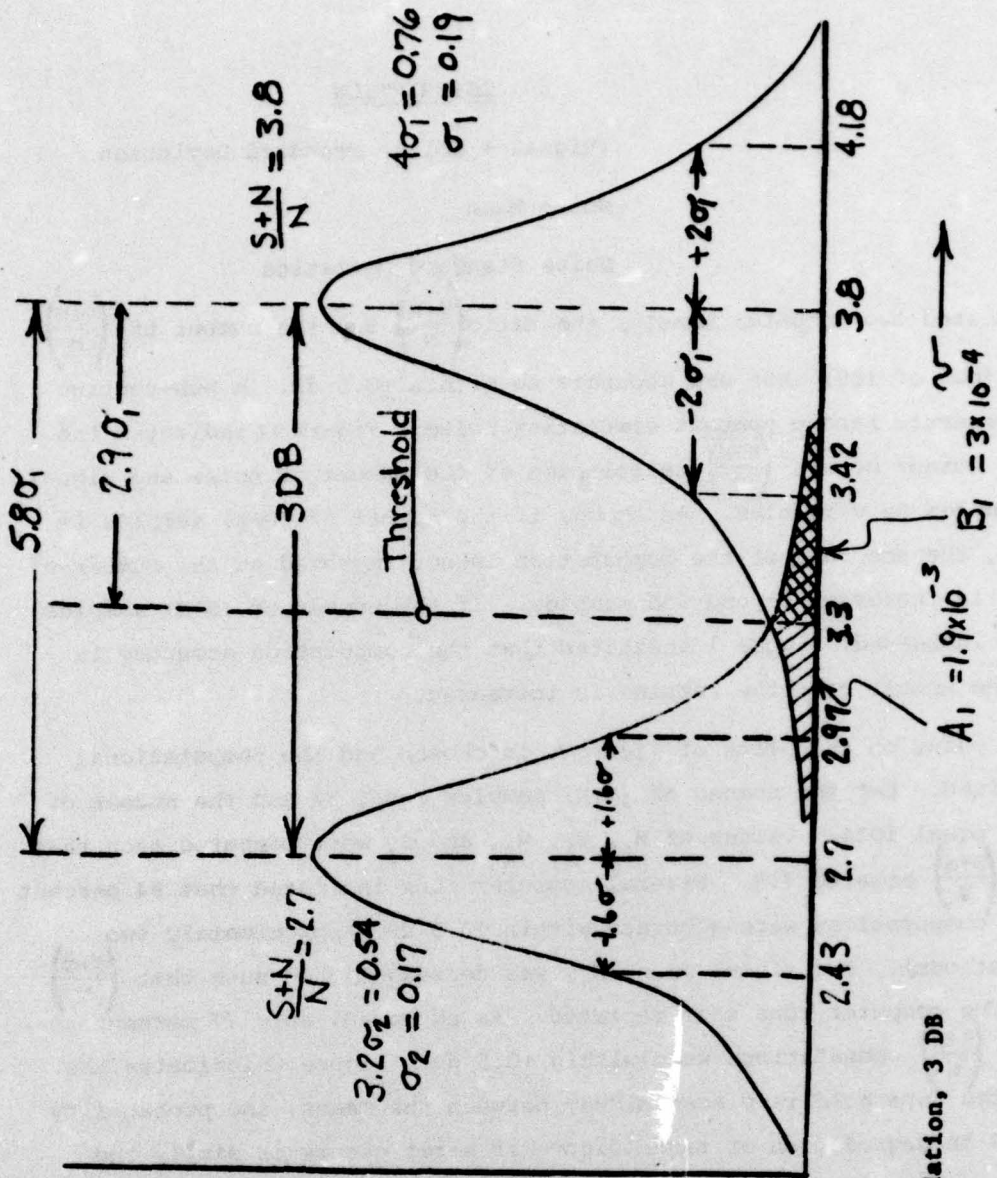


Figure A1. NUMBER OF (S+N) SAMPLES



- (1)  $(S+N) = 32$  Samples
- (2)  $N = 1024$  Samples
- (3)  $\frac{S+N}{N} = 3.8/1$
- (4) Figure of Merit Degradation, 3 DB
- (5) 1 Scan

Figure A2. Statistical Relationship Between False Alarm and Miss for Equidistant Threshold

<u>INPUT</u>	<u>DESCRIPTION</u>
$S_1$	(Signal + Noise) Standard Deviation
$M_2$	Noise Mean
$S_2$	Noise Standard Deviation

The program listed two outputs; namely, the ratio  $\left(\frac{S+N}{N}\right)$  and the number of  $\left(\frac{S+N}{N}\right)$  computations (out of 100) that are accurate to within  $\pm 0.5$  dB. A sub-routine was used to generate random numbers simulating noise. Figure A1 indicates the statistical accuracy of the  $\left(\frac{S+N}{N}\right)$  calculation of the number of noise and signal plus noise samples as variables. As shown, if the number of (S+N) samples is limited to 32, the accuracy of the computation is not improved as the number of noise samples is increased beyond 500 samples. If the number of (S+N) samples per sector is increased, Figure 1 indicates that the computation accuracy is improved as the number of noise samples is increased.

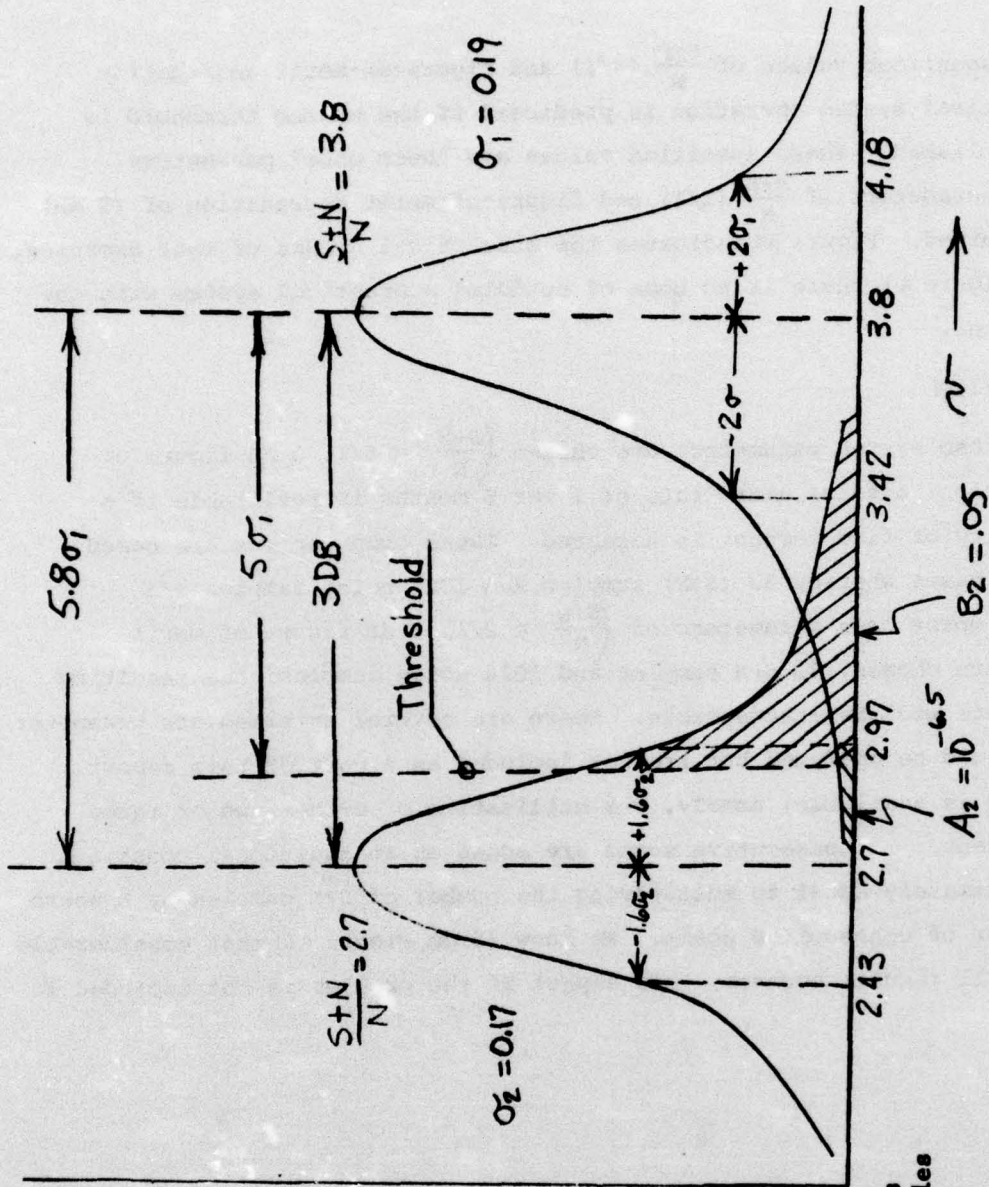
A single point on the plots of Figure A1 is chosen and the computational accuracy examined. Let the number of (S+N) samples equal 32 and the number of noise samples equal 1024. Values of  $M_1$ ,  $S_1$ ,  $M_2$ , and  $S_2$  were computed such that the ratio of  $\left(\frac{S+N}{N}\right)$  equaled 3.8. Several computer runs indicated that 94 percent of the  $\left(\frac{S+N}{N}\right)$  computations were accurate within  $\pm 0.5$  dB (approximately two standard deviations). The signal mean,  $M_1$ , was decreased 3 dB such that  $\left(\frac{S+N}{N}\right)$  became 2.7. The computer runs were repeated. As expected, only 77 percent (1.6) of the  $\left(\frac{S+N}{N}\right)$  computations were within  $\pm 0.5$  dB. Figure A2 indicates the process. If the threshold is placed midway between the means, the probability that a false 3 dB degradation of radar figure of merit occurs is simply the area  $A_1$ . Conversely, if the figure-of-merit degrades 3 dB the probability that the degradation will not be reported is the area  $B_1$ . Area  $A_1$  results in the probability of  $1.9 \cdot 10^{-3}$ . Area  $B_1$  yields a probability of  $3.10^{-4}$ .

If an antenna scan rate of  $15 \frac{\text{rev}}{\text{min}}$  is assumed, and the threshold is placed as shown in Figure A2 a false 3 dB degradation of figure of merit will be reported every 127 minutes. If the threshold is placed as shown in Figure A3 (for the same scan rate) a false 3 dB degradation of figure of merit will be reported every six months. However, as a result, five percent of the time when the figure of merit degrades 3 dB the sensor will not report the fact as shown by the area  $B_2$ . The designer has control of system operation by selection of the threshold.

For the specified values of  $\frac{S+N}{N}$  (4/1) and figure-of-merit degradation (3 dB) a practical system operation is predicted if the system threshold is properly established. These specified values are "best case" parameters. "Worst Case" parameters of  $\frac{S+N}{N}$  (1/1) and figure-of-merit degradation of (2 dB) were also examined. Figure A4 indicates the statistical nature of that exercise. As shown in Figure A4, there is no hope of building a practical system with the listed parameter.

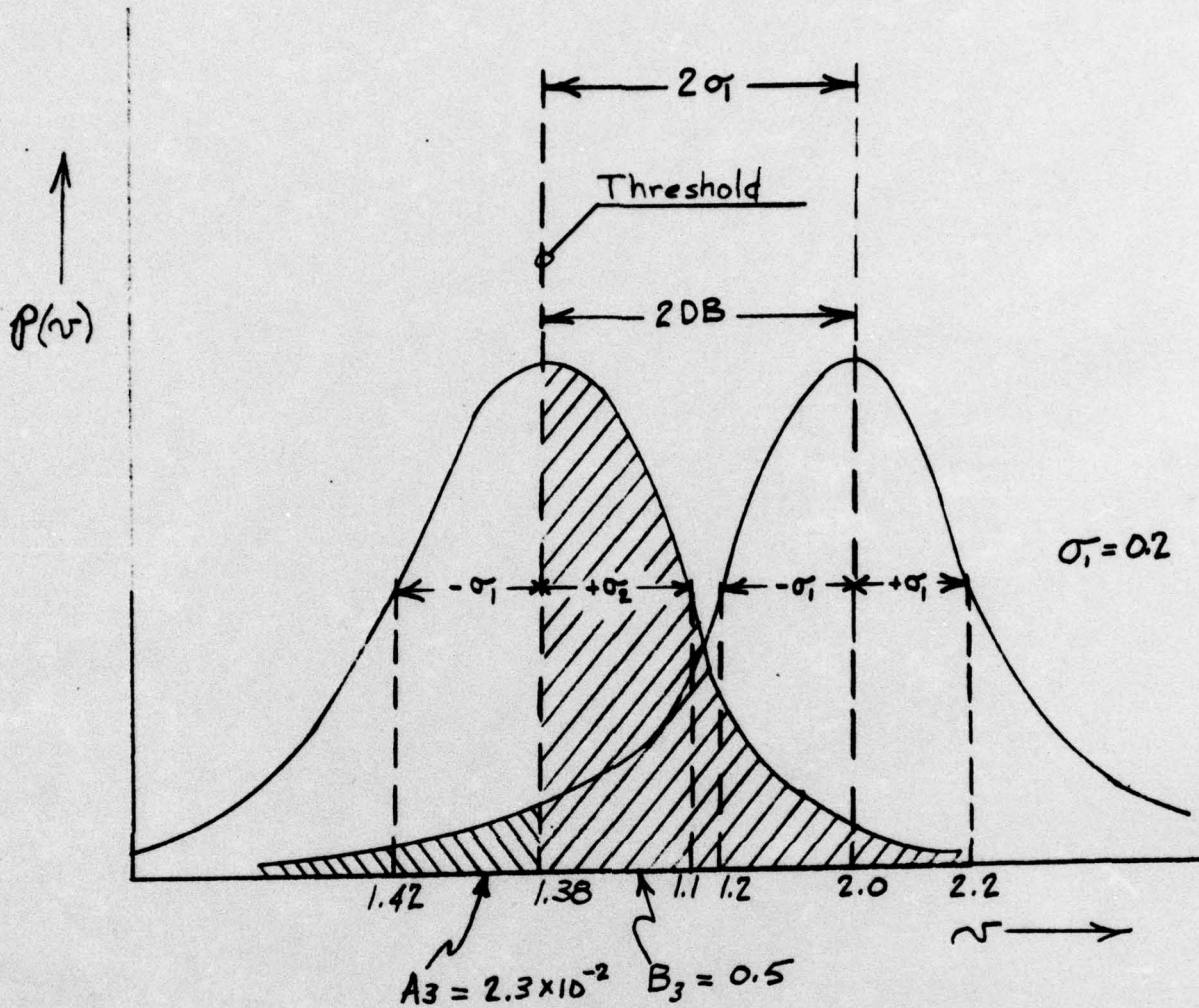
### 3.0 CONCLUSION

If best case system parameters are chosen ( $\frac{S+N}{N} = 4/1$ , 3 dB figure of merit degradation) a false alarm rate of 1 per 6 months is realizable if a miss probability of five percent is accepted. These computations are based on a per scan basis whereby 32 (S+N) samples and 1024 noise samples are utilized. If worst case parameters of ( $\frac{S+N}{N} = 2/1$ , 2 dB figure of merit degradation) are chosen, 32 S+N samples and 1024 noise samples, the resulting false alarm rate will be unacceptable. There are several intermediate parameter values that could be analyzed but are not included as a part of this report. Another option is available; namely, the utilization of either two or three consecutive scans. If consecutive scans are added as an additional constraint this is approximately equal to multiplying the number of S+N samples by N where N is the number of consecutive scans. We know (from Figure A1) that considerable improvement will result; however, this aspect of the problem is not included in this report.



- (1)  $(S+N)$  = 32 Samples
- (2)  $N$  = 1024 Samples
- (3)  $\frac{S+N}{N}$  = 3.8/1
- (4) Figure of Merit Degradation
- (5) 1 Scan

Figure A3. Statistical Relationship Between False Alarm and Miss for Weighted Threshold



- (1)  $(S+N)$  = 32 Samples
- (2)  $N$  = 1024 Samples
- (3)  $\frac{S+N}{N}$  = 2/1
- (4) Figure of Merit Degradation, 2 DB
- (5) 1 Scan

Figure A4. Statistical Relationship Between False-Alarm and Miss for Weighted Threshold (Worst Case)

APPENDIX B  
RADAR PERFORMANCE MONITOR  
MTI CANCELLATION RATIO

The Radar Performance Monitor measures the IF cancellation ratio of the ASR-5 radar by injecting IF test targets at the input of the MTI-IF amplifier (FA-5758A) in the ASR-5 radar. Figure B1 is a simplified functional block diagram showing the portion of ASR-5 radar monitored and the Radar Performance Monitor instrumentation associated with the cancellation ratio measurement. The IF test target source, shown in Figure B1, is a 30 MHz oscillator which is phase locked to the radar coho by using the radar coho lock pulse. The 30 MHz signal from the oscillator is amplitude modulated to simulate antenna scan modulation and then range gated to produce pairs of in-phase and quadrature IF test targets equal to radar pulsewidth. The resulting signal at point A of Figure B1 is three pairs of IF pulses (in-phase and quadrature) at the end of each radar PRT. The first and last test target pairs are injected into the radar by enabling the fixed target gate. These pulses are at fixed phase relative to the radar coho and simulate fixed or clutter targets. The fixed targets are injected into MTI IF at the end of the PRT with the IF switch gating off the front end MTI receiver noise to ensure sufficient video dynamic range at the output of the radar MTI. The resulting fixed target residue from the radar MTI is sampled and multiplexed into the Radar Performance Monitor. To evaluate the uncanceled residue level, a total of 1024 range cells are sampled. The corresponding I and Q range cells are first quadrature-added and then the residue from the 1024 range cells is averaged and stored for further computation. The second pair of the I and Q IF pulses at point A in Figure B1 is attenuated (20 dB) and applied to the moving target gate. This gate causes the 30 MHz test target phase to shift 180° on alternate PRT's simulating optimum velocity IF target, which is summed in quadrature with the fixed target. The resulting signal at point B in Figure B1 is a fixed target on which there is a superimposed moving target at 90 degrees with respect to the fixed target.

The moving target amplitude with respect to the fixed target is as preset by the attenuator at the input to the moving target gate. The total number of fixed-plus-moving pulses injected into the MTI receiver is one maximum run-length or 32. These pulses are sampled at the output of the radar MTI and processed in the same manner as previously described for the fixed target. The averaged moving target level and the previously computed average of the fixed target residue are then used to compute moving + fixed to fixed ( $\log M/F$ ) target ratio which is then stored for further computation. During the azimuth assigned for Radar Performance Monitor calibration one run-length of fixed IF targets and one run-length of moving target (not superimposed with fixed targets) are applied to an amplitude detector. The amplitude detected fixed and moving targets are applied directly to the sensor and the fixed-to-moving test target ratio at the input to the radar MTI is measured in a manner identical to the processing of radar video. The input fixed-to-moving target ratio ( $\log F1/M1$ ) is then added to the previously computed moving-to-fixed ratio to compute the cancellation ratio of the MTI canceller, which is offset to zero by a calibrate switch for nominal performance. Degradation of MTI canceller will cause this output to deviate from zero and when the threshold following the calibrate adder is exceeded an alarm condition will be sensed.

The measured cancellation ratio is greater than the overall system cancellation ratio and the thresholds must be set higher than 2 or 3 dB to avoid false alarms. The threshold value for the measured cancellation ratio can be analytically related to any given overall cancellation ratio as shown in the following discussion.

The overall MTI radar cancellation ratio  $I_R$  is a result of cancellation ratio limitations of all the radar subsystems:

$$\frac{1}{I_R} = \left[ \frac{1}{I_X} \right]$$

where  $I_X$  are the cancellation ratio limitations due to the individual subsystems of the radar, such as scan modulation, timing instability, cancellation ratio of the canceller, and the transmitter, stalo and coho phase instabilities. For a known overall MTI radar cancellation ratio required canceller performance may be determined from

$$\frac{1}{I_R} = \frac{1}{I_S} + \frac{1}{I_C}$$

where  $I_C$  is the canceller cancellation ratio and  $I_S$  are all other limitation on MTI cancellation ratio. For  $I_C \gg I_S$  then  $I_R = I_S$ , and for  $I_C \ll I_S$  then  $I_R = I_C$ . Intermediate points of  $I_C$  are plotted for  $I_R = 27$  dB in Figure B2.

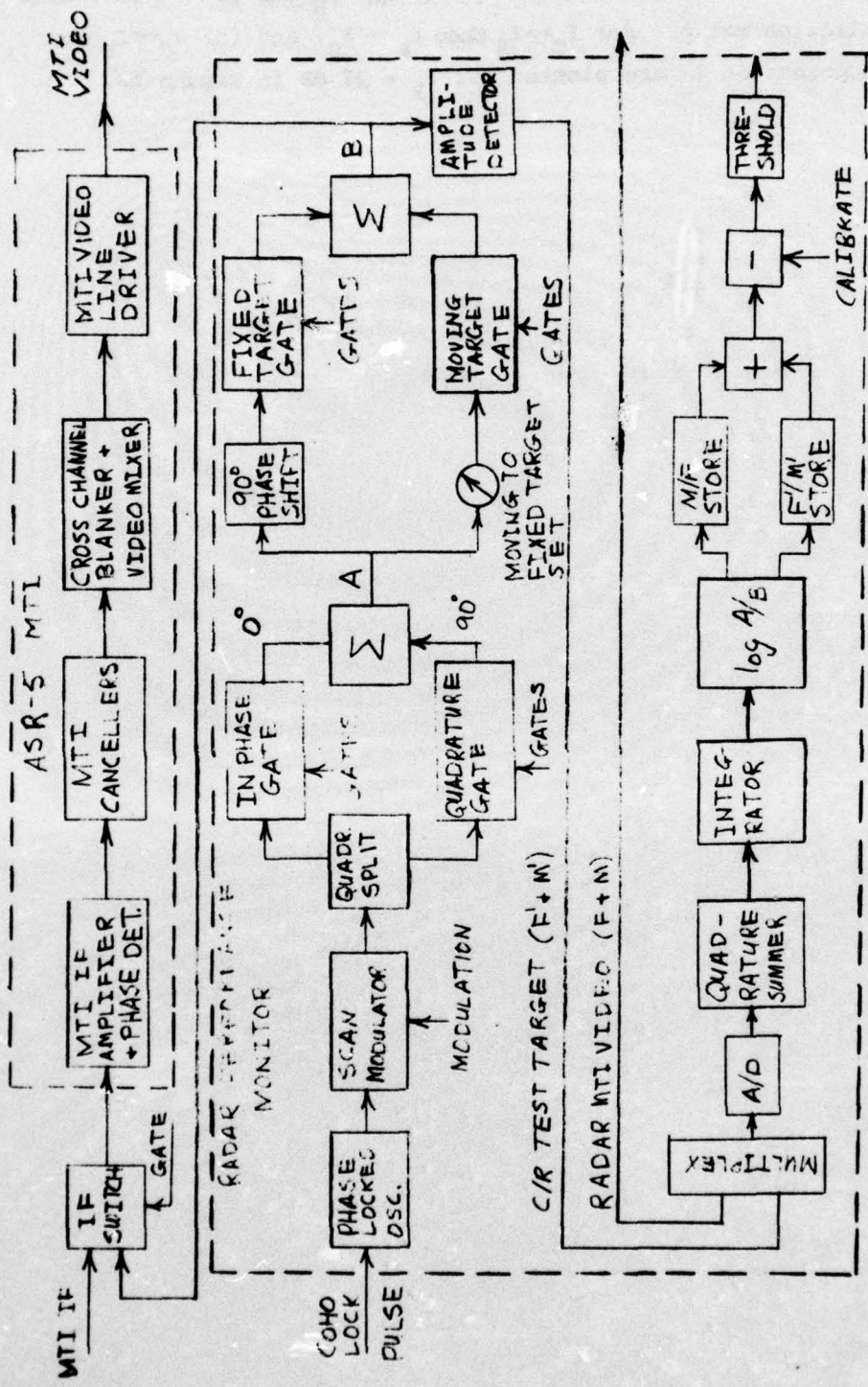


Figure B1. MTI Cancellation Ratio Monitor Functional Block Diagram

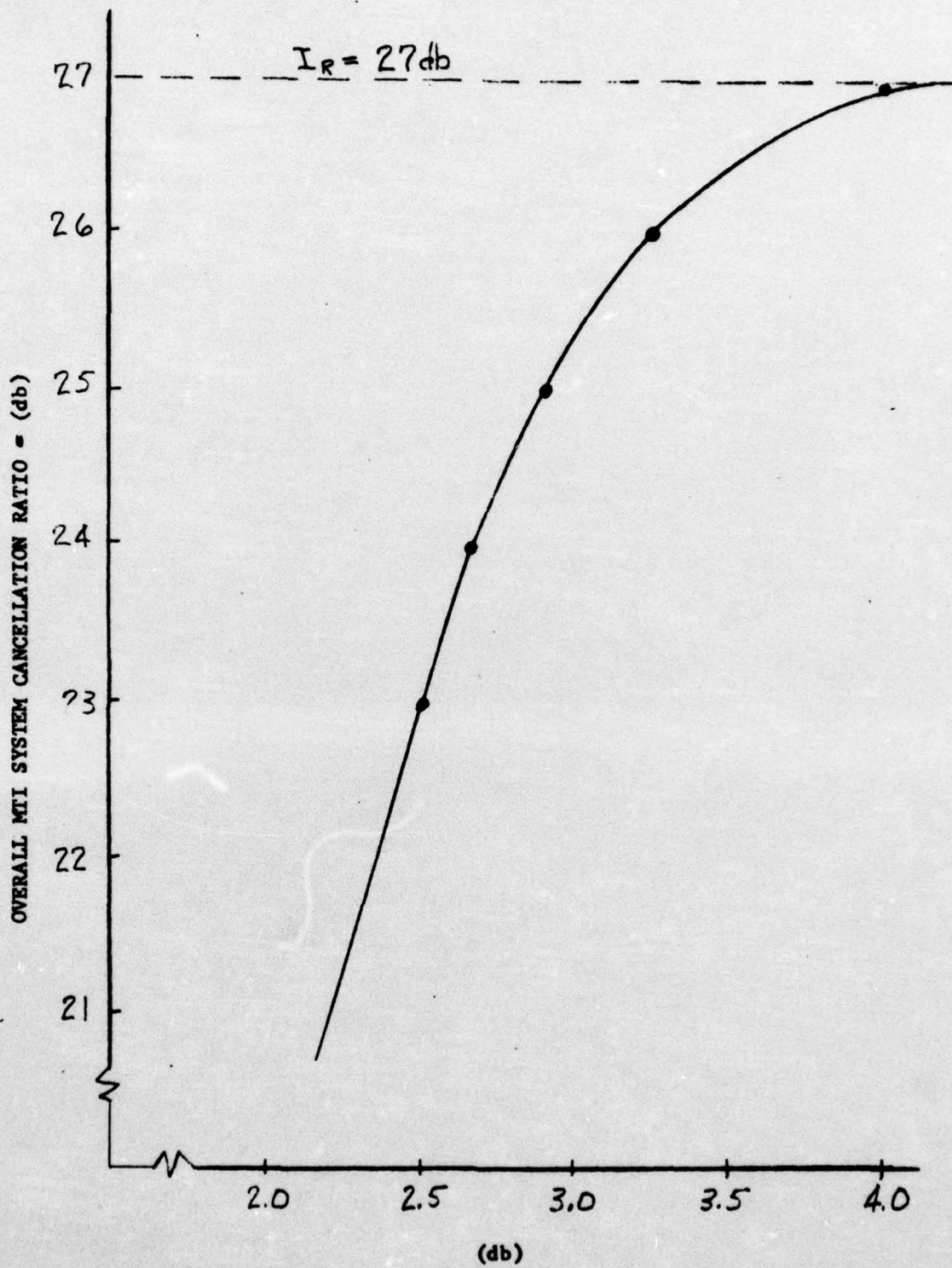


Figure B2. Cancellor - C/R

B-5/B-6

GPO 912-281

(5) 96